

Unlocking Flexibility: Risk-Aware Operational Water and Energy Management

van der Heijden, T.J.T.

DOI

[10.4233/uuid:f067975a-cc23-441d-bb75-c62985094a80](https://doi.org/10.4233/uuid:f067975a-cc23-441d-bb75-c62985094a80)

Publication date

2024

Document Version

Final published version

Citation (APA)

van der Heijden, T. J. T. (2024). *Unlocking Flexibility: Risk-Aware Operational Water and Energy Management*. [Dissertation (TU Delft), Delft University of Technology].
<https://doi.org/10.4233/uuid:f067975a-cc23-441d-bb75-c62985094a80>

Important note

To cite this publication, please use the final published version (if applicable).
Please check the document version above.

Copyright

Other than for strictly personal use, it is not permitted to download, forward or distribute the text or part of it, without the consent of the author(s) and/or copyright holder(s), unless the work is under an open content license such as Creative Commons.

Takedown policy

Please contact us and provide details if you believe this document breaches copyrights.
We will remove access to the work immediately and investigate your claim.

Unlocking flexibility

Risk-aware operational water
and energy management



Teunis Johannes Theodorus van der Heijden

UNLOCKING FLEXIBILITY

RISK-AWARE OPERATIONAL WATER AND ENERGY MANAGEMENT

UNLOCKING FLEXIBILITY

RISK-AWARE OPERATIONAL WATER AND ENERGY MANAGEMENT

Proefschrift

ter verkrijging van de graad van doctor
aan de Technische Universiteit Delft,
op gezag van de Rector Magnificus prof. dr. ir. T.H.J.J. van der Hagen,
voorzitter van het College voor Promoties,
in het openbaar te verdedigen op donderdag 24 oktober 2024 om 12:30 uur

door

Teunis Johannes Theodorus VAN DER HEIJDEN

Master of Science in Civil Engineering,
Technische Universiteit Delft, Delft, Nederland,
geboren te Wageningen, Nederland.

Dit proefschrift is goedgekeurd door de promotoren.

Samenstelling promotiecommissie:

Rector Magnificus,
Prof. dr. P. Palensky
Prof. dr. ir. N.C. van de Giesen
Dr. ir. E. Abraham

voorzitter
Technische Universiteit Delft, promotor
Technische Universiteit Delft, promotor
Technische Universiteit Delft, promotor

Onafhankelijke leden:

Prof. dr. M. Gibescu
Prof. dr. I. Oleinikova
Prof. dr. A.F. Castelletti
Prof. dr. ir. B.H.K. de Schutter
Prof. dr. P.J. Vardon

Universiteit Utrecht
Norwegian U. of Science and Technology
Politecnico di Milano, Italy
Technische Universiteit Delft
Technische Universiteit Delft, reservelid

Keywords: Demand Response, Operational Water Resources Management, Energy Markets, Operational Uncertainty, Forecasting, Control, Energy Management, Renewable Energy Integration

Printed by: Proefschrift All in One

Front & Back: Cover art and chapter transitionings were designed using generative Artificial Intelligence (Chat-GPT and Dall-E).

Copyright © 2024 by T.J.T. van der Heijden

ISBN 978-94-93406-14-8

An electronic version of this dissertation is available at
<http://repository.tudelft.nl/>.

I knew exactly what to do.

*But in a much more real sense,
I had no idea what to do.*

Michael Scott

*You will be alone with the gods,
and the nights will flame with fire.*

*Do it. Do it...Do it!
All the way.*

Charles Bukowski



CONTENTS

Summary	xi
Samenvatting	xiii
1 Introduction	1
1.1 The European energy transition landscape	2
1.1.1 Goals and challenges.	2
1.1.2 Evolving markets.	2
1.2 Flexibility, the new renewable.	4
1.2.1 Demand response	4
1.2.2 Uncertainty & operational challenges	5
1.3 The Dutch water-energy nexus	7
1.3.1 Energy transition status	7
1.3.2 The water management system	8
1.4 This thesis	9
1.4.1 Case study area for demand response	9
1.4.2 Thesis structure	10
2 Pumping when the wind blows	17
2.1 Introduction	18
2.1.1 Demand response in the Netherlands	18
2.1.2 Current status of DR applications	18
2.2 Market and balancing mechanisms	19
2.2.1 Grid balancing mechanisms	20
2.2.2 Carbon intensity of grid electricity	21
2.3 Methods: Modelling the water system and DR participation in the case study area	23
2.3.1 Water system modelling	24
2.3.2 Economic MPC formulation with multiple markets	24
2.3.3 Water system constraints	26
2.3.4 MPC optimisation problem	28
2.4 Results & discussion	31
2.4.1 System dynamics	31
2.4.2 Evaluation of DR profitability	31
2.4.3 aFRR potential analysis	33
2.5 Conclusion	34

3	Modelling operational uncertainty for control	43
3.1	Probabilistic forecasting	44
3.1.1	Combined quantile regression deep neural networks	44
3.1.2	Feature and hyperparameter optimization.	44
3.2	Scenario generation and selection	45
3.2.1	Non-parametric bayesian networks	45
3.2.2	Energy distance clustering	46
3.2.3	Scenario tree reduction	48
3.2.4	Proof of concept	49
3.3	Conclusion	50
4	Electricity price forecasting in European day ahead markets	55
4.1	Introduction	56
4.2	Electricity price forecasting methods	58
4.2.1	LASSO and Elastic-net	58
4.2.2	Lasso estimated auto regressive model.	59
4.2.3	Deep neural network.	60
4.2.4	Diebold-Mariano test	60
4.2.5	Greedy algorithm for European feature search	61
4.3	Data and tools	62
4.4	European feature importance analysis	63
4.5	Dutch DAM price forecasting with EU Market Integration	68
4.5.1	Model training	68
4.5.2	Dutch benchmark	68
4.5.3	Greedy search for European features.	69
4.5.4	Temporal variation in performance	74
4.6	Conclusion	76
5	Incorporating risk in operational water resources management	85
5.1	Introduction	86
5.2	Demand response in the Netherlands: case study IJmuiden	88
5.2.1	The Noordzeekanaal–Amsterdam–Rijnkanaal	88
5.2.2	Energy markets in the Netherlands.	90
5.3	Risk-aware optimal control	91
5.3.1	Stochastic model predictive control	91
5.3.2	Water system constraints	94
5.3.3	Multi-market trading objective.	95
5.3.4	Full MPC control problem	96
5.4	Results and discussion	97
5.4.1	Probabilistic forecasting	98
5.4.2	Scenario generation and reduction	100
5.4.3	Stochastic MPC	102
5.4.4	Closed-loop simulation testing	103
5.5	Summary and conclusion.	105

6	RayCast: a satellite-based quantile regression irradiance nowcast	113
6.1	Introduction	114
6.2	Methodology	115
6.2.1	Adversarial extrapolation neural network	115
6.2.2	Study set-up	117
6.2.3	Hyperband pruning	117
6.2.4	Model validation	118
6.3	Spatiotemporal modelling of cloud characteristics	119
6.4	Translating cloud characteristics to irradiance quantiles	120
6.5	Results and discussion	122
6.5.1	Model output	122
6.5.2	Spatially distributed performance metrics	123
6.5.3	Temporal variation in model performance	123
6.5.4	Model validation with DSO data	124
6.6	Conclusion	128
7	Conclusions and recommendations	133
7.1	Conclusions.	133
7.2	Societal impact	135
7.3	Suggestions for future research	136
7.4	Practical considerations for operational water resources management	140
	Acknowledgements	145
	About the author	147
	List of Publications	149



SUMMARY

This thesis explores risk-aware operational decision-making methods to support the integration of Renewable Energy Sources (RES) into the energy system by enhancing energy flexibility under operational uncertainty. Amidst the urgent global shift towards RES to combat climate change, this work identifies and addresses the challenges posed by the intermittent and uncertain nature of renewable energies, such as wind and solar power, to grid stability and energy reliability.

Central to this objective is the use of Demand Response (DR) strategies to balance energy supply and demand dynamically using electricity spot markets, mitigating the risks associated with the variability and uncertainty of renewable energy sources. A significant contribution of this work lies in the examination of the water-energy nexus through a case study of the Noordzeekanaal–Amsterdam–Rijnkanaal in the Netherlands. This area serves as a prime example of how critical water management infrastructure can be optimized to support and advance the country's energy transition goals without compromising its primary function of flood protection. This thesis presents a new pump-scheduling strategy that provides DR services by optimising the energy cost of pumping based on hourly electricity prices. We analyse the cost-saving potential through DR, showing significant benefits can be gained by exploiting the flexibility in the water system. By analysing both the Dutch and German markets with different RES penetration over multiple years, this thesis also shows that as renewable energy penetration increases, the potential benefits are expected to increase.

Operational uncertainty, arising from the intermittent nature of RES, fluctuating demand, and the volatility of electricity prices, presents significant challenges to maintaining grid stability and optimising energy use. The complexity of decision-making is further compounded by the involvement of various mechanisms such as markets, balancing, and congestion management, each introducing its own set of uncertainties to actors willing to exploit energy flexibility. To depict the consequential operational uncertainty, this thesis describes predictive models and stochastic methods that aid in navigating the intricacies of operational uncertainty effectively. By employing deep learning techniques, specifically a neural network architecture designed to forecast multiple distribution quantiles simultaneously, we enhance the process of operational uncertainty estimation. This thesis also presents methods for generating realistic scenarios that consider the autocorrelation in data, enabling risk-aware DR strategies through scenario-based stochastic programming. However, as the amount of sources of uncertainty increase, the computational burden of such an approach increases exponentially. To mitigate this curse of dimensionality and alleviate the computational burden of control methods, this thesis presents a subset selection and scenario tree generation method that allows for developing sparse uncertainty representations.

Accurate forecasts are essential for effective energy planning and management, which is an increasingly difficult task as the energy landscape becomes more complex and in-

terconnected. In this context, the ability to predict Day Ahead Market (DAM) prices with higher accuracy enables stakeholders to make more informed bidding and operational decisions, potentially reducing costs and enhancing the efficiency of the energy system as a whole. Recognising the significance of market integration in electricity price forecasting, this thesis explores how European markets influence one another and the implications for DAM price forecasting models. It presents an EU-wide data analysis to reveal the dynamics between interconnected markets and their collective impact on price settlements to improve price forecasting performance for the Dutch market.

Integrating stochastic predictive and optimisation techniques into DR strategies offers opportunities to unlock the flexibility of energy assets under uncertainty. By implementing this thesis' proposed framework for risk-aware pump scheduling, we quantify the uncertainties within the energy market and meteorological conditions and optimise the operational decision-making process for pump-controlled open canal systems. This approach's core is the stochastic Model Predictive Control (MPC) problem that incorporates scenario forecasts of future inflows, sea water levels, and hourly electricity prices. Integrating Exceedance Risk constraints within the stochastic MPC allows for managing the risks associated with water level violations, enabling an informed trade-off between minimising energy costs and maintaining water safety. This risk-aware decision-making model represents a departure from traditional deterministic control methods, providing a more nuanced approach that acknowledges and accommodates the unpredictable nature of weather phenomena and electricity market volatility.

As a natural extension to modelling uncertainty and adopting risk-aware decision-making approaches to accommodate the volatile nature of RES, this presents the application of the proposed techniques in electricity grid management. As solar becomes a more dominant component of the Dutch power system, grid congestion emerges as an urgent issue. Addressing this, this thesis presents RayCast, an irradiance nowcasting model that utilises satellite-derived cloud characteristics to forecast solar irradiance quantiles. The proposed approach advances the capability to predict solar energy generation in space and time, thus addressing one of the grid operators' main hurdles: the uncertainty in incoming radiation. The application of RayCast in a real-world scenario shows that by integrating the model into operational practices, as demonstrated with data provided by Dutch DSO Alliander, a tangible improvement can be realised in forecasting congestion related to solar generation.

All proposed approaches for modelling uncertainty and optimal control aid in efficiently managing energy resources and support the broader goal of integrating RES by providing a framework for risk-aware operational decision-making.

SAMENVATTING

Dit proefschrift onderzoekt risicobewuste operationele besluitvormingsmethoden om de integratie van hernieuwbare energiebronnen (RES) in het energiesysteem te ondersteunen door de energieflexibiliteit onder operationele onzekerheid te vergroten. Onder de dringende mondiale verschuiving naar hernieuwbare energiebronnen om klimaatverandering te mitigeren, identificeert en adresseert dit proefschrift de uitdagingen die het grillige en onzekere karakter van hernieuwbare energiebronnen, zoals wind- en zonne-energie, voor de stabiliteit en de betrouwbaarheid van de energievoorziening met zich meebrengt.

Centraal bij deze doelstelling staat het gebruik van Demand Response (DR)-strategieën om vraag en aanbod van energie dynamisch in evenwicht te brengen met behulp van elektriciteitsspotmarkten, waardoor de risico's die gepaard gaan met de variabiliteit en onzekerheid van hernieuwbare energiebronnen worden beperkt. Een belangrijke bijdrage van dit proefschrift ligt in water-energie nexus onderzoek door middel van een case study van het Noordzeekanaal-Amsterdam-Rijnkanaal in Nederland. Dit gebied dient als voorbeeld van hoe de kritieke infrastructuur voor waterbeheer kan worden geoptimaliseerd om de energietransitiedoelstellingen van het land te ondersteunen en te bevorderen, zonder de primaire functie van bescherming tegen overstromingen in gedringte te brengen. Dit proefschrift presenteert een nieuwe strategie voor het maken van pompschema's die DR-diensten levert door de energiekosten van gemalen te optimaliseren op basis van uurlijkse elektriciteitsprijzen. We analyseren het potentieel voor kostenbesparing via DR, waaruit blijkt dat er aanzienlijke voordelen kunnen worden behaald door de flexibiliteit in het watersysteem te benutten. Door zowel de Nederlandse als de Duitse markt met verschillende RES-penetratie over meerdere jaren te analyseren, laat dit proefschrift ook zien dat naarmate de penetratie van hernieuwbare energie toeneemt, de potentiële voordelen naar verwachting zullen toenemen.

Operationele onzekerheid, die voortkomt uit het onderbroken karakter van hernieuwbare energiebronnen, de fluctuerende vraag en de volatiliteit van de elektriciteitsprijzen, vormt een aanzienlijke uitdaging voor het handhaven van de stabiliteit van het elektriciteitsnet en het optimaliseren van het energieverbruik. De complexiteit van de besluitvorming wordt versterkt door de betrokkenheid van verschillende mechanismen zoals markten, balancering en congestiebeheer, die elk hun eigen reeks onzekerheden introduceren bij actoren die bereid zijn energieflexibiliteit te exploiteren. Om de operationele onzekerheid die uit deze mechanismes voortvloeit in beeld te brengen, beschrijft dit proefschrift voorspellende modellen en stochastische methoden die helpen bij het navigeren van de complexiteit die operationele onzekerheid met zich meebrengt. Door gebruik te maken van deep learning-technieken, met name een neurale netwerkarchitectuur die is ontworpen om meerdere distributiekwantielen tegelijkertijd te voorspellen, verbeteren we het proces van operationele onzekerheidsschatting. Dit proefschrift presenteert ook methoden voor het genereren van realistische scenario's die rekening hou-

den met de autocorrelatie in tijdreeksen, waardoor risicobewuste DR-strategieën mogelijk worden gemaakt door middel van op scenario's gebaseerde stochastische programming methoden. Naarmate het aantal bronnen van onzekerheid toeneemt, neemt de rekenlast van een dergelijke benadering exponentieel toe. Om deze vloek van dimensionaliteit te verzachten en de rekenlast van controlemethoden te verlichten, presenteert dit proefschrift een methode voor het selecteren van subsets en het genereren van scenario-bomen die het mogelijk maakt om schaarse onzekerheidsrepresentaties te ontwikkelen.

Nauwkeurige verwachtingen zijn essentieel voor effectieve energieplanning en -beheer, en dat wordt steeds moeilijker naarmate het energielandschap toeneemt in complexiteit en onderlinge verbondenheid. In deze context stelt het vermogen om Day Ahead Market (DAM)-prijzen met grotere nauwkeurigheid te voorspellen, belanghebbenden in staat beter geïnformeerde biedingen en operationele beslissingen te nemen, waardoor mogelijk de kosten worden verlaagd en de efficiëntie van het energiesysteem als geheel wordt verbeterd. Dit proefschrift erkent het belang van marktintegratie bij het voorspellen van elektriciteitsprijzen en onderzoekt hoe Europese markten elkaar beïnvloeden en de implicaties voor DAM-prijsverwachtingsmodellen. Het presenteert een EU-brede data-analyse om de dynamiek tussen onderling verbonden markten en hun collectieve impact op prijschikking bloot te leggen om zo de prestaties van prijsverwachtingsmodellen voor de Nederlandse markt te verbeteren.

Het integreren van stochastische verwachtingsmethoden en optimalisatietechnieken in DR-strategieën biedt mogelijkheden om de flexibiliteit van energieactiva onder onzekerheid te ontsluiten. Door het in dit proefschrift voorgestelde raamwerk voor het risicobewust opstellen van pompschema's te implementeren, kwantificeren we de onzekerheden binnen de energiemarkt en meteorologische omstandigheden en optimaliseren we het operationele besluitvormingsproces voor pompgestuurde open kanaalsystemen. De kern van deze benadering is het stochastische Model Predictive Control (MPC)-probleem dat scenarioverwachtingen van toekomstige instromen, zeevaterstanden en uurlijkse elektriciteitsprijzen omvat. Door beperkingen op het gebied van overschrijdingsrisico's binnen het stochastische MPC te integreren, kunnen de risico's die gepaard gaan met overschrijdingen van het waterpeil worden beheerd, waardoor een weloverwogen afweging kan worden gemaakt tussen het minimaliseren van de energiekosten en het handhaven van de waterveiligheid. Dit risicobewuste besluitvormingsmodel wijkt af van traditionele deterministische controlemethoden en biedt een meer genuanceerde aanpak die de onvoorspelbare aard van weersverschijnselen en de volatiliteit van de elektriciteitsmarkt erkent en accommodeert.

Als natuurlijke uitbreiding van het modelleren van onzekerheid en het aannemen van risicobewuste besluitvormingsmethoden om tegemoet te komen aan de volatiele aard van RES, presenteert dit proefschrift een toepassing van de voorgestelde technieken in het beheer van elektriciteitsnetwerken. Nu zonne-energie een steeds dominant onderdeel van het Nederlandse energiesysteem wordt, wordt netcongestie op het elektriciteitsnetwerk een steeds urgenter probleem. Om hieraan bij te dragen presenteert dit proefschrift RayCast, een 'irradiance nowcasting'-model dat gebruik maakt van satelliet-afgeleide wolkkarakteristieken om zonnestralingkwantielen te modelleren. De voorgestelde aanpak vergroot het vermogen om een verwachting van de opwekking van zonne-energie in ruimte en tijd te maken, en adresseert daarmee een van de belangrijkste

ste hindernissen voor de netbeheerders: de onzekerheid in de binnenkomende straling. De toepassing van RayCast in een echt scenario met gegevens van de Nederlandse DSO Alliander, laat zien dat door het model te integreren in operationele praktijken een tastbare verbetering kan worden gerealiseerd in het voorspellen van congestie gerelateerd aan de opwekking van zonne-energie.

Alle voorgestelde benaderingen voor het modelleren van onzekerheid en optimale operationele besluitvorming helpen bij het efficiënt beheren van energiebronnen en ondersteunen het bredere doel van het integreren van RES door een raamwerk te bieden voor risicobewuste operationele besluitvorming.



1

INTRODUCTION

*We're marooned on a small island, in an endless sea.
Confined to a tiny spit of sand, unable to escape.*

But tonight, it's heavy stuff.

Pendulum

This thesis aims to assist in integrating Renewable Energy Sources (RES) into the energy system. In doing so, it explores methods that allow for the exploitation of energy flexibility under uncertainty. The focus lies on operational decision-making under uncertainty, where several approaches are considered for quantifying operational uncertainty and its application in optimal real-time control. One key case study area for the exploitation of flexibility through Demand Response is the Noordzeekanaal–Amsterdam–Rijnkanaal, an essential waterbody for flood defences in the Netherlands that is operated by large under-shot gates and a pumping station to redirect water into the North Sea. The area represents an interesting case where meteorological uncertainties affect both safety-critical processes (i.e. water level management) and the energy system they operate in. This thesis offers insights into how physical and market risk can be estimated and considered in water- and energy management, unlocking flexibility in a world rich in uncertainty.

1.1. THE EUROPEAN ENERGY TRANSITION LANDSCAPE

The energy transition represents a path towards sustainability and resilience in the face of global climate change. In Europe, this journey is characterized by the integration of intermittent *Renewable Energy Sources* (RES), the smooth operation of an integrated European energy market, and the transition from a centralized to a distributed grid infrastructure. These elements are key in achieving the *European Union's* (EU) goals for a climate-neutral future. However, overcoming challenges in infrastructural limitations, policy and market dynamics, and the variability of RES is essential to secure an independent and climate-neutral energy system.

1.1.1. GOALS AND CHALLENGES

Wind and solar energy led the European energy transition, marking a significant change in the energy production landscape. As of 2023, renewables contributed to 44% of Europe's electricity generation, with wind energy surpassing gas in electricity production for the first time [1]. This reflects not only the technological advancements that are made but also the success of the EU policy framework, for example, through the European Green Deal, which sets a target to reduce greenhouse gas emissions by at least 55% by 2030 from 1990 levels with the ambition of a climate-neutral continent by 2050 [2].

However, as the more readily accessible opportunities for renewable energy deployment become more scarce, the focus shifts towards innovation in energy storage [3] and management and expanding renewable capacity in less accessible locations. The variability and intermittency introduced by renewable sources like wind and solar power pose significant challenges to grid stability and reliability. This necessitates advanced energy and grid management strategies to ensure a consistent balance between supply and demand, prevent the local congestion of grids, safeguard against potential blackouts, and ensure power quality.

1.1.2. EVOLVING MARKETS

To support renewable integration, a shift was made to spot markets and short-term trading. The *Day Ahead Market* (DAM) and *Intraday Market* (IDM) are the two main instruments in balancing the supply and demand of electricity in real-time by offering variable prices of electricity based on the expected (change in) renewable energy availability. Figure 1.1 depicts the energy delivery timeline with the markets and roles in the energy system.

On the DAM, energy is traded daily, with bids made for the following day. Consumers buy energy in hourly blocks and are responsible for consuming it within the period for which it is purchased. Every day at 12:00 CET, bids are collected by the market operator and the market is cleared at the price where supply meets demand.

On the other hand, the IDM is a continuous market where participants trade 15-minute, 30-minute or hourly energy blocks throughout the day, up to 5 minutes before delivery. On the IDM, buy- and sell orders are matched individually, leading to varying contract prices. This thesis treats the volume-weighted price over the three hours before delivery (ID3-price) as the closing price. In practice, every bid would have a different price. This would result in a distinct price for each trade, depending on the time of trading or even the specific party traded with. The IDM allows users to buy and sell energy

throughout the day, correcting their day ahead plan while preventing them from causing imbalance. The IDM is seen as the market containing the highest potential to trade renewable energy in the future [4], as it accommodates the uncertain and intermittent nature of renewables through short-term trading in short blocks.

Besides the regular market mechanisms, DSOs and TSOs employ several mechanisms to mitigate imbalances and congestion. TSOs apply aFRR and mFRR to mitigate imbalances by activating participants beforehand, where they apply FCR for immediate response. DSOs are tasked with congestion management, which they do by calling in flexibility or changing topology. However, participating in these mechanisms can require strict constraints to satisfy, making them less accessible to regular assets.

Both the DAM and the IDM incentivise participants to adjust energy planning for favourable prices that reflect the scarcity of supply and the marginal cost of production. In this thesis, we focus primarily on these two markets. However, the Futures and aFRR markets are included in the analysis presented in Chapter 2.

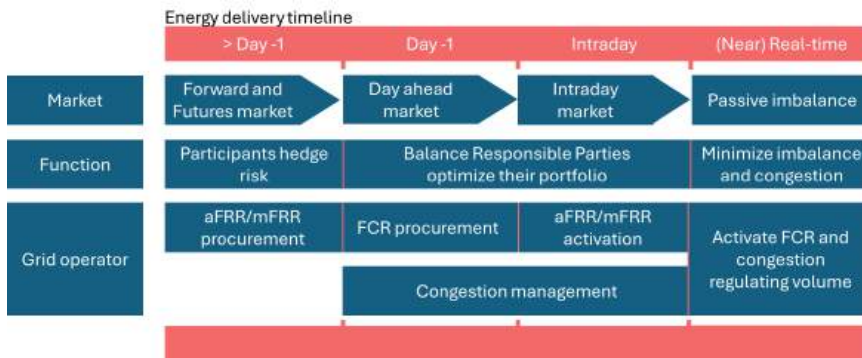


Figure 1.1: The energy delivery timeline depicting the energy markets, their function, and the role of the activity of the grid operators at several stages before time of delivery.

A fully integrated European energy market envisions the free flow of energy across borders, optimizing renewable resource use and enhancing energy security by leveraging diverse meteorological conditions across Europe [5]. Initiatives like market coupling (XBID) [6] make cross-border trading more easily accessible and improve renewable resource utilization and electricity supply security, but also cause price convergence within the European system [7]. The price waves travelling through the European bidding zones observed during the recent energy crises highlight the integrated system's shared strengths and weaknesses, underscoring that national energy transition policies must consider the broader European context.

The move towards more responsive and efficient markets is facilitating the reduction of reliance on fossil fuels and moves us towards achieving the EU's climate goals. However, this transition introduces new complexities and volatilities into the energy market, demanding adaptive regulatory frameworks. The European Agency for the Cooperation of Energy Regulators (ACER) emphasizes the importance of regulatory evolution to support effective spot markets and short-term trading, highlighting the need for market de-

signs that ensure transparency, security, and flexibility [8]. As markets accommodate and reward flexibility, participants need to adopt energy management strategies that exploit flexibility and unlock the balancing potential of spot markets.

1.2. FLEXIBILITY, THE NEW RENEWABLE

Flexibility in the energy sector is increasingly recognized as a cornerstone for successfully integrating RES into the power grid [9]. As countries move towards more sustainable energy solutions, the inherent intermittency of variable renewable resources such as wind and solar power presents new challenges, as depicted in Figure 1.2. In Europe, we keep our grid operating at a 50 Hz frequency, to which we have adjusted our appliances and infrastructure to operate optimally. This frequency stays stable when demand and supply are in balance, where the frequency increases with a generation surplus (positive imbalance) and the frequency decreases with a generation deficit (negative imbalance). Unlike traditional energy sources that can be controlled to meet demand, renewable energy generation is variable and dependent on factors like weather conditions and time of day. This variability introduces the need for innovative approaches to maintain a stable and reliable energy supply—enter the concept of flexibility.

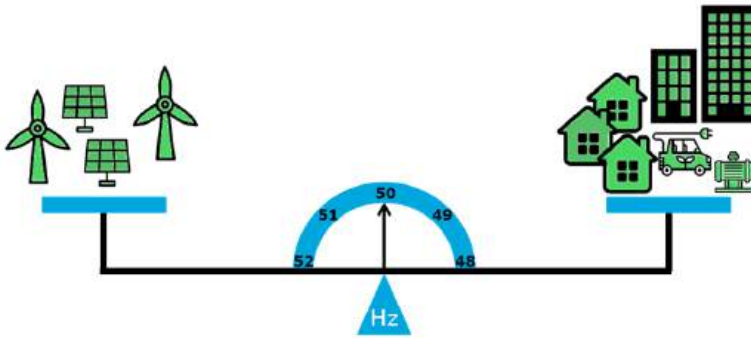


Figure 1.2: A depiction of the challenge of balancing the electricity grid. It is a metaphor for how renewable electricity supply (left) is balanced with demand (right) in order to maintain a grid frequency of 50 Hz.

1.2.1. DEMAND RESPONSE

Demand Response (DR) refers to the changes in electric usage by end-use customers from their normal consumption patterns. These signals are achieved through prices that reflect scarcity of supply and marginal cost of production. The variable supply of renewables leads to changing electricity prices over time, and induce lower electricity use at times of high market prices. The *Transmission System Operator* (TSO) and *Distribution System Operator* (DSO) can send activation signals to flexible assets when grid reliability is jeopardized to prevent system failure. By enabling dynamic adjustments of demand, DR contributes to the grid's stability, reduces the need for peak generation capacity, and optimizes energy costs for consumers. European spot markets are designed to incen-

tivise consumers to adjust their energy usage in response to variable prices, giving DR its business case. By incorporating DR into energy systems, consumers can leverage market mechanisms to achieve a more resilient, cost-efficient, and sustainable energy system.

Besides leading to cost-efficiency, DR helps renewable integration through the merit-order effect as depicted in Figure 1.3. The merit-order describes the activation order of electricity production sources by their marginal cost of production. As demand increases, the necessary generation capacity to fulfil demand increases, requiring a new and more expensive source to start producing electricity and driving up the electricity price. By actively steering consumption towards low electricity prices, consumers automatically aim for a higher share of renewables in the mix, potentially preventing more polluting sources further down the merit order from being activated.

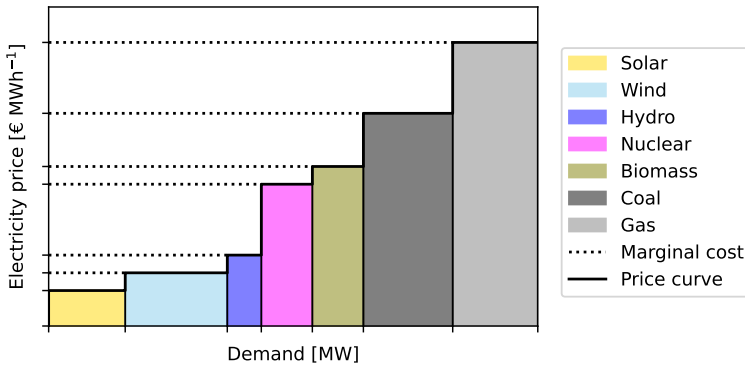


Figure 1.3: The merit-order curve where electricity production sources are activated in order of their marginal cost of production, and thereby shapes the price-volume curve. The bar width indicates the available generation capacity of different electricity sources, whereas their height represents their marginal cost of production.

Figure 1.4 shows a toy example of how flexibility can be exploited to minimize energy costs for a given consumer. In this example, we compare a demand profile that is applied when there a fixed price scenario with DAM and IDM optimised energy demand. We constrain the maximum power to be 3.5 kW, the minimum power to be 0.5 kW, the maximum ramp rate to be 0.75 kW per hour, and the total energy consumption to be the same for all scenarios. The demand is redistributed by optimizing hourly demand over DAM prices, realizing 22.8% energy cost savings compared to the original demand. After DAM closure, re-optimizing the demand over the IDM prices leads to a total of 56% cost decrease. In this toy example, there is a single opportunity to capitalize on price differentials between the DAM and IDM; in reality, this differential varies throughout time, leading to multiple trading opportunities for the same energy.

1.2.2. UNCERTAINTY & OPERATIONAL CHALLENGES

In the previous sections of this Introduction, we show that many available mechanisms (markets, balancing, and congestion) can benefit from DR strategies. Opportunities

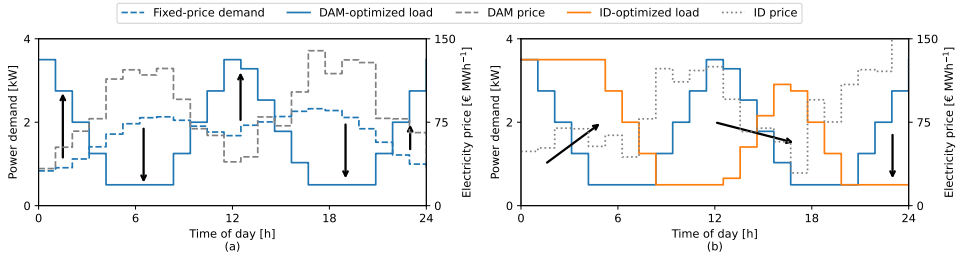


Figure 1.4: Toy example of a user that has peak demand in mornings and early evenings. This user, however, can optimize operations as it has inherent flexibility in its system. This flexibility is exploited by optimising demand over (a) DAM and (b) IDM prices. The arrows indicate how the optimized load differs from the initial schedule with the same total energy use, constrained minimum and maximum demand, and constrained ramping.

might arise from different markets and mechanisms simultaneously. Including more markets increases the complexity of decision-making and the sources of uncertainty for participants. Still, it is likely to amplify the business case for DR since it is possible to capitalize on opportunities in separate processes of the electricity system, as shown in the toy example in Figure 1.4. Portfolio optimization on both the DAM and IDM allows for the exploitation of day-ahead forecast inaccuracies in the market, with multiple possible opportunities before delivery. As numerical weather models give updates every few hours, expected conditions can change with every new update, leading to new trading opportunities.

Different combinations of mechanisms require customised control that can make trade-offs between the various opportunities. This gets complicated by the operational uncertainty in prices or activation signals. Figure 1.4 shows a two-step optimization using a single price-curve for each market. Including multiple mechanisms would require a constant trade-off for profitability, while the signals or prices can be subject to high volatility and uncertainty. At the same time, in the case of DR from complex systems, there are likely local processes, also affected by uncertainty, that constrain the load profile and limit the flexibility.

One approach for controlling processes under operational uncertainty is ‘predict-and-optimise’ [10], where prices or activation signals are forecast and used to optimise decisions or portfolios based on the most recent knowledge. However, a strategy relying on forecasts must also cope with forecast errors. These errors involve financial risk through market participation at disadvantageous times, uncertain net demand or supply, and physical risk in user processes or grid infrastructure.

In DR, the uncertainty emanates from weather phenomena, fossil fuel markets, fluctuating demand, and, consequently, electricity prices and activation signals. Since many energy management activities are currently performed on a day-ahead basis, the expected day-ahead forecast error plays a large role in real-time management, for example, through the IDM where *Balance Responsible Parties* (BRPs) correct their positions.

This unpredictability and complexity call for enhanced predictive models that adequately reflect the operational uncertainty given the latest information. Moreover, integrating stochastic optimization methods into DR strategies can mitigate the risks associated with operational uncertainty. These methods enable the consideration of multiple possible future scenarios in the decision-making process, thus providing a more comprehensive strategy that accounts for a wide range of outcomes. By adopting a probabilistic approach to forecasting and optimization, stakeholders can better prepare for and adapt to the inherent volatility associated with RES and demand fluctuations and the operational risk involved in their processes.

The increased complexity in operational decision-making under varied sources of uncertainty motivates this thesis to explore operational uncertainty quantification and risk management methods. It proposes methods to capture dependencies between weather, markets, and control decisions, and shows how to exploit these in control. By unlocking DR potential from assets without violating local constraints, this thesis aids with integrating variable renewable energy into the energy system.

1.3. THE DUTCH WATER-ENERGY NEXUS

The water-energy nexus represents the interdependent relationship between water and energy management. It is an active area of study in the pursuit of sustainable development, capturing the intersections across various fields, including drinking water supply [11], heating systems [12], and electricity generation [13], each showing their unique ways that water and energy are intertwined.

Historically, the Netherlands has been utilizing windmills to pump water and manage water levels within networks of canals, dykes, and polders. The transition to fuels-based and electric pumping stations offered more reliable, controllable, and thereby faster-responding water management systems. Besides enhancing the efficiency of managing the Netherlands' water systems, it also caused a growing interdependence between the water and energy sectors.

This thesis evaluates the water-energy nexus within the context of the Netherlands' open canal systems, exploring how this historic and critical infrastructure can be optimized to support the country's energy transition goals.

1.3.1. ENERGY TRANSITION STATUS

The Netherlands has set ambitious environmental targets, outlined in the National Climate Agreement and the EU Green Deal. These frameworks collectively aim to substantially reduce carbon emissions by 2030 and establish a carbon-neutral energy system by 2050. Recent statistics reveal a promising trajectory towards these goals, with RES having a significant presence in the Dutch energy system. In 2022, renewable electricity's contribution rose by 20% from the previous year, accounting for 40% of the country's total electricity production [14]. Arguably, the COVID pandemic's role in the electricity consumption patterns also affected the statistics. The share of renewable energy in the Netherlands' final energy consumption has also seen an uptick, reaching 15% in 2022. Solar energy, in particular, witnessed a 45% increase in consumption due to the substantial rise in installed capacity, now exceeding 19 GW. Wind energy production capacity

grew by 14% in the same period, with onshore wind energy being the larger share [15].

Despite these positive trends, challenges remain in meeting the 2030 target of a 49% reduction in *greenhouse gas* (GHG) emissions set by the Climate Act [16]. The Netherlands faces the task of significantly accelerating its efforts in renewable energy deployment and GHG emissions reduction to align with these ambitious goals. The transition away from natural gas, especially with the phase-out of Groningen gas production, further increases the urgency for alternative energy solutions and the reinforcement of renewable energy infrastructures [17]. The rapid integration of rooftop *photovoltaic* (PV) systems, driven by high electricity prices and net metering policies, has introduced substantial stress on the national grid, leading to imbalances and congestion. TenneT, the Dutch TSO, mentions that flexibility is a key building block for a reliable and affordable grid [18].

1.3.2. THE WATER MANAGEMENT SYSTEM

The Netherlands is a low-lying country in the Rhine-Meuse delta, with the rivers Rhine, Meuse and Scheldt flowing through it. A large part of the country lies below mean sea level, making managing water levels of local and national waterways necessary. The water levels and type of management (fixed, flexible or dynamic) are decided locally, by a waterboard, for the smaller canals. Nationally, the Dutch Ministry of Infrastructure and Water Management, *Rijkswaterstaat* (RWS), determines water levels typically based on agricultural needs, land-subsidence mitigation, shipping requirements and flood risk. Many of these canals are controlled with *Model Predictive Control* (MPC), which still is an active research topic in water resources management [19].

Water system control involves a sophisticated infrastructure network that redirects, stores, and pumps excess rainfall from below-sea-level areas to the North Sea. This system operates in stages: from drainage canals in polder areas to main drainage canals, and finally out to rivers or the sea. Managing this water system currently consumes approximately 147 GWh of electricity annually [20]. However, with the anticipated rise in sea levels, groundwater seepage and pump head are expected to increase, leading to a corresponding rise in the operational energy consumption of the water system [21].

Designed to withstand extreme weather events, the system's capacity for significant water level increases provides a buffer in critical times. Incorporating variable speed pumps offers additional flexibility, enhancing energy use efficiency within the water system [11]. Allowing for more dynamic water levels in everyday cases would increase the flexibility in pump scheduling and unlock DR strategies. It could be used to reduce the CO₂ emission caused by the pumping stations' electricity consumption during the energy transition, and could contribute to stabilising the Dutch electricity grid and energy system.

The Dutch water system has an installed pump capacity of 200 MW and potential energy storage of 1700 MWh in the canals [22]. By harnessing the inherent flexibility within the water management system, the Netherlands has an opportunity to pioneer by optimizing its necessary pump usage to facilitate the energy transition. This approach echoes the historical practice of "pumping when the wind blows," illustrating a full-circle moment where traditional methods merge with modern technologies to address environmental challenges.

1.4. THIS THESIS

In this thesis, we seek to unlock flexibility potential in the energy system with a probabilistic and risk-aware control framework. By examining the operational flexibility of electric pumping stations and their role in the broader energy system, this thesis aims to contribute to a more sustainable and integrated approach to managing the interdependencies between water and energy in the Netherlands. However, the proposed techniques in this thesis are not limited to operational water management and could be applied in any operational control under uncertainty.

This thesis aims to answer the question

How to exploit flexibility in energy-related processes such that benefits, in terms of reducing cost, CO₂ emissions, and increasing balance and congestion regulating volume, are generated while complying to localized constraints and objectives under uncertainty?

In answering this question, we build on the 'predict-and-optimize' approach and extend it to incorporate operational uncertainty. Special attention is paid to the Noordzeekanaal–Amsterdam–Rijnkanaal water system, a critical system for water defence controlled by a 6 MW pumping station, which is used to showcase DR applications from safety-critical systems.

1.4.1. CASE STUDY AREA FOR DEMAND RESPONSE

One main aspect of the Dutch water management system is the *Noordzeekanaal–Amsterdam–Rijnkanaal* (NZK–ARK). It's an intricate open canal system equipped with multiple undershot gates and has a pumping station at IJmuiden, which aids in consistently directing water into the North Sea, regardless of the sea's variable water levels. Water from four regional water boards flows into the NZK–ARK, helping in the redirection of excess rainwater. This water is methodically channelled or pumped out to the North Sea. A detailed representation of this water system, focusing on the inflow and outflow mechanisms, is provided in Figure 1.5.

At IJmuiden, the gate operations are dictated by specific water level differentials. They can be activated when there's a 16 cm water level difference and deactivated at 12 cm. This modulation is necessary to account for the contrasting densities of salt and freshwater, along with inherent system friction [23]. With automated controls in place, these gates have a maximum discharge rate of $500 \text{ m}^3 \text{ s}^{-1}$, a precaution to protect the foundation of the gate complex. The IJmuiden station incorporates six distinct pumps, with a combined maximum discharge of $260 \text{ m}^3 \text{ s}^{-1}$ and peak power consumption nearing 6 MW, underscoring the system's energy-intensive nature.

The NZK–ARK's considerable surface area, coupled with its variable water level capabilities and significant energy demands for pumping, positions it as an exemplary case for exploring DR strategies. However, given its critical role in the Netherlands' main flood defence infrastructure, any implementation of DR must not compromise flood risk management. In addition to that, the pumping station is positioned in a congested area of the grid [24], necessitating the adoption of sophisticated, reliable control techniques that can seamlessly integrate energy efficiency measures without undermining the system's primary purpose of flood protection.

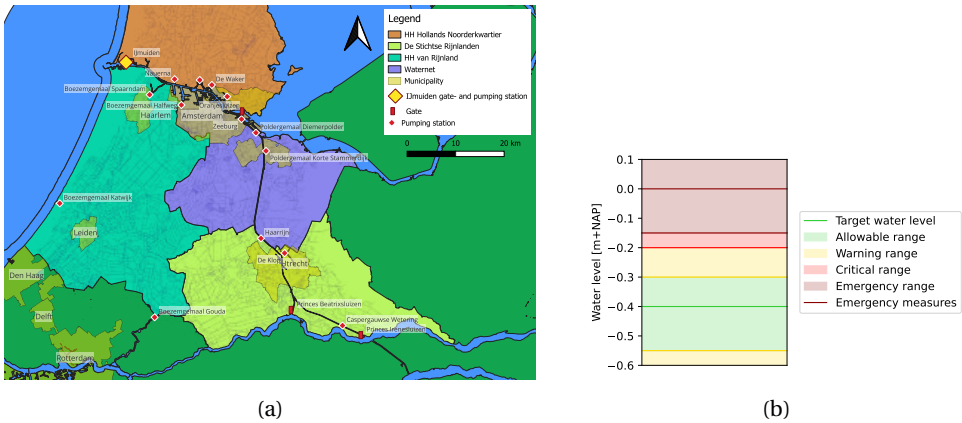


Figure 1.5: The Netherlands, Noordzeekanaal–Amsterdam–Rijnkanaal. a) The water management area of different local water authorities are shown by color. Pumping stations owned by local water authorities are shown by red diamonds, gate structures with red rectangles, and the IJmuiden gate- and pumping station with a yellow diamond. b) The water level regime of the NZK-ARK showing target ranges and warning/emergency levels.

1.4.2. THESIS STRUCTURE

Chapter 2 aims to answer the question: *What are the potential benefits in terms of cost reduction and CO₂ mitigation of applying DR strategies to safety-critical systems like water pumping stations?* This chapter explores the potential benefits of applying DR to the NZK-ARK, a critical piece of the Dutch water defence system and a large energy consumer. By formulating a new MPC problem, in which we propose a multi-market strategy, DAM and IDM prices are used to optimize energy-cost optimal pump schedules. Using Dutch and German market data over different years and variable renewable energy market penetration, we show that the potential benefits of applying DR are high, where up to 56% of cost savings can be made with perfect foresight. The difference between the German and Dutch markets indicates that as variable renewable energy market penetration increases, so does the potential profitability of DR. The analysis with perfect foresight serves as a benchmark for evaluating performance when considering operational uncertainty, and allows us to establish the benefits of multi-market DR separately from the predictive capacity of uncertainty models..

Chapter 3 asks: *What are effective methods for estimating operational uncertainty to improve control performance and decision-making in water and energy systems?* This chapter describes several methodologies applied to model operational uncertainty in multiple parts of this thesis. It details how neural networks are trained and optimized for forecasting purposes, what architecture is used to quantify uncertainty and generate probabilistic forecasts, a method for multi-distribution sampling with fixed correlation between variables is explored for the purpose of time series sampling, and a scenario-reduction method is proposed to condense a large uncertainty representation into an

optimal subset and sparse scenario tree representation.

Chapter 4 addresses the question: *How does European energy market integration impact DAM price forecasting, and what features improve the accuracy of these forecasts?* This chapter explores how data on European market integration can be used to inform DAM price forecasts. We perform an extensive analysis of features for national price forecasting models, giving insights into the mechanisms that make markets affect each other. We show that flexibility in the energy system could be important for the influence the system has on price settlement in a connected market. This knowledge is then used to develop a DAM price forecasting model, where EU market integration features are shown to improve forecasting accuracy of Dutch DAM prices with statistical significance. The findings in this chapter are later applied in Chapter 5 to investigate the effect of operational uncertainty in DR.

Chapter 5 examines: *How does operational uncertainty affect the performance of the DR strategies and control framework applied to the NZK-ARK system?* This chapter evaluates the performance of the operational forecasting and control framework, as defined in Chapter 2, when applied to the NZK-ARK case study area. We develop probabilistic forecasting models for the incoming pumped discharge, North Sea water level, and DAM and IDM electricity prices to be used in a stochastic MPC in a receding horizon fashion. We apply risk-aware constraint formulations for a computationally efficient and pragmatic trade-off between energy cost savings and water level violations.

Chapter 6 poses the question: *How can probabilistic irradiance forecasting models improve grid management and congestion mitigation in regions with high solar penetration?* This chapter showcases the potential application of earlier proposed uncertainty estimation tools in a different context than water resources management. We introduce RayCast, a spatially distributed Quantile Regression irradiance nowcast, that proficiently predicts irradiance quantiles using satellite data. We showcase its potential for grid management through a case study with Dutch DSO Alliander, where we improve the coverage percentage of a QR net-load forecast at a transformer station characterized by its high degree of solar penetration and grid congestion.

In Chapter 7, we summarize our conclusions and the societal impact of our work, and give suggestions on further research directions that would complement the work described in this thesis. The chapter ends with practical considerations for operational water resource management aimed at the Dutch sector and acknowledgements to people either directly or indirectly involved in this thesis.

This thesis describes a risk-aware framework for DR services under operational uncertainty. This framework is depicted in Figure 1.6, describing how the steps in the proposed framework are connected to the chapters in this thesis.

The mathematical notation applied in this thesis is specific to each chapter. Therefore, the meaning of the symbols used in the following chapter should be obtained from the corresponding text rather than from a different chapter.

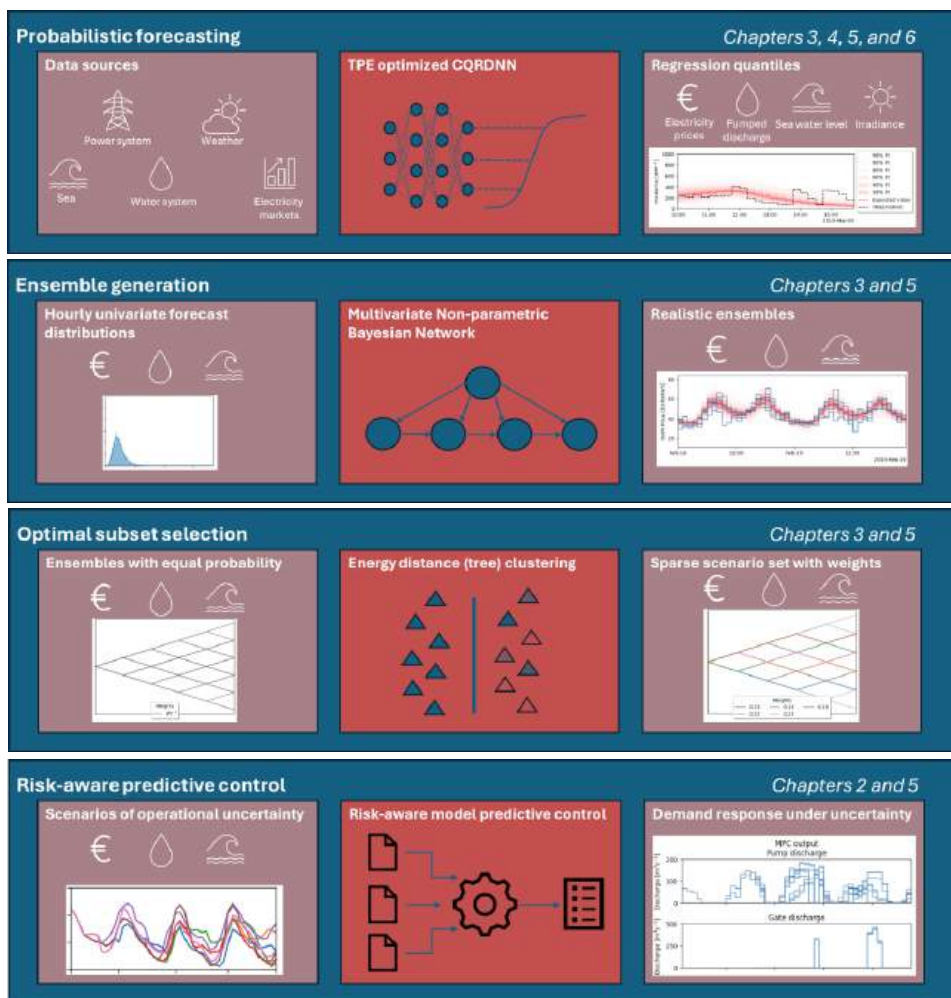


Figure 1.6: The proposed framework for DR under operational uncertainty and how it is connected to the chapters of this thesis.

BIBLIOGRAPHY

- [1] Sarah Brown and Dave Jones. *European Electricity Review 2024*. Tech. rep. Ember, 2024. URL: <https://ember-climate.org/insights/research/european-electricity-review-2024/#supporting-material>.
- [2] European Commission and Directorate-General for Communication. *European green deal – Delivering on our targets*. Publications Office of the European Union, 2021. DOI: [doi/10.2775/373022](https://doi.org/10.2775/373022).
- [3] Dan Tong et al. “Geophysical constraints on the reliability of solar and wind power worldwide”. In: (). DOI: [10.1038/s41467-021-26355-z](https://doi.org/10.1038/s41467-021-26355-z). URL: <https://doi.org/10.1038/s41467-021-26355-z>.
- [4] Jacques De Jong et al. *Improving the Market for Flexibility in the Electricity Sector*. Tech. rep. Centre for European Policy Studies, 2017, p. 30. URL: http://aei.pitt.edu/92294/1/CEPS%7B%5C_%7DTFR%7B%5C_%7DFlexibility%7B%5C_%7DElectricity%7B%5C_%7DMarkets.pdf.
- [5] European Commission and Directorate-General for Energy. *Clean energy for all Europeans*. Publications Office, 2019. DOI: [doi/10.2833/9937](https://doi.org/10.2833/9937).
- [6] EPEX Spot. *Single Intraday Coupling (XBID) Information Package*. Tech. rep. EPEX Spot, 2021.
- [7] TenneT. *Annual Market Update 2021*. Accessed: 2024-02-08. 2021. URL: https://tennet-drupal.s3.eu-central-1.amazonaws.com/default/2022-07/Annual_Market_Update_2021_0.pdf.
- [8] David Merino and Charles Esser. *Annual Report on the Results of Monitoring the Internal Electricity and Natural Gas Markets in 2019*. 2020. URL: <https://acer.europa.eu/sites/default/files/documents/Publications/ACER%20Market%20Monitoring%20Report%202019%20-%20Electricity%20Wholesale%20Markets%20Volume.pdf>.
- [9] *Infrastructure Outlook 2050*. Tech. rep. TenneT and Gasunie, 2022.
- [10] Adam N. Elmachtoub and Paul Grigas. “Smart “Predict, then Optimize””. In: *Management Science* 68.1 (Jan. 2022), pp. 9–26. ISSN: 1526-5501. DOI: [10.1287/mnsc.2020.3922](https://doi.org/10.1287/mnsc.2020.3922). URL: <http://dx.doi.org/10.1287/mnsc.2020.3922>.
- [11] R. Menke et al. “Extending the Envelope of Demand Response Provision through Variable Speed Pumps”. In: *Procedia Engineering* 186 (2017), pp. 584–591. ISSN: 18777058. DOI: [10.1016/j.proeng.2017.03.274](https://doi.org/10.1016/j.proeng.2017.03.274). URL: <http://dx.doi.org/10.1016/j.proeng.2017.03.274>.

- [12] Chelsea Kaandorp, Nick van de Giesen, and Edo Abraham. “The water use of heating pathways to 2050: analysis of national and urban energy scenarios”. English. In: *Environmental Research Letters* 16.5 (2021), pp. 1–11. ISSN: 1748-9326. DOI: [10.1088/1748-9326/abede7](https://doi.org/10.1088/1748-9326/abede7).
- [13] Jeroen Verhagen, Pieter van der Zaag, and Edo Abraham. “Operational planning of WEF infrastructure: quantifying the value of information sharing and cooperation in the Eastern Nile basin”. English. In: *Environmental Research Letters* 16.8 (2021). ISSN: 1748-9326. DOI: [10.1088/1748-9326/ac1194](https://doi.org/10.1088/1748-9326/ac1194).
- [14] Centraal Bureau van de Statistiek. *Renewable electricity share up by 20 percent in 2022*. 2022. URL: <https://www.cbs.nl/en-gb/news/2023/10/renewable-electricity-share-up-by-20-percent-in-2022>.
- [15] Centraal Bureau van de Statistiek. *Renewable energy share rose to 15 percent in 2022*. 2022. URL: <https://www.cbs.nl/en-gb/news/2023/22/renewable-energy-share-rose-to-15-percent-in-2022>.
- [16] Rijksoverheid. *Klimaatakkoord*. Tech. rep. Rijksoverheid, 2019. URL: <https://open.overheid.nl/documenten/ronl-7f383713-bf88-451d-a652-fbd0b1254c06/pdf>.
- [17] *The Netherlands 2020 Energy Policy Review*. Tech. rep. International Energy Agency, 2020. URL: <https://www.iea.org/reports/the-netherlands-2020>.
- [18] *Industrial flexibility is a key building block for a reliable and affordable grid*. Tech. rep. TenneT, 2021.
- [19] Xin Tian et al. “Efficient multi-scenario Model Predictive Control for water resources management with ensemble streamflow forecasts”. In: *Advances in Water Resources* 109 (2017), pp. 58–68. ISSN: 03091708. DOI: [10.1016/j.advwatres.2017.08.015](https://doi.org/10.1016/j.advwatres.2017.08.015). URL: <https://doi.org/10.1016/j.advwatres.2017.08.015>.
- [20] Ruben Dahm. *Energieverbruik nationaal en regionaal waterbeheer*. Tech. rep. Deltares, 2009.
- [21] Rens Kolkhuis Tanke et al. *Energievoorziening: beschikbaar, betrouwbaar en betaalbaar (E3B)*. Tech. rep. Stichting Toegepast Onderzoek Waterbeheer, 2023.
- [22] Ivo Pothof et al. *Slim malen*. Tech. rep. STOWA, 2019. URL: <https://www.stowa.nl/sites/default/files/assets/PUBLICATIES/Publicaties%202019/STOWA%202019-27%20slim%20malen%20defdefversie.pdf>.
- [23] H. Janssen. *Effect selectieve onttrekking IJmuiden op waterbeheer*. Tech. rep. Rijkswaterstaat, 2017. URL: https://www.platformparticipatie.nl/binaries/Effect%5C%20selectieve%5C%20onttrekking%5C%20IJmuiden%5C%20op%5C%20waterbeheer%5C_tcm117-377563.pdf.
- [24] *Capaciteitskaart afname elektriciteitsnet*. 2024. URL: <https://capaciteitskaart.netbeheernederland.nl/>.



2

PUMPING WHEN THE WIND BLOWS

This is where our worlds collide, this is where we come alive.

Koven

In this chapter, we propose the use of multiple electricity spot markets to enable price-based Demand Response for open canal systems in the Netherlands, where many large pumping stations are used for flood mitigation and control of groundwater levels. In the new strategy for pump-scheduling we combine the Day Ahead and Intraday electricity markets to be used in a hierarchical receding horizon economic Model Predictive Control (MPC). A cost analysis is performed for the potential of multiple market-strategies and the automatic Frequency Restoration Reserves, using actual market and water system data. We show new insights in the trade-off between CO₂ emissions and operating cost, the difference between the German and Dutch market, and temporal changes in market conditions and Demand Response profitability due to increased renewable energy market-penetration.

We observe that the German energy market is rewarding DR more than the Dutch equivalent, due to the higher renewable energy market penetration. The proposed multi-market strategy leads to a cost decrease of 10% and 16% in the Netherlands in 2017 and 2019, respectively. When applying German market scenarios, we found a cost saving potential of 56% and 50% in 2017 and 2019, respectively. The cost-saving potential for the aFRR-market was found to be up to 12% in the Netherlands and 28% in Germany, through a conservative analysis. The results suggest that the proposed control system, optimising costs over the day ahead, intraday and possibly the aFRR markets, is profitable compared to the current strategy in both the current and future electricity market.

Parts of this chapter have been published in the Journal of Hydroinformatics [1].

2.1. INTRODUCTION

2.1.1. DEMAND RESPONSE IN THE NETHERLANDS

With climate change mitigation as a driving force, *Renewable Energy Sources* (RES) are becoming a larger part of the energy mix [2]. The Netherlands has passed a climate law, in which the country commits to a 49% reduction of carbon dioxide (CO₂) emission by 2030 and 95% reduction by 2050 (compared to emission levels in 1990) [3]. Solar and wind energy are promising RES, and are becoming more profitable due to technological advancements. While these generating techniques are valuable for the energy transition, they bring some new challenges. One of these challenges is that the amount of energy generated at a certain time is as predictable as the weather. Big consumers will have to be more active when energy is available, and less when it isn't. The availability of energy is reflected in the price of flexible energy markets through scarcity of a product. This economic incentive to customers to shift energy use in time is known as *Demand Response* (DR) [4, 5].

Currently, energy prices are correlated with sustainable energy production, as shown in Section 2.2.2. When wind power generation peaks unexpectedly, the price of energy decreases. This price decrease can even result in negative energy prices since paying consumers can, at times, be less expensive than shutting down inflexible power plants. By consuming energy at the right time, money can be saved, or even earned by energy users; this gives DR a business case. DR can be enabled by participating in flexible energy markets, which give incentives to change energy usage through time-of-use pricing. Currently, these markets are changing to accommodate sustainable energy and flexibility in consumption [6].

Since the Dutch market currently has a low share of renewable energy, we take the German market as a representative of a future scenario for the Dutch market. Germany's energy mix is increasingly dominated by wind and solar energy [7], which are the same sources the Dutch energy transition is moving towards [8]. In addition, the market structures are relatively similar in the two countries. Both countries make use of a *Day Ahead Market* (DAM) and *Intraday Market* (IDM). However, the balancing services are not open for public participation in Germany; this has already been realised in the Netherlands, where any *Balance Responsible Party* (BRP) can participate in the imbalance market [9].

2.1.2. CURRENT STATUS OF DR APPLICATIONS

With rapid advances in intelligent electricity demand management systems and the growth of aggregators, many more energy users are participating in DR [10]. In fact, even power network expansion and renewable energy investment decisions have to explicitly consider a future with DR [11]. Currently, some new assets that participate in DR include drinking water systems and Heating, Ventilation and Air-Conditioning systems. The DR strategies applied mostly involve a DAM. However, there is still variation in strategy. Some research the economic potential of the IDM [12], while others combine the DAM with the IDM to optimise cost [13]. Considering multiple market mechanisms can significantly improve economic efficiency of DR [14]. This type of spot market-based DR is called time-of-use pricing and is part of the price-based DR class [5]. The potential cost- and emission-reduction through DR increases with renewable energy penetration [15].

DR strategies that include a short-term flexible energy market (like the IDM or market-based balancing services) typically use mixed-integer formulations of the optimisation problem to indicate buy/sell scenarios [5]. When studying DR literature, applications relate to energy markets in France [16], the UK [12], Canada [17], the USA [18], Denmark [13], and South-Africa [19]. The Dutch or German market is hardly ever taken as case-study. Some studies show the economic potential of the *Frequency Restoration Reserves* (FRR) for photovoltaic-battery systems [20], where a rule-based control was simulated with Dutch market data. FRR potential was also explored for heat pumps in Germany [21] by simulating with a rule-based control system. In [22], a stochastic *Model Predictive Control* (MPC) was applied in a simulation of residential heating, energy storage and community-integrated energy systems in order to explore the technical feasibility and economic potential.

In this chapter, we propose a new pump scheduling strategy that combines both the DAM and IDM, and consider scenarios with both the Dutch and German markets over two years. We analyse market data from both countries, showing the effect of renewable energy market-penetration on the correlation between the *carbon intensity* (CI) of electricity and the DAM price (Section 2.2.2). Actual open-source market data for the DAM, *automatic Frequency Restoration Reserves* (aFRR), and German IDM markets were used, and licensed Dutch IDM data was used. The MPC formulated (Section 2.3.2) results in a *Mixed Integer Quadratic Program* (MIQP), which is solved to near global optimality using Gurobi [23], and applied in a closed-loop simulation in receding horizon fashion. The MIQP formulation results from water system constraints that indicate pump- and gate-discharge possibilities, electricity market participation is formulated continuously. The proposed multi-market strategy is compared with a reference strategy, where energy use is minimised and energy is traded on the futures market for a monthly fixed price. The analysis was performed for the years 2017 and 2019 to show temporal changes in market conditions. More recent data was excluded to purely explore market changes due to the increase in renewable energy integration, and to exclude effects from the pandemic or the invasion of Ukraine. Besides participation in spot markets (Section 2.4.2), we present an estimate of the economic potential for participating in the aFRR market, for which the potential of successful activation for downward regulation is analysed (Section 2.4.3).

2.2. MARKET AND BALANCING MECHANISMS

We evaluate the following mechanisms for DR purposes: the DAM, IDM, futures market and aFRR market. Direct participation in the aFRR market is not simulated, but its potential is explored based on a post-analysis using actual aFRR activation data (Section 2.4.3) and MPC simulations with participation on the DAM and IDM (Section 2.4.2). Both the DAM and the IDM incentivise participants to adjust energy planning for favourable prices that reflect scarcity of supply and marginal cost of production. Minimising the operational cost of energy will lead to a shift in energy use when prices change, a mechanism known as price-based DR [5].

The German market is taken as representative for a future Dutch market. The German RES mix is similar to the planned future mix in the Netherlands [7, 8], while the countries have a similar market structure, climate and socio-economically driven electricity consumption patterns. Germany uses similar market mechanisms as the Nether-

lands, although the markets do differ in some rules and in volume. Alternative markets have significantly different conditions: Denmark has a relatively small market dominated by RES, the Norwegian system is dominated by hydropower generation, the French market is dominated by nuclear generation, the Belgian mix doesn't contain a high share of intermittent renewables, and the UK market contains a relatively low degree of interconnectivity with other markets. Therefore we deem the German market as most feasible representative for a future Dutch market.

Figure 2.1 shows the 2-Dimensional *Kernel Density Estimate* (KDE) of the Dutch (Figure 2.1a) and German (Figure 2.1b) DAM and IDM price over recent years. The price difference between the two markets causes change in the scheduled energy use or production. The distribution of the Dutch prices is varying more over the years than the distribution of the German prices. A possible explanation is the maturity of the markets: the German market is more mature in volume and therefore possibly more stable.

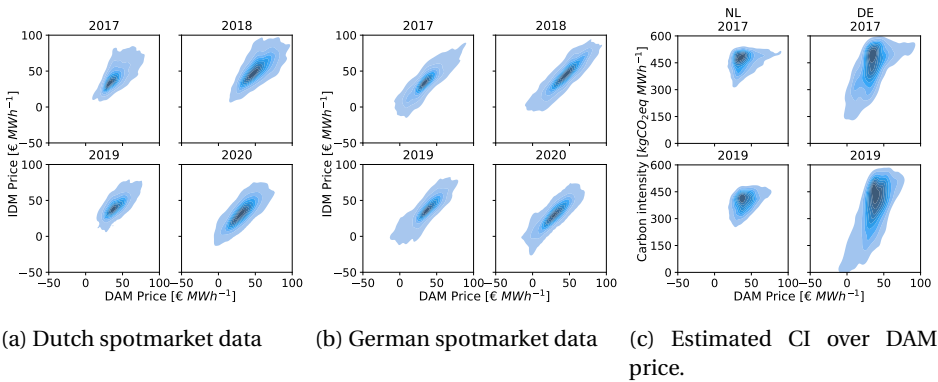


Figure 2.1: 2-Dimensional KDE of the Dutch (a) and German (b) DAM and IDM price, and the estimated CI over the DAM price (c). Darker color indicate a higher empirical probability.

2.2.1. GRID BALANCING MECHANISMS

The integration of RES has introduced a growing complexity in energy systems, leading to the need for advanced balancing mechanisms to minimize energy imbalances. Short-term trading and flexibility in energy use have been identified as effective strategies to address this challenge. The Dutch *Transmission System Operator* (TSO), TenneT, is responsible for balancing the grid. It does so by employing balancing mechanisms, like the imbalance market. Because large volumes of energy cannot yet be stored with economic efficiency, power supply and demand have to be matched continuously. Imbalance on the grid can negatively affect power quality or can eventually result in damage to the infrastructure itself. TenneT balances the grid using back-up (emergency) production capacity or asking producers to reduce production. Another option is to ask large consumers to in- or decrease consumption, which is currently being applied to greenhouses, hospitals, and small industries. Demand-side balancing of the grid is mostly

implemented using automated control, powered by a near-real-time feed of the imbalance and energy price [9].

Positive contributions to the imbalance are rewarded, while negative contributions will be penalized. This is called 'passive contribution', and the feed is freely available while BRPs act on this market automatically [24]. Participation in the imbalance market requires strategic energy consumption, a challenge for operations with fixed ramp-up times like pumping stations, indicating a need for tailored solutions. Therefore, imbalance should be minimized using short-term trading and flexibility in energy use, reflecting the growing complexity introduced by the integration of RES and the need for advanced balancing mechanisms.

Positive contributions to the imbalance are rewarded, while negative contributions will be penalised. This is called 'passive contribution', and the feed is freely available while BRPs act on this market automatically [9]. To act profitably on the imbalance market, the balancing party would want to consume as much energy as possible within 15 minutes. For a pumping station like the one in IJmuiden, which takes about 15 minutes to boot-up and then preferably keeps running for at least one hour, participation on the the imbalance market would probably result in minimum financial gains or even losses. Therefore, imbalance should be minimised using short-term trading and flexibility in energy use.

The aFRR is a reserve capacity market used to restore the grid frequency automatically when deviations from 50 Hz occur. In this market, BRPs can bid for upward regulation or downward regulation. Bidding is done in 15-minute blocks, and the BRP gets a 15-minute notice before activation. This market would be feasible for a pumping station to participate in, due to the 15-minute ramp-up time. The aFRR does constrain its participants to a minimum bid of 1 MW, a constraint that can be avoided by partnering with an aggregator that combines multiple small bids into larger bids. Figure 2.2 shows the probability of occurrence of downward activation on the aFRR market for certain downward regulating prices and activation sequence lengths. The German market shows a higher profit potential for downward regulating services. Interestingly, the data shows small differences over the years, indicating that the increase in renewable energy generation does not increase the demand for downward regulation through the aFRR. The IDM, which is more easily accessible to BRPs, might be providing the necessary balancing while allowing BRPs to mitigate risks of trading for disadvantageous prices.

2.2.2. CARBON INTENSITY OF GRID ELECTRICITY

Optimising on energy costs can lead to a decrease in emitted CO₂ [15] due to the correlation between sustainable energy production and energy price. Two national markets are evaluated: the Dutch and the German market. The Netherlands has a low share of RES, while the German energy mix contains a larger share. The merit-order effect, where RES with low marginal costs of electricity are activated before more polluting sources with higher marginal costs, increases the correlation between CI and energy price in the German market.

Due to incorrect *European Network for Transmission System Operators in Europe* (ENTSO-E) Electricity generation by source time series, a CI time series of the grid was not easily estimated. First, historic solar and wind generation time series are calculated using

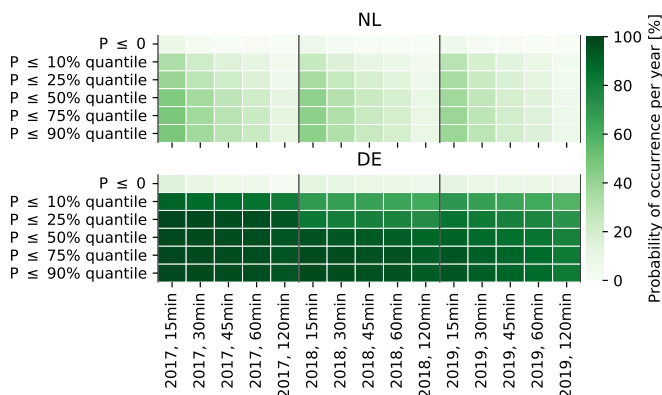


Figure 2.2: Probability of occurrence of downward activation through the aFRR market. The figure shows the percentage of time at which downward activation occurred in color, the year and the length of the activation sequence (15min, 30min, 45min, 60min) on the x-axis. On the y-axis is the downward regulating price at ≤ 0 , or less than a quantile value of the DAM prices that year.

'Renewables.Ninja' capacity factor time series [25, 26] for both the Netherlands and Germany. The yearly installed capacities were linearly interpolated over time in order to have time series of installed capacity. The resulting renewable energy generation time series are corrected with the yearly produced renewable energy volumes by scaling the time series to match the reported yearly produced generation volumes. For every hour, the emitted carbon from renewables is calculated based on the CI of electricity produced by renewable sources [27, 28]. The total emitted carbon per year is then calculated using the load and the reported yearly averaged CI [29, 30]. The yearly emitted carbon from renewables is then calculated, and subtracted from the total emitted carbon. Consequently, the emitted carbon from non-renewable sources remains. The yearly average 'rest' CI is calculated using the previously calculated non-renewable carbon emission, and the amount of load not supplied by renewables. The yearly averaged CI is then linearly interpolated over the intermittent dates to a 'rest' CI time series. The CI time series of all generation is consequently calculated by dividing the emitted carbon at each hour by the load.

Figure 2.1c shows the estimated CI of the two national grids plotted over the DAM prices for 2017 and 2019. For both considered markets, a correlation can be seen between the DAM price and the CI of energy. In Germany, the spread of the CI is larger than in the Netherlands. The Netherlands contains relatively efficient coal- and gas-fired power plants, while Germany still uses brown-coal plants to produce electricity to some degree [31]. Also, Germany has a larger share of renewables which at some times can even fulfill all the electricity demand, leading to a strong correlation between DAM prices and CI.

Table 2.1: Pump power and discharge curves [33].

Pump	RPM/Discharge	Q-dH relationship [m ³ /s], [m]	P-dH relationship [kWh], [m]
1&3	n = 64.3 rpm	$Q = -5.4174 \cdot dH + 44.93$	$P = 208.08 \cdot dH + 536.85$
	n = 64.3 rpm	$Q = -5.4174 \cdot dH + 44.93$	$P = 208.02 \cdot dH + 536.85$
2&4	n = 48.2 rpm	$Q = -6.4977 \cdot dH + 33.149$	$P = 192.36 \cdot dH + 217.26$
	n = 50 m ³ /s	$Q = -1.9822 \cdot dH^2 + 1.9726 \cdot dH + 44.93$	$P = 443.91 \cdot dH + 476.3$
5&6	n = 40 m ³ /s	$Q = -1.8544 \cdot dH^2 + 7.774 \cdot dH + 44.93$	$P = 379.09 \cdot dH + 373.18$
	n = 30 m ³ /s	$Q = -7.1021 \cdot dH + 48.164$	$P = 282.97 \cdot dH + 417.32$

2.3. METHODS: MODELLING THE WATER SYSTEM AND DR PARTICIPATION IN THE CASE STUDY AREA

We apply the multi-market strategy to the water system of the NZK-ARK. The NZK-ARK is a complex open canal system, containing multiple undershot gates and a pumping station at IJmuiden to enable the discharge of water into the North Sea, whether the sea water level is high or low. The system receives water from four waterboards (local water authorities) who discharge excess rainwater into the system, which is then pumped or sluiced out to the North Sea. The NZK-ARK is also used for ship traffic, which imposes a strict lower and upper bound on the water level. These constraints prevent cargo-ships from hitting the bottom and to make sure ships can pass bridges. Figure 1.5a shows the water system and its incoming and outgoing fluxes.

At IJmuiden, the gates are opened at a difference in water level of 16cm, and closed at 12cm [32]. This difference in pressure is needed to overcome the difference in density of fresh and salt water together with internal friction. The gate is controlled automatically and has a maximum discharge of 500 m³s⁻¹, resulting from a physical constraint to ensure stability of the bed of the gate-complex. The pumping station in IJmuiden contains six pumps, with a combined maximum power consumption of around 5 MW. The pumps can only pump up to a certain water level difference, when the height differential is too high they will automatically shut down. Currently, pumping station IJmuiden is controlled through an MPC that minimises energy use while energy is bought on the futures market. In this MPC, the prediction horizon is 24 hours, and the water level is kept between -0.3m+NAP and -0.5m+NAP. For DAM participation, a prediction horizon of at least 36 hours is necessary to submit a full bid before market closure. In this chapter, a prediction horizon of 48 hours was applied to investigate the economic potential of DR for the water system.

Table 2.1 contains the Q-dH (discharge - pump height), and P-dH (power - pump height) relationships for each of the six pumps. To solve a single MPC problem for the whole pumping station, we formulate a single simplified Q-dH curve by using the separate Q-dH curves for the pumping station as described in Section 2.3.3. We used the P-dH curves in Table 2.1 to formulate a single equivalent PQH-curve for the pumping station, which describes pump power consumption as function of pump discharge and pump height. The novel method we have applied to formulate the representative PQH-curve is described in Section 2.3.3.

2.3.1. WATER SYSTEM MODELLING

In the MPC's internal model, we represent the canals of the system as simple storage components: i.e. a bucket with a fixed surface area that is used to describe the relationship between storage and water level in the canals. A similar model is currently being applied in the control system of the NZK-ARK. Large depth and width cause low flow speeds to occur, resulting in negligible friction [34]. The incoming fluxes are the water-board discharge and the discharge measured in Maarsse, the outgoing fluxes are the pump- and gate-discharge into the North Sea. Delay or routing is not taken into account and is assumed negligible due to the low flow speeds taking place in the system, leading to negligible friction.

The gate-complex in IJmuiden has 7 square tubes, which contract in the middle to regulate discharge. They are 5.9m wide and the height of the "throat" of a tube is 4.8m above the bottom. It has a maximum discharge of $500 \text{ m}^3\text{s}^{-1}$, imposed for the stability of the bed and structure [35]. These seven square tubes can be (partially) closed to regulate the flow. The equation describing its behaviour is [36]

$$Q_{max}[t] = n \cdot \alpha \cdot B \cdot h_k \cdot \sqrt{2 \cdot g \cdot (h_i[t] - h_o[t])}, \quad (2.1)$$

with $Q_{max}[t]$ as the maximum discharge at time t , n the amount of tubes, α the contraction coefficient, B the width of a tube, h_k the height of the center of the tube, g the gravitational constant, $h_i[t]$ the water level of the NZK at time t and $h_o[t]$ the water level of the North Sea at time t .

The pumping station in IJmuiden consists of 6 pumps: two fixed-speed pumps, two pumps with two settings, and two variable speed pumps. The combined maximum discharge is $260 \text{ m}^3\text{s}^{-1}$. The pumping station is modelled by simplifying it to a single pump. Pump-characteristics are combined to estimate the equivalent characteristics. Since there are 6 pumps present in the pumping station, with different properties, multiple Q-dH curves and power-curves are used to describe the station. Table 2.1 shows these curves for all three types of pumps present in the station. To account for the effect of the wind on the water level, wind data of the *Royal Netherlands Meteorological Institute* (KNMI) station in IJmuiden has been used to estimate the water level change.

We solve the MPC problem to determine the optimal control settings for multiple gates and the pumping station at IJmuiden. The gates and pumping stations are represented using a single gate and single pump with an aggregated Q-dH and QPH-relationship.

2.3.2. ECONOMIC MPC FORMULATION WITH MULTIPLE MARKETS

We propose a two-stage MPC for participating in DR through the use of both the DAM and IDM. The MPC involves buying energy on the DAM for 24 hours and then iteratively deciding on how to deviate from this plan based on rewards on the IDM. As such it solves two optimisation problems in a receding horizon fashion subject to physical constraints for the water system. IDM trading occurs with a shrinking horizon stretching until the next DAM-bid is made. The combination of both the DAM and IDM has been shown to significantly improve performance compared to participating in a single market [14]. While the other alternative, the current strategy involving the futures market, does not reward flexibility in consumption.

The two-stage MPC applying the multi-market strategy is compared to a reference scenario without DR, where energy use is minimised and energy is purchased for a fixed price on the futures market.

Two objective functions belong to the proposed multi-market strategies, where an objective function is formulated for both the day ahead planning and the intraday trading phase. A third objective function is applied in the reference strategy without DR. For the DAM planning, an indication of the hourly prices of the next day is needed. In this research we have assumed perfect knowledge, where we minimise costs based on the observed prices to estimate economic potential for DR participation. In future work we will include probabilistic forecasts of the DAM and IDM price, for example by generating price scenarios and apply tree-based MPC [37]. The economic objective function for DAM bidding is

$$\min J_1 := \underbrace{\sum_{t=0}^N (P[t] \cdot \frac{\Delta t}{\gamma_c} \cdot c_{da}[t])}_{\text{day ahead bid}}, \quad (2.2)$$

where

$$P[t] := a_p \cdot Q_p[t]^2 + b_p \cdot dH_p[t]^2 \cdot Q_p[t] + c_p \cdot Q_p[t] \cdot dH_p[t], \quad (2.3)$$

$$dH_p[t] := h_{ns}[t-1] - h[t-1] - dh_w[t-1], \quad (2.4)$$

and $P[t]$ is the pumping power in kW, Δt the timestep size in seconds, γ_c is used to convert kW to MWh, c_{da} is the DAM price in [€/MWh], t is the timestep index, N is the prediction horizon length in number of timesteps, a_p , b_p , c_p are the fitted parameters for the pump power-curve, dh_w and h_{ns} stand for the increment of water level at the gates and pumps due to wind effects and the water level of the North Sea, respectively.

The IDM allows for extra flexibility since the market allows trading up to 5 minutes before consumption. This makes the IDM a valuable addition to the DAM, since unforeseen external disturbances on the water system could be made up for or exploited by trading the energy surpluses or deficits during the day. We used the ID3 IDM price, which is the volume weighted price of a certain delivery hour in a 3 hour window preceding delivery. The economic objective function used for IDM trading is

$$\min J_2 := \underbrace{\sum_{t=0}^{t_d} ((P[t] \cdot \frac{\Delta t}{\gamma_c} - E_{plan}[t]) \cdot c_{id}[t])}_{\text{intraday trading}} + \underbrace{\sum_{t=t_d}^N (P[t] \cdot \frac{\Delta t}{\gamma_c} \cdot c_{da}[t])}_{\text{day ahead bid preparation}}, \quad (2.5)$$

where $E_{plan}[t]$ the energy bought on the DAM for time t , c_{id} the IDM price, t_d the timestep at which the next DAM bid starts. The first term allows for IDM trading, where deviations from the DAM bid are allowed at IDM prices for the time a DAM bid has been made (until t_d). The second term prepares the next DAM bid (starting at t_d) where costs are minimised based on DAM prices for the remaining length of the prediction horizon (N).

We compare the proposed multi-market strategy with a reference strategy where energy is bought on the futures market for a monthly fixed price. In the reference strategy,

the objective is to minimise energy use of pumping, resembling the current strategy employed by RWS. The objective function for the reference scenario is

$$\min J_3 := \underbrace{\sum_{t=0}^N P[t] \cdot \frac{\Delta t}{\gamma_c}}_{\text{energy use minimisation}}, \quad (2.6)$$

with $P[t]$, Δt , N and γ_c as defined above.

2.3.3. WATER SYSTEM CONSTRAINTS

There are various safety and performance constraints (e.g. water level and discharge limits) that need to be dealt with explicitly by the model predictive controller.

Although the lower bound on water level is a strict constraint for transport purposes, it may be tolerable to marginally violate the upper bound for small time periods. Therefore, the upper bound of the water level constraint was relaxed with a slack variable, and a penalty for exceeding the upper bound was introduced in the objective function. This was done to improve robustness of the computational model, so the problem would not become infeasible in high-water situations but rather the small violations could be analysed a posteriori. The lower and upper water-level bound constraints are reformulated as

$$h[t] \geq h_{min}, \quad (2.7)$$

$$h[t] \leq h_{max} + s[t], \quad (2.8)$$

where the discretised slack variable $s[t]$ represents the constraint violations on the maximum water height h_{max} at timestep t . The upper bound relaxation is implemented as a lazy constraint, meaning it is only active when a constraint violation on the un-relaxed upper-bound occurs. The penalty function

$$f_1(\cdot) := \gamma_s \cdot \sum_{t=0}^N s[t]. \quad (2.9)$$

sums up the discrete slack variables (i.e. bound violations per timestep), which automatically minimises the time and magnitude of constraint violations. This is added to the economic cost in the MPC optimisation problem in Equation (2.4), Equation (2.5) and Equation (2.6). The constant γ_s was chosen a posteriori to be sufficiently high, in order to prevent compromises between energy costs and constraint violation.

The water level associated with a given storage is calculated using a mass balance: the difference in water level is equal to the net flux that leaves or enters the body, divided by the surface area of the wetted water body. Because water is assumed in-compressible, a mass balance can be expressed in terms of volume

$$h[t] = h[t-1] + \frac{\Delta t}{A_{nzk}} * (Q_{in}[t-1] - Q_g[t-1] - Q_p[t-1]), \quad (2.10)$$

where $h[t]$ is the water level of the NZK-ARK at time t in m+NAP, Δt the timestep size in seconds, A_{nzk} the surface area of the NZK-ARK in m^2 , $Q_{in}[t]$ the incoming discharge of

the ARK (the discharge in Maarsse, water coming from the Oranjesluizen and pumped discharge from the waterboards) at time t in m^3/s , $Q_g[t]$ the discharge from the gates, and $Q_p[t]$ the discharge of the pumping station in IJmuiden at time t in m^3/s .

The gates can only discharge when the water level of the North Sea is lower than the water level of NZK-ARK, and the pumping station can only discharge when the water level of the North Sea is higher than the water level of the NZK-ARK. To ensure this, a big-M formulation is applied. Two binary variables, z_g and z_p are introduced, which indicate the possibility of using the gates or pumping station, respectively

$$h[t] - h_{ns}[t] - dH_{g,min} + (1 - z_g[t]) \cdot M_g \geq 0, \quad (2.11)$$

$$h[t] - h_{ns}[t] - dH_{g,min} - z_g[t] \cdot M_g \leq 0, \quad (2.12)$$

$$h_{ns}[t] - h[t] - dH_{p,min} + (1 - z_p[t]) \cdot M_p \geq 0, \quad (2.13)$$

$$h_{ns}[t] - h[t] - dH_{p,min} - z_p[t] \cdot M_p \leq 0, \quad (2.14)$$

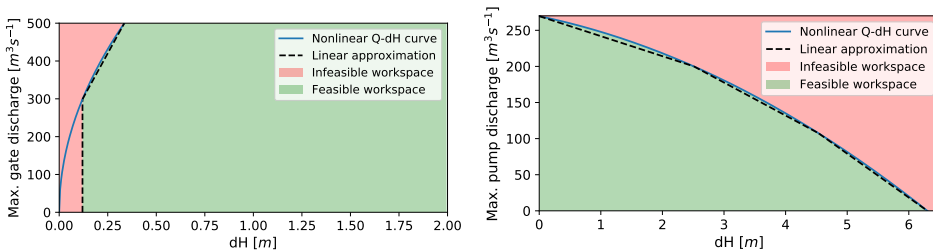
where h_{ns} is the water level of the North Sea, $dH_{g,min}$ the minimum water level difference needed to discharge with the gate, and $dH_{p,min}$ the minimum water level difference needed to discharge with the pumps. The big-M constants, M_g and M_p were chosen sufficiently large.

The discharge of the gate is a decision variable in the optimisation problem. The gate discharge relationship in Equation (2.1) was simplified through *piecewise linearisation* (PL). The feasible gate discharge region and the PL can be see in Figure 2.3a. The majority of the feasible region is constrained by the upper bound on gate discharge, rather than the Q-dH relationship. The gate discharge is bound to $[0, 500]$, and the upper bound on gate discharge is multiplied with the binary variable z_g that indicates gate discharge possibilities

$$Q_g[t] \leq (a_g \cdot dH_g[t] + b_g[t]) \cdot z_g[t], \quad (2.15)$$

$$dH_g[t] := h[t] - h_{ns}[t], \quad (2.16)$$

with $Q_g[t]$ being the gate discharge at time t , and a_g and b_g being the fitted parameters for the PL of the upper bound on gate discharge.



(a) Q-dH relationship for the undershot gates. (b) Q-dH relationship for the pumping station.

Figure 2.3: Feasible (green) and infeasible (red) region for the discharge from undershot gates (a) and the pumping station (b) in IJmuiden.

Pump discharge capacity given a certain pump height is generally described through the use of Q-dH curves, where the (maximum) discharge is a function of the pump height. In the case of IJmuiden, six pumps are present with different curves describing their maximum discharge as a function of pump height. In order to represent the pumping station as one big pump, the different Q-dH relationships of the 6 separate pumps found in Table 2.1 are aggregated. For a given water level difference dH_p , the maximum discharge of the six pumps combined is equal to the sum of the maximum discharges for the individual pumps

$$Q_p[t] \leq \sum_{i=1}^6 Q_i(dH_p[t]), \quad (2.17)$$

$$dH_p[t] := h_{ns}[t] - h[t], \quad (2.18)$$

with $Q_p[t]$ being combined pump discharge for the pumping station, and Q_i the maximum discharge of pump i as function of the pump-height dH_p . The resulting quadratic description of the Q-dH relationship is approximated through PL, as shown in Figure 2.3b. The PL is applied as an upper bound constraint on pump discharge, where the total upper bound is multiplied with the binary variable z_p indicating pump discharge possibilities

$$Q_p[t] \leq (a_p[i] \cdot (h_{ns}[t] - h[t]) + b_p[i]) \cdot z_p[t] \text{ for } i \in (1, 2, 3), \quad (2.19)$$

with a_g and b_p representing the coefficients of the PL-approximation of the Q-dH relationship.

In practice, the power consumption of the pump station can vary, depending on multiple operating conditions like pump configuration, pump height and discharge. The derived Q-dH curve for the pumping station acts as upper bound constraint for discharge at a given head difference. However, when deciding a combination of (Q_p, dH_p) , energy use should be considered. Although the energy use of the pumping station could be directly represented using binary variables to act as an on/off switch for every separate pump, this results in computationally infeasible large scale mixed-integer nonlinear programs [38]. A novel approach that is in-between was applied. In the approach, the pumping station was represented using a single aggregate power curve so that the resulting MPC optimisation problem is a non-convex MIQP. Discretising the feasible domain in Equation (2.17) results in solving a MIQP for each aggregate (Q_p, dH_p) combination, optimising individual pump combinations and their respective discharges in order to minimise pump power consumption. Gurobi [23] was used to solve the MIQP. The function

$$P[t] := a_p \cdot Q_p[t]^2 + b_p \cdot dH_p[t]^2 \cdot Q + c_p \cdot dH_p[t] \cdot Q_p[t] \quad (2.20)$$

was fitted through these points, where parameters of the least squares fit were found to be: $a_p = 0.033$, $b_p = 0.061$ and $c_p = 11.306$. This equivalent power curve was used in the objective function as described in Equation (2.3).

2.3.4. MPC OPTIMISATION PROBLEM

For our system, two aspects of important are i) water level constraints cannot be violated at any time step and ii) financial optimality needs to be close to global optimality since

we are exploring economic potential for the approach. As such mathematical optimisation methods that certify closeness to global optimality and satisfy physical constraints are applied. To calculate optimal control settings for pumps and gates, the model is expressed as a non-convex MIQP, to be solved with certification on bounds to global optimality with Gurobi [23]. The NonConvex parameter was set to 2, the MIPGap set to 2%, the Absolute MIPGap set to €1,-, and the time limit set to 15min. Figure 2.4 shows the percentage that combined termination conditions occurred for the individual optimisation problems. The figure shows that in all scenarios over 99.8% of the optimisation problems is solved at the termination conditions, rather than cut-off at the time limit.

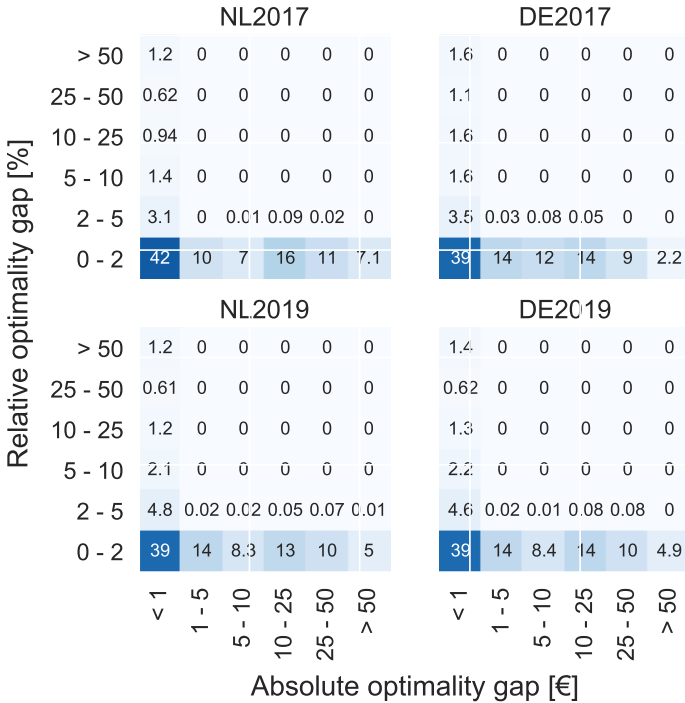


Figure 2.4: Percentage of occurrence of the combined termination conditions for the individual optimisation problems. Gurobi termination settings are at an absolute optimality gap of €1, or at a relative optimality gap of 2%.

The MPC implementation then solves the two optimisation problems (to minimise J_1 and J_2) in a receding horizon fashion, where the DAM participation (J_1) is optimised for every t_d time steps, and participation in the IDM is decided by solving J_2 every hour in a shrinking horizon fashion. The iterative two phase optimisation problem, and the reference problem (J_3) can be stated as:

$$\text{DAM planning phase: } \min_{(\cdot)} J_1(\cdot) + f_1(\cdot), \quad (2.21a)$$

$$\text{IDM trading phase: } \min_{(\cdot)} J_2(\cdot) + f_1(\cdot), \text{ and} \quad (2.21b)$$

$$\text{Futures market trading: } \min_{(\cdot)} J_3(\cdot) + f_1(\cdot). \quad (2.21c)$$

The above are solved subject to the following constraints:

$$h_{min} \leq h[t] \leq h_{max} + s[t] \quad (2.22a)$$

$$h[t] - (h[t-1] + \frac{\Delta t}{A} \cdot (Q_{in}[t-1] - Q_g[t-1] - Q_p[t-1])) \leq \delta_{wb} \quad (2.22b)$$

$$h[t] - (h[t-1] + \frac{\Delta t}{A} \cdot (Q_{in}[t-1] - Q_g[t-1] - Q_p[t-1])) \geq -\delta_{wb} \quad (2.22c)$$

$$h[t] - h_{ns}[t] - dH_{g,min} + (1 - z_g[t]) \cdot M_g \geq 0 \quad (2.22d)$$

$$h[t] - h_{ns}[t] - dH_{g,min} - z_g[t] \cdot M_g \leq 0 \quad (2.22e)$$

$$Q_g[t] \leq (a_g \cdot (h[t] - h_{ns}[t]) + b_g[t]) \cdot z_g[t] \quad (2.22f)$$

$$h_{ns}[t] - h[t] - dH_{p,min} + (1 - z_p[t]) \cdot M_p \geq 0 \quad (2.22g)$$

$$h_{ns}[t] - h[t] - dH_{p,min} - z_p[t] \cdot M_p \leq 0 \quad (2.22h)$$

$$Q_p[t] \leq (a_g[i] \cdot (h_{ns}[t] - h[t]) + b_p[i]) \cdot z_p[t] \text{ for } i \in (1, 2, 3) \quad (2.22i)$$

$$dH^2[t] = (h_{ns}[t] - h[t])^2 \quad (2.22j)$$

$$z_g \in (0, 1) \quad (2.22k)$$

$$z_p \in (0, 1) \quad (2.22l)$$

with

$$P[t] := a_p \cdot Q_p[t]^2 + b_p \cdot dH^2[t] \cdot Q_p[t] + c_p \cdot Q_p[t] \cdot dH_p[t], \quad (2.22m)$$

$$dH_p[t] := h_{ns}[t-1] - h[t-1] - dh_w[t-1] \quad (2.22n)$$

and the decision variables h , Q_g , Q_p stand for, respectively, the water level of the NZK, gate discharge and pump discharge. The slack variable s stands for the upper bound relaxation for water level constraints. The variables Q_{in} stand for the discharge flowing into the NZK-ARK system. Constants h_{min} , h_{max} , Δt , A , δ_{wb} , a_g , b_g , d_p , e_p , f_p , $dH_{g,min}$ and $dH_{p,min}$ stand for minimum and maximum water level allowed in the NZK-ARK, timestep size, storage area of the NZK-ARK, relaxation of the water balance constraint, fitted parameters for gate and pump discharge approximates and minimum water level difference needed for gate and pump discharge. Variables z_g and z_p are binary variables indicating gate- and pump-discharge possibilities through big-M constraints on the water level difference between the canal and the North Sea. The additional objective function terms $f_1(\cdot)$ (Equation (2.9)) is a linear penalty function on upper bound violations of the water level.

2.4. RESULTS & DISCUSSION

We simulate two 1-year periods, where costs are minimised using the multi-market strategy. We also simulate a reference scenario without DR, where energy use is minimised and energy costs are calculated using a monthly fixed futures market price. For the electricity markets, two years of real market data were used (2017, 2019). The hydrological forcings (incoming discharge and sea water level) of the system for the period (01-04-2017 - 31-03-2018) are used for both 2017 and 2019 simulations. The hydrological data was kept the same in order to be able to distinctly study the effect of a changing market and RES market penetration on DR profitability. Actual DAM and IDM data is used, where for the IDM the ID3 IDM price was aggregated from the separate bids. For both the market data and the hydrological forcings, perfect forecasts are assumed. The use of perfect forecasts gives a economic potential, where actual performance in practice would also rely on forecast accuracy. Given the uncertain nature of renewables and their influence on electricity prices, a stochastic problem is likely to give superior results. This is will be discussed in Chapter 5. For the reference scenarios, the monthly-averaged futures market price is assumed. In practice, the actual price depends on the time the contract was signed and for how long, and can therefore differ significantly per user. In the Dutch case, this is the ENDEX market price while the Phelix-DE market price was used in the German case. The combination of minimising energy use while buying on the futures market is equivalent to the current strategy applied by RWS.

2.4.1. SYSTEM DYNAMICS

Figure 2.5 shows the actual and planned (at the time of the day ahead bid) fluxes (a, c), energy use and electricity prices (b, d) of water system using the multi-market strategy. The figure shows both the Dutch (left) and the German (right) market scenarios. The MPC tends to focus pumping on times where the water level difference with the North Sea is low when prices are positive, decreasing energy use. Both the gates and pumps don't violate the big-M constraint, forcing water to flow downwards and be pumped upwards only. In the depicted day, the North Sea is too high for the gates to be used. Negative prices can be seen in the German DAM, while they only occur in the Dutch IDM. Minimising cost when negative prices occur effectively leads to a maximisation of energy use. In the Dutch market, the MPC decides to sell energy bought for October 28th on the IDM for advantageous prices, and buys extra energy for October 29th for negative prices, counteracting a positive imbalance on the grid. On the German market, the MPC already maximises energy use on the DAM, restricting trade options on the IDM. However, some energy is sold on October 29th where positive prices occur on the IDM, counteracting a negative imbalance on the grid.

2.4.2. EVALUATION OF DR PROFITABILITY

The summarised performance of different scenarios can be seen in Table 2.2. It shows the relative costs of the proposed multi-market strategy compared to the reference futures market strategy. The relative energy use, the relative CO₂ emission, the average price of the used energy, the average CI of the used energy, and the percentage of energy that was used for negative energy prices are shown in the picture.

In both markets, optimising costs over the DAM and IDM leads to a significant cost

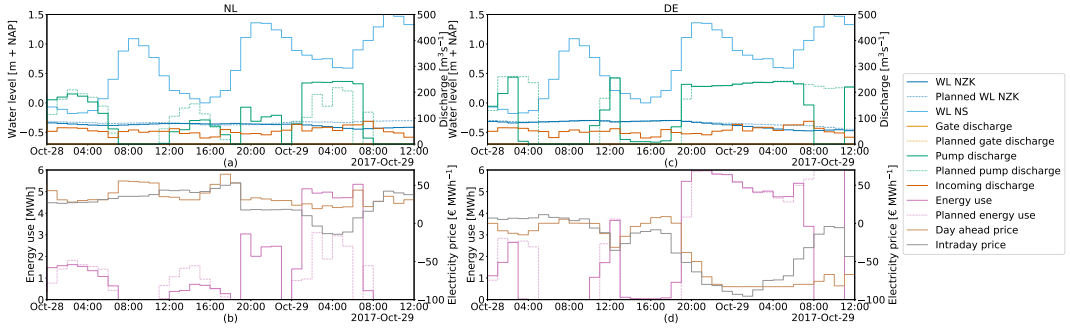


Figure 2.5: Optimised fluxes of the NZK-ARK (a, c), pump energy use and energy prices (b, d) for the Dutch market (left) and the German market (right). Thin and dashed lines show the planned course of action and the resulting water level at the time of day ahead market closing. Filled and thicker lines show the actual actions performed and the resulting water level after intraday trading.

decrease. In the German market the difference between spot and futures market participation is the largest, which can be explained by the higher share of renewable energy generation. Inflexible supply can lead to higher price volatility [39], rewarding flexibility. Uncertainty in energy generation makes a guaranteed base-load more expensive. Inflexibility in energy use is penalised when there is a higher market penetration of renewable energy and a lack of storage solutions, leading to negative energy prices.

Also, the large difference in relative costs between the market strategies can be explained by the increased price on carbon emission allowance [40]. This increased price creates a larger price difference between renewable (with low CI) and fossil energy (with high CI). Due to their unpredictable nature, renewable energy makes up a higher share of the spot markets volume. This makes the increased carbon emission price mostly noticeable in the futures market, where base-load contracts can be supplied through the use of fossil sources, explaining the relatively low spot market prices in Germany compared to the futures market prices. If both futures (i.e. Endex, Phelix-De) and spot markets (i.e. DAM, IDM) have a low penetration of renewable energy, like in the Dutch scenario, the spot market would experience the same price increase as the futures market. This would explain why the difference between the German DAM and Futures market is higher than the difference between their Dutch equivalents.

In both the Dutch and German scenario, energy use is higher for the spot market scenarios than in the reference scenarios (where energy use is minimised), explaining the increase in carbon emission. The carbon emission does increase more slowly than the energy use, indicating a lower average CI of the used energy. The average price and CI of the used energy can be seen in Table 2.2, in both markets the average price of the used energy is lower for the spot market scenarios. The increase in energy use does not lead to an increase in costs. In the German case, the average price for the spot market scenarios is about a third of the average price for the reference scenarios. Also, a significant percentage of energy was used for negative prices, causing the MPC problem to maximise

energy use. This explains the low average price, high cost savings, and high amount of extra energy use.

Even though the average price of the energy differs significantly between the futures and spot market scenarios, the average CI of the used energy is relatively similar. This shows that the base-level of the CI of the energy is not low enough to make up for the extra amount of energy being used. This holds for both the Dutch and the German markets. However, the average CI of the used energy is somewhat lower for the spot market scenarios, which can be explained by the correlation between CI and energy price shown in Figure 2.1c. In the German 2019 scenario, a 29% increase in energy use leads to a 5% CO₂ emission increase. This indicates that Germany is nearing a point where an increase in energy use would not lead to increased CO₂ emissions. Something that can possibly already be realised by limiting the energy use maximisation when negative prices occur, even though it's optimal for balancing the markets. However, these numbers should be taken as an indication since the CI time series was estimated as described in Section 2.2.2 and not measured.

The relative cost differences show the influence of a higher futures market price on the potential cost savings through DR. Higher uncertainty in generation due to renewables make futures prices carry more risk-premiums, rewarding flexibility on the spot market while penalising inflexibility on baseload contracts.

Table 2.2: Relative profitability of DR over spot markets compared to futures market participation with fixed monthly prices. The rows show four scenarios of applying the multi-market MPC in DE and NL, using market data from two different years. The profitability of the multi-market strategy is divided by the profitability of the reference strategy without DR.

Country	Year	Rel. costs	Rel. energy use	Rel. CO ₂	Average energy price		Average CI		% of energy volume used with negative prices
					Spot	Futures	Spot	Futures	
NL	2017	0.90	1.07	1.05	31.81	37.60	421.22	428.84	0.00
	2019	0.84	1.29	1.16	30.94	47.31	271.59	301.51	0.92
DE	2017	0.44	1.32	1.15	11.93	35.44	319.52	365.43	11.44
	2019	0.50	1.29	1.05	17.67	45.43	222.10	273.41	14.25

2.4.3. AFRR POTENTIAL ANALYSIS

To investigate the potential for pumping station IJmuiden to be active on the aFRR market, we perform an analysis on the previous results where the pumping station is active on the DAM and IDM. The simulation data was used to determine if and when there was room within the constraints to realise a larger pump discharge. We assume the upper limit on the possible discharge to be the amount of water flowing into the system while being constrained by the Q-h curve of the pumping station, i.e. the added pumped volume would never lower the water level in the system. This ensures that water level constraints would not be violated by the additional use of the pumps, leading to a conservative estimate of extra pump capabilities. The extra room for pump use is translated into the amount of energy corresponding to this combination of maximum discharge and pump height. The energy already bought on the DAM and IDM is subtracted from this amount.

Table 2.3: Summarised results of aFRR market economic potential analysis: downward regulating volume and relative cost savings for scenarios with individual and aggregated market participation.

Country	Year	aFRR cost savings [%]		Downward regulating volume [MWh]	
		Individual	Aggregated	Individual	Aggregated
NL	2017	7.68	12.65	150.61	234.07
	2019	3.84	5.23	75.59	103.26
DE	2017	18.60	27.85	485.90	773.61
	2019	12.33	20.70	216.36	369.12

The resulting data is used for two different analyses. In the first analysis, all DR events resulting in extra power consumption of more than 1 MW are selected to analyse aFRR potential during individual market participation (i.e. in the absence of an aggregator). In the second analysis, all DR events are selected to analyse aFRR potential when cooperating with an aggregator, thus allowing for small bids to be placed. In both cases, we selected the periods where downward activation in the aFRR market occurred simultaneously with a negative downward activation price. This allows us to calculate the maximum additional amount of energy that could have been profitably used for grid balancing purposes per timestep.

Table 2.3 shows the summary of results for the aFRR potential analysis. The results show that the aFRR market has the potential to compensate a part of the energy cost for pumping station IJmuiden. Although cost savings seem small, this analysis doesn't take the selling of energy due to aFRR participation into account. The DAM and IDM bids are not corrected for the energy bought on the aFRR, and the remaining pump schedule remained unchanged. Besides that, the maximum amount of pumping for aFRR purposes was constrained to keep the water level equal. Re-optimising pump schedules and spot-market participation after aFRR activation would result in a less conservative estimate of the actual economic potential for aFRR participation. This will be left for future work. The results show that partnering with an aggregator could allow for substantial extra cost savings and regulating volume compared to participating on the market as a single bidder. The supplied downward regulating volume decreased from 2017 to 2019 in both the Dutch and German market scenario's. This indicates that the IDM is capable of supplying the necessary extra regulating volume due to renewable energy generation. The IDM is more accessible to BRPs, and carries relatively lower risk of disadvantageous prices due to the possibility to trade before delivery.

2.5. CONCLUSION

In this chapter, we propose an economic two-stage MPC scheme to enable a large flood defense pumping station to participate in DR services. We explore how participating on the DAM gives more certainty of supply and costs while the IDM allows for short-notice trading, to make up for or exploit unforeseen events or dealing with uncertainties in the state of the open canal system. Therefore, a multi-market strategy is proposed, where

pumping is scheduled a day ahead by buying energy on the DAM and then adjusted in a receding horizon fashion (every hour) when energy prices of the IDM are rewarding. We show that a larger profit can be realised for the pumping station when energy prices are more volatile, which can be expected to accompany a higher RES market penetration.

To demonstrate this, we explore the difference between the German and Dutch markets, whose grids have a significantly different energy mix. We show that the proposed MPC is able to counteract both positive and negative imbalances on the grid through price-based DR. We also explore the effect of temporal market changes by using both 2017 and 2019 market data. A 56% and 50% cost decrease was found in the German market scenarios for the years 2017 and 2019 respectively, compared to the reference scenario. Negative energy prices on the German market were found to result in increased energy use and CO₂ emissions. The Dutch market scenario shows a 10% and 16% cost decrease in 2017 and 2019, respectively. The difference in potential cost saving shows that the German market rewards flexibility more than the Dutch market.

We have shown that CO₂ savings are not yet present or well quantifiable in both German and Dutch cases. The efficiency of pumping is time-dependent due to tides, resulting in an increased energy use when shifting pumping schedules for DR while the CI of the grid does not decrease enough for CO₂ emission savings to be present. Besides that, negative energy prices can lead to a significant increase in energy use. Although this is optimal from a market-perspective, it might not be preferred by the stakeholders. Also, generation by source time series are incorrect in the ENTSO-E transparency platform, requiring us to estimate the CI time series through renewable energy production, observed load and reported CI estimates.

We show that participating in the aFRR market has economic potential, resulting in cost savings of up to 28% in the aggregated German scenario in 2017 based on our conservative analysis. Receiving a warning signal 15-minutes before activation makes the market feasible for the pumping station to participate in. The analysis shows that aggregating participants, allowing them to circumvent the 1 MW minimum-bid constraint through pooling, results in higher participation and lower costs. In both German and Dutch markets, the aFRR economic potential decreased from 2017 to 2019. The supplied downward regulating volume decreased as well, indicating that the IDM could be providing the extra balancing services required for renewable energy.

To conclude, we have shown that the economic potential for DR applied to open water systems is significant. However, it would be interesting to quantify the impact of uncertainty in system state, hydrological forcings (e.g. incoming discharge and sea water level) and energy prices. Operationalising the strategy in a feasible way would probably require the consideration of uncertainty. However, this chapter focuses on the economic potential of DR participation, leaving the consideration of uncertainty for Chapter 5. It is also known that variable speed pumps and more efficient configurations of more smaller pumps, in comparison to a single large pump, can expand the envelope for participation in DR [12]. Therefore, cost benefit analysis for the upgrading of the pumping station should be evaluated also explicitly considering performance in DR.

BIBLIOGRAPHY

- [1] Ties van der Heijden et al. “Multi-market demand response from pump-controlled open canal systems: an economic MPC approach to pump-scheduling”. In: *Journal of Hydroinformatics* 24 (4 July 2022), pp. 838–855. ISSN: 14651734. DOI: [10.2166/hydro.2022.018](https://doi.org/10.2166/hydro.2022.018).
- [2] International Energy Agency. *Renewables 2017: Analysis and Forecast to 2022*. Tech. rep. International Energy Agency (IEA), 2017.
- [3] Ministry of Economic Affairs and Climate Policy. *Climate policy*. Accessed: 2019-05-28. 2019. URL: <https://www.government.nl/topics/climate-change/climate-policy>.
- [4] European Commission. *2050 low-carbon economy roadmap*. Tech. rep. European Commission, 2016. URL: https://ec.europa.eu/clima/policies/strategies/2050%5C_en (visited on 06/13/2018).
- [5] A. Rezaee Jordehi. “Optimisation of demand response in electric power systems, a review”. In: *Renewable and Sustainable Energy Reviews* 103. July 2018 (2019), pp. 308–319. ISSN: 18790690. DOI: [10.1016/j.rser.2018.12.054](https://doi.org/10.1016/j.rser.2018.12.054). URL: <https://doi.org/10.1016/j.rser.2018.12.054>.
- [6] Liander. *Liander wil flexibiliteitsmarkt starten in Nijmegen-Noord*. 2017. URL: <https://www.alliander.com/nl/media/nieuws/liander-wil-flexibiliteitsmarkt-starten-nijmegen-noord> (visited on 06/16/2018).
- [7] Fraunhofer Institute for solar energy systems ISE. *Net Public Electricity Generation in Germany in 2018*. Tech. rep. Fraunhofer Institute for solar energy systems ISE, 2019. URL: https://www.ise.fraunhofer.de/content/dam/ise/en/documents/News/Stromerzeugung%5C_2018%5C_2%5C_en.pdf.
- [8] Ministerie van Economische Zaken. *Energierapport: transitie naar duurzaam*. Tech. rep. Ministerie van Economische Zaken, 2016. URL: <https://www.rijksoverheid.nl/binaries/rijksoverheid/documenten/rapporten/2016/01/18/energie-rapport-transitie-naar-duurzaam/energie-rapport-transitie-naar-duurzaam.pdf>.
- [9] Paolo Bertoldi, Paolo Zancanella, and Benigna Boza-Kiss. *Demand Response status in EU Member States*. Tech. rep. European Commission, 2016, pp. 1–153. DOI: [10.2790/962868](https://iet.jrc.ec.europa.eu/energyefficiency/sites/energyefficiency/files/publications/demand%7B%5C_%7Dresponse%7B%5C_%7Dstatus%7B%5C_%7Din%7B%5C_%7Ddeu28%7B%5C_%7Dmember%7B%5C_%7Dstates-online.pdf). URL: https://iet.jrc.ec.europa.eu/energyefficiency/sites/energyefficiency/files/publications/demand%7B%5C_%7Dresponse%7B%5C_%7Dstatus%7B%5C_%7Din%7B%5C_%7Ddeu28%7B%5C_%7Dmember%7B%5C_%7Dstates-online.pdf.

- [10] Kritika Saxena and Rohit Bhakar. “Impact of LRIC pricing and demand response on generation and transmission expansion planning”. In: *IET Generation, Transmission and Distribution* 13.5 (2019), pp. 679–685. ISSN: 17518687. DOI: [10.1049/iet-gtd.2018.5328](https://doi.org/10.1049/iet-gtd.2018.5328).
- [11] J. G. Kirkerud, N. O. Nagel, and T. F. Bolkesjø. “The role of demand response in the future renewable northern European energy system”. In: *Energy* 235 (2021), p. 121336. ISSN: 03605442. DOI: [10.1016/j.energy.2021.121336](https://doi.org/10.1016/j.energy.2021.121336). URL: <https://doi.org/10.1016/j.energy.2021.121336>.
- [12] R. Menke et al. “Extending the Envelope of Demand Response Provision through Variable Speed Pumps”. In: *Procedia Engineering* 186 (2017), pp. 584–591. ISSN: 18777058. DOI: [10.1016/j.proeng.2017.03.274](https://doi.org/10.1016/j.proeng.2017.03.274). URL: <http://dx.doi.org/10.1016/j.proeng.2017.03.274>.
- [13] Rasmus Elbæk Hedegaard, Theis Heidmann Pedersen, and Steffen Petersen. “Multi-market demand response using economic model predictive control of space heating in residential buildings”. In: *Energy and Buildings* 150 (2017), pp. 253–261. ISSN: 03787788. DOI: [10.1016/j.enbuild.2017.05.059](https://doi.org/10.1016/j.enbuild.2017.05.059). URL: <http://dx.doi.org/10.1016/j.enbuild.2017.05.059>.
- [14] Daniel Schwabeneder et al. “Business cases of aggregated flexibilities in multiple electricity markets in a European market design”. In: *Energy Conversion and Management* 230. August 2020 (2021), p. 113783. ISSN: 01968904. DOI: [10.1016/j.enconman.2020.113783](https://doi.org/10.1016/j.enconman.2020.113783). URL: <https://doi.org/10.1016/j.enconman.2020.113783>.
- [15] Madeleine McPherson and Brady Stoll. “Demand response for variable renewable energy integration: A proposed approach and its impacts”. In: *Energy* 197 (2020), p. 117205. ISSN: 03605442. DOI: [10.1016/j.energy.2020.117205](https://doi.org/10.1016/j.energy.2020.117205). URL: <https://doi.org/10.1016/j.energy.2020.117205>.
- [16] Chouaib Mkireb et al. “Robust Optimization of Demand Response Power Bids for Drinking Water Systems”. In: *Applied Energy* 238 (2019), pp. 1036–1047. ISSN: 03062619. DOI: [10.1016/j.apenergy.2019.01.124](https://doi.org/10.1016/j.apenergy.2019.01.124). URL: <https://doi.org/10.1016/j.apenergy.2019.01.124>.
- [17] Gianni Bianchini et al. “Demand-response in building heating systems: A Model Predictive Control approach”. In: *Applied Energy* 168 (2016), pp. 159–170. ISSN: 03062619. DOI: [10.1016/j.apenergy.2016.01.088](https://doi.org/10.1016/j.apenergy.2016.01.088). URL: <http://dx.doi.org/10.1016/j.apenergy.2016.01.088>.
- [18] Faran A. Qureshi, Tomasz T. Gorecki, and Colin N. Jones. *Model predictive control for market-based demand response participation*. Vol. 19. IFAC, 2014, pp. 11153–11158. ISBN: 9783902823625. DOI: [10.3182/20140824-6-ZA-1003.02395](https://doi.org/10.3182/20140824-6-ZA-1003.02395). URL: <http://dx.doi.org/10.3182/20140824-6-ZA-1003.02395>.
- [19] Ditiro Setlhaolo, Xiaohua Xia, and Jiangfeng Zhang. “Optimal scheduling of household appliances for demand response”. In: *Electric Power Systems Research* 116 (2014), pp. 24–28. ISSN: 03787796. DOI: [10.1016/j.epsr.2014.04.012](https://doi.org/10.1016/j.epsr.2014.04.012). URL: <http://dx.doi.org/10.1016/j.epsr.2014.04.012>.

- [20] G.B.M.A. Litjens, E. Worrell, and W.G.J.H.M. van Sark. “Economic benefits of combining self-consumption enhancement with frequency restoration reserves provision by photovoltaic-battery systems”. In: *Applied Energy* 223 (2018), pp. 172–187. ISSN: 0306-2619. DOI: <https://doi.org/10.1016/j.apenergy.2018.04.018>. URL: <http://www.sciencedirect.com/science/article/pii/S0306261918305622>.
- [21] Laura Romero Rodríguez et al. “Heuristic optimization of clusters of heat pumps: A simulation and case study of residential frequency reserve”. In: *Applied Energy* 233-234 (2019), pp. 943–958. ISSN: 0306-2619. DOI: <https://doi.org/10.1016/j.apenergy.2018.09.103>. URL: <http://www.sciencedirect.com/science/article/pii/S0306261918314247>.
- [22] Peng Li et al. “Two-stage optimal operation of integrated energy system considering multiple uncertainties and integrated demand response”. In: *Energy* 225 (2021), p. 120256. ISSN: 03605442. DOI: [10.1016/j.energy.2021.120256](https://doi.org/10.1016/j.energy.2021.120256). URL: <https://doi.org/10.1016/j.energy.2021.120256>.
- [23] Gurobi Optimization, LLC. *Gurobi Optimizer Reference Manual*. Tech. rep. Gurobi Optimization, LLC, 2018. URL: <http://www.gurobi.com>.
- [24] Paolo Zancanella, Paolo Bertoldi, and Benigna Kiss. *Demand response in EU member states*. Tech. rep. European Commission, 2016. URL: <https://publications.jrc.ec.europa.eu/repository/handle/JRC101191> (visited on 02/26/2024).
- [25] Stefan Pfenninger and Iain Staffell. “Long-term patterns of European PV output using 30 years of validated hourly reanalysis and satellite data”. In: *Energy* 114 (2016), pp. 1251–1265. ISSN: 03605442. DOI: [10.1016/j.energy.2016.08.060](https://doi.org/10.1016/j.energy.2016.08.060). URL: <http://dx.doi.org/10.1016/j.energy.2016.08.060>.
- [26] Iain Staffell and Stefan Pfenninger. “Using bias-corrected reanalysis to simulate current and future wind power output”. In: *Energy* 114 (2016), pp. 1224–1239. ISSN: 03605442. DOI: [10.1016/j.energy.2016.08.068](https://doi.org/10.1016/j.energy.2016.08.068). URL: <http://dx.doi.org/10.1016/j.energy.2016.08.068>.
- [27] Michaja Pehl et al. “Understanding future emissions from low-carbon power systems by integration of life-cycle assessment and integrated energy modelling”. In: *Nature Energy* 2 (2017), pp. 939–945. ISSN: 2058-7546. DOI: [10.1038/s41560-017-0032-9](https://doi.org/10.1038/s41560-017-0032-9). URL: <https://doi.org/10.1038/s41560-017-0032-9>.
- [28] Alexandra Bonou, Alexis Laurent, and Stig I. Olsen. “Life cycle assessment of on-shore and offshore wind energy-from theory to application”. In: *Applied Energy* 180 (2016), pp. 327–337. ISSN: 03062619. DOI: [10.1016/j.apenergy.2016.07.058](https://doi.org/10.1016/j.apenergy.2016.07.058). URL: <http://dx.doi.org/10.1016/j.apenergy.2016.07.058>.
- [29] Centraal Bureau van de Statistiek. *StatLine - Elektriciteit en warmte; productie en inzet naar energiedrager*. Accessed: 2019-07-17. 2019. URL: <https://opendata.cbs.nl/statline/%5C#/CBS/nl/dataset/80030ned/table?fromstatweb%7D>.
- [30] European Environment Agency. *Greenhouse gas emission intensity of electricity generation*. 2020. URL: https://www.eea.europa.eu/data-and-maps/visualization/co2-emission-intensity-14/#tab-googlechartid_chart_41.

- [31] ENTSO-E. *ENTSO-E Transparency Platform*. 2018. URL: <https://transparency.entsoe.eu/>.
- [32] H. Janssen. *Effect selectieve onttrekking IJmuiden op waterbeheer*. Tech. rep. Rijkswaterstaat, 2017. URL: https://www.platformparticipatie.nl/binaries/Effect%5C%20selectieve%5C%20onttrekking%5C%20IJmuiden%5C%20op%5C%20waterbeheer%5C_tcm117-377563.pdf.
- [33] R.D. van Weissenbruch. “Onderzoek Energieverbruik gemaal IJmuiden”. MA thesis. TU Delft, 2003.
- [34] A Goedbloed. “Kwaliteitsanalyse Beslissingen Ondersteunend Systeem Noordzeekanaal / Amsterdam-Rijnkanaal”. MA thesis. TU Delft, 2006.
- [35] HKV. *Doorontwikkeling DEZY 2.0*. Tech. rep. HKV, 2016.
- [36] C. Geerse and B. Kuijper. *Probabilistisch model frequentielijnen IJsselmeergebied: Hoofdrapport van model DEZY*. Tech. rep. HKV, 2015.
- [37] J. M. Maestre et al. “Distributed tree-based model predictive control on a drainage water system”. In: *Journal of Hydroinformatics* 15.2 (2013), pp. 335–347. ISSN: 14647141. DOI: [10.2166/hydro.2012.125](https://doi.org/10.2166/hydro.2012.125).
- [38] Ruben Menke et al. “Exploring optimal pump scheduling in water distribution networks with branch and bound methods”. In: *Water Resources Management* 30.14 (2016), pp. 5333–5349.
- [39] Stephanía Mosquera-López and Anjali Nursimulu. “Drivers of electricity price dynamics: Comparative analysis of spot and futures markets”. In: *Energy Policy* 126. October 2018 (2019), pp. 76–87. ISSN: 03014215. DOI: [10.1016/j.enpol.2018.11.020](https://doi.org/10.1016/j.enpol.2018.11.020). URL: <https://doi.org/10.1016/j.enpol.2018.11.020>.
- [40] TenneT. *Annual Market Update 2018*. Accessed: 2019-07-19. 2018. URL: https://www.tennet.eu/fileadmin/user%5C_upload/Company/Publications/Technical%5C_Publications/Dutch/Annual%5C_Market%5C_Update%5C_2018%5C_-%5C_Final.pdf.



3

MODELLING OPERATIONAL UNCERTAINTY FOR CONTROL

*Bounce with it, rock with it,
lean with it, drop with it,
snap with it.*

All my fellas tip your hat with it.

Acraze & Cherish

The previous chapter showed the significant economic potential for Demand Response participation from the Noordzeekanaal–Amsterdam-Rijnkanaal. However, this potential was estimated using a simulation with perfect foresight. This chapter introduces the methods applied in the remainder of this thesis to model operational uncertainty. First, the techniques that are used for probabilistic forecasting are described. After that, we discuss multivariate sampling techniques that allow us to sample time series. Finally, techniques for selecting an optimal subset are discussed, which allow for a sparse representation of operational uncertainty by generating weighted scenario fans and trees. The proposed techniques are validated in a Proof of Concept, where Day Ahead Market arbitrage using a battery is simulated under uncertainty, showing increased performance over naive benchmarks.

Parts of this chapter have been published in other work [1, 2, 3]

3.1. PROBABILISTIC FORECASTING

3.1.1. COMBINED QUANTILE REGRESSION DEEP NEURAL NETWORKS

In this thesis, we propose the use of *Quantile Regression* (QR), where quantiles of a probability density of a value are given instead of merely an expected value. Specifically, we apply the *Combined Quantile Regression Deep Neural Network* (CQRDNN), as depicted in Figure 3.1, which was introduced to mitigate the crossing quantile problem encountered in ensemble models, where each quantile is represented by a separate model [4]. The CQRDNN mitigates this issue by employing a combined quantile loss function, enabling simultaneous training of multiple quantiles within a single Deep Neural Network. This is achieved by applying a distinct loss to each output node while minimizing the average loss across all output nodes. Consequently, the CQRDNN prevents divergence of separate quantile models to different local optima due to stochastic sampling during training, thereby improving the quantiles consistency in exhibiting monotonic increase.

To train the CQRDNN model, a combination of pinball loss functions [5] is utilized, defined as

$$L_{CQ} = \frac{1}{N} \sum_{\tau \in T} L_{\tau}, \text{ where} \quad (3.1)$$

$$L_{\tau} = \max(\tau \cdot e, (\tau - 1) \cdot e), \text{ and} \quad (3.2)$$

$$e = z - y, \quad (3.3)$$

where N represents the number of quantiles considered, T denotes the set of quantiles $\{\tau_i, i = 1 : n\}$, L represents the loss, τ denotes a quantiles in T , and e represents the quantile forecast error, with y indicating the observed value and z denoting the quantile forecast. Due to the asymmetrical penalization of over- and under-predictions, the CQRDNN learns to regress a variable that is anticipated to exceed the actual target for a fraction τ of the samples, representing a quantile.

3.1.2. FEATURE AND HYPERPARAMETER OPTIMIZATION

For accurate and effective application of ML models it is necessary to optimize both the features applied in the model and the hyperparameters of the model. The *Tree Parzen Estimator* (TPE) algorithm, which is a variant of *Sequential Model Based Optimization*, is capable of simultaneously optimizing both features and hyperparameters [6, 7, 4]. It allows for the construction of a custom search space with a large number of dimensions which can be either discrete, continuous, or a combination.

The TPE employs Bayes' rule to create a surrogate model. The primary differentiator here is how the TPE segments the search space by evaluating the likelihood of the observed loss being above or below a threshold, typically denoted as y^* . In this work, we apply the TPE to optimize the features and hyperparameters of our CQRDNNs, where the loss being optimized for is the combined pinball loss function.

This surrogate model describes the probability of the loss being higher ($h(x)$) or lower ($l(x)$) than a specified threshold value (y^*) as a function of the search space instantiation:

$$p(y|x) = \frac{p(x|y) \cdot p(y)}{p(x)}, \quad (3.4)$$

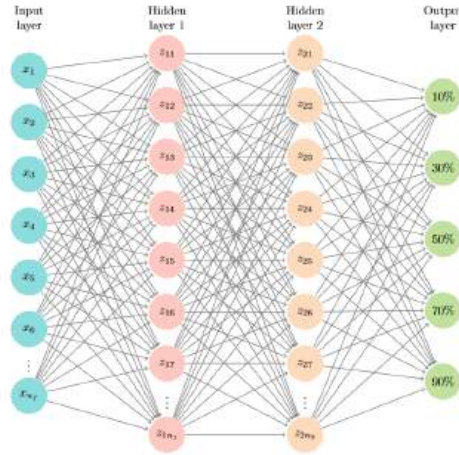


Figure 3.1: Architecture of the QQRDNN with n_f features, n_1 nodes in the first hidden layer, n_2 nodes in the second hidden layer, and 5 quantile output nodes representing the same random variable [4].

In the above equation, y represents the model performance, and x denotes a search space instantiation.

Consequently, the model performance is estimated based on the features and hyper-parameters, where $p(x|y)$ is defined as

$$p(x|y) = \begin{cases} l(x) & \text{if } y < y^* \\ h(x) & \text{if } y \geq y^*. \end{cases} \quad (3.5)$$

Within the TPE algorithm, samples are drawn from both $l(x)$ and $h(x)$, after which the ratio $\frac{l(x)}{h(x)}$ is evaluated for all samples. The next suggested candidate is the one with the highest expected improvement, i.e., the candidate with the largest ratio between low and high probabilities in $l(x)$ and $h(x)$, respectively. In our case, we apply the combined pinball loss function (Equation (3.1)).

3.2. SCENARIO GENERATION AND SELECTION

3.2.1. NON-PARAMETRIC BAYESIAN NETWORKS

To assess decision-making processes in uncertain environments, generating operational scenarios is essential. The *Non-Parametric Bayesian Network* (NPBN) approach is useful here. It employs univariate parametric distributions based on quantiles from the QQRDNN to depict the marginal distributions of the variable at a timestep, while bivariate copulae are used to model temporal dependencies as observed in the data. Particularly, in the NPBN, Gaussian copulas are used¹ due to their ability to effectively han-

¹In previous literature, Non-Parametric Bayesian Networks are sometimes referred to "Gaussian copula-based" Bayesian Networks.

de a large number of variables by simplifying the process of joint distribution sampling [8]. This feature makes NPBN effective for scenario generation [3] with scenarios that obey both the forecast marginal distribution and the observed auto-correlation. In this thesis, we apply NPBNs to sample scenarios containing multiple time steps of incoming waterboard discharge, the water level of the North Sea, and the *Day Ahead Market* (DAM) and *Intraday Market* (IDM) electricity prices.

In NPBNs, multivariate distributions are characterized by univariate marginals and a copula to represent the dependencies. The joint density of an NPBN with n variables is factorized as:

$$f_{1,\dots,n}(x_1, \dots, x_n) = f_1(x_1) \prod_{i=2}^n f_{i|Pa(i)}(x_i|x_{Pa(i)}), \quad (3.6)$$

Here, $f_{1,\dots,n}$ denotes the joint density of the n variables, f_i represents the marginal distribution of each variable, and $f_{i|j}$ represents the conditional distributions. Each random variable x_i is associated with a node i , and the parent nodes of node i form the set $Pa(i) = i_1, \dots, i_{p(i)}$. The arcs in the NPBN are assigned one-parameter conditional copulas [9], parameterized by Spearman's rank correlations [10]. The arc from the parent node i_m to node i is assigned a conditional rank correlation.

3.2.2. ENERGY DISTANCE CLUSTERING

While generating a set of scenarios that fully describes the uncertainty space is invaluable, it is equally valuable to have a practical size, especially in simulation and optimization contexts where computational resources are constrained. Hence, it is beneficial to distil the original scenario set into an optimal subset with statistical properties that best approximates the properties of the original set. The criterion we use for this selection is the "minimal energy distance" between the reduced set and the original set of scenarios. The energy distance was applied since it tends to show better statistical approximation properties than the more widely used Wasserstein distance [11].

The energy distance quantifies the dissimilarity between two distributions. This metric describes the distances between the elements of X and X^* , and then corrects these with the distances found between members within X and X^* themselves [11, 12].

Mathematically, the energy distance is formulated as

$$E_p(X, X^*) = 2 \sum_{i \in \mathcal{I}} \sum_{j \in \mathcal{I}^*} p_i p_j^* d_{ij}^p - \sum_{i \in \mathcal{I}} \sum_{j \in \mathcal{I}} p_i p_j d_{ij}^p - \sum_{i \in \mathcal{I}^*} \sum_{j \in \mathcal{I}^*} p_i^* p_j^* d_{ij}^p, \quad (3.7)$$

$$d_{ij}^p = |\mathbf{x}_i - \mathbf{x}_j|^p, \quad (3.8)$$

$$(3.9)$$

where X denotes the original scenario set with index set \mathcal{I} , and scenarios (time series set elements) \mathbf{x}_i for $i \in \mathcal{I}$ with respective probabilities p_i . X^* denotes the considered subset with index set $\mathcal{I}^* \subset \mathcal{I}$, with corresponding scenarios \mathbf{x}^* , and probabilities p^* . The term d_{ij}^p denotes the p -norm distance between two scenarios, with $p = 1$ being our choice for this study. Since the primary set (X) remains unaltered when during scenario selection, the middle term is often neglected. This revised metric is termed the Energy

Score. Probabilities p^* of X^* can be optimized for the minimal Energy Score relative to X using the quadratic program

$$\begin{aligned} p^* &= \operatorname{argmin}_{p^*} E_p(X, X^*), \\ \text{s.t. } \sum p^* &= 1. \end{aligned} \quad (3.10)$$

To select an optimal subset X^* (i.e. the subset for which the chosen distance metric is minimal), we can compute the Energy distances for all potential subsets where $|\mathcal{S}| = N$. This method works for small scenario sets but becomes impractical for larger sets. The forward selection algorithm [13] was suggested to greedily append scenarios to the subset X^* until the required subset size is attained. This approach is detailed in Algorithm 1, accompanied by an illustrative example founded on the Bernoulli walk, presented in Figure 3.2.

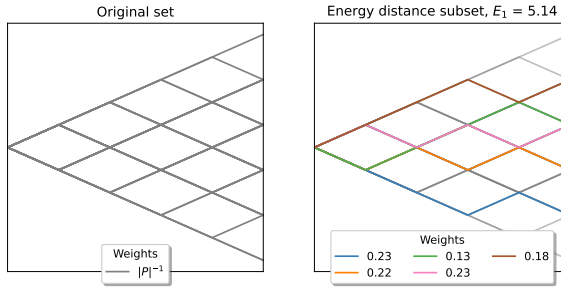


Figure 3.2: Scenario reduction and weight redistribution of the Bernoulli walk using the Forward Selection algorithm and the Energy distance metric.

Algorithm 1: Forward Selection(X, \mathcal{S}, N)

```

1  $X^* \leftarrow \emptyset$ 
2  $\mathcal{S}^* \leftarrow \emptyset$ 
  while  $|\mathcal{S}^*| < N$  do
    // Execute the forward selection algorithm, adding scenarios to the
    // subset until reaching N.
3    $i^* \leftarrow \operatorname{argmin}_{i \in \mathcal{S} \setminus \mathcal{S}^*} \text{Distance}(X, X^* \cup \mathbf{x}_i)$  // Acquire the scenario index
    // yielding the smallest Energy Score.
4    $\mathcal{S}^* \leftarrow \mathcal{S}^* \cup i^*$  // Update the optimal subset's index set.
5    $X^* \leftarrow X^* \cup \mathbf{x}_{i^*}$  // Update the optimal subset.
  end
6  $p^* \leftarrow \text{Probabilities}(X^*)$  // Extract the scenario probabilities of the
    // optimal subset either through the optimal redistribution rule or
    // using the quadratic program defined in Equation (3.10).
7 return  $X^*, \mathcal{S}^*, p^*$ 

```

3.2.3. SCENARIO TREE REDUCTION

Building on the concept of scenario reduction, scenario trees further simplify the task by offering a structured representation. The core principle here is to model the inherent growth of uncertainty over forecast horizons. To transition from scenario subsets to tree representations, we utilize a method inspired by [13]. However, we search for the optimal tree shape and use the energy distance [11] instead of the wasserstein distance to calculate distances. The subsequent trees model the progression of uncertainty over time, as depicted in Figure 3.3.

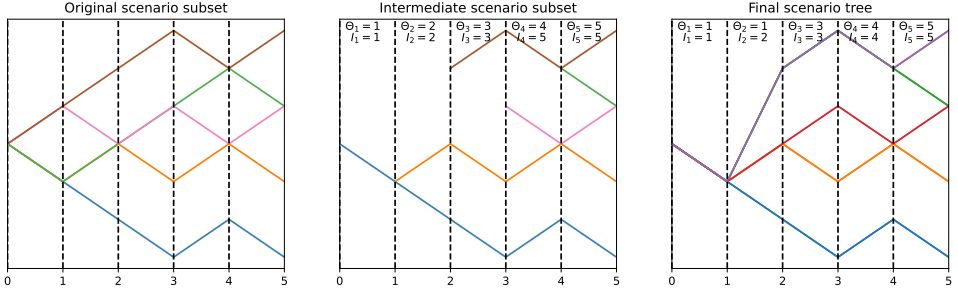


Figure 3.3: Tree construction for the Bernoulli walk using the Energy distance.

The Backward Tree Reduction method depicted in Figure 3.3, while effective, has its limitations. It relies on predefined parameters like node locations (Φ) and the maximum children count per node (Θ), while fixing these parameters can yield suboptimal trees. To circumvent this limitation, a Genetic Algorithm (GA) is used to dynamically adjust these parameters. GAs can search effectively through complex search spaces with non-linear constraints and objectives. We apply it to optimize tree structures for a given scenario set by solving the optimization problem

$$\begin{aligned} \Phi^*, \Theta^* &= \underset{\Phi, \Theta}{\operatorname{argmin}} \operatorname{Distance}(\tilde{X}, X^*) \\ \text{s.t. } \sum_{x \in \tilde{X}} \frac{|x|}{N \cdot H} &\leq \beta, \end{aligned} \quad (3.11)$$

where we solve for optimal split locations (Φ^*) and number of nodes (Θ^*) by minimizing the distance between tree \tilde{X} and original subset X^* . We define tree complexity as the number of time-discretized variables necessary to describe the scenario set (i.e. the sum of the length of all sub-scenario time series in each node of the tree), where the length of a sub-scenario time series is defined as $|x|$. The solution is constrained to a tree complexity reduction fraction, β , of the original complexity defined by subset size N and time series length H . In this work, we apply a β value of 0.5 to constraint tree complexity. In this thesis, we apply a β value of 0.5 to constraint tree complexity reduction with a minimum of 50%, which was selected a posteriori based on the speed at which the GA could find feasible solutions.

3.2.4. PROOF OF CONCEPT

To illustrate the performance of the scenario generation and reduction methods discussed in this chapter, we present a proof of concept involving a battery storage system engaged in DAM arbitrage. The objective is to maximize arbitrage profits by optimally charging and discharging the battery, based on forecast DAM prices. The system is controlled by an MPC scheme that relies on probabilistic forecasts of future prices, maximizing the expected profit of a DAM bid.

We benchmark the following approaches:

- *Naive random sampling*: 10 random samples are generated from the marginal distributions at each time step without considering temporal relationships.
- *Naive sampling with energy distance clustering*: 100 random time series are generated using the same method as in the naive approach, but energy distance clustering is applied to select the 10 optimal weighted time series that best represent the uncertainty space.
- *NPBN sampling with energy distance clustering*: Scenarios are generated using the NPBN approach, which preserves temporal dependencies and uses energy distance clustering to select 10 optimal weighted scenarios.

Closed-loop simulations are performed with a 48-hour control horizon, where only the first 24 hours are used for bidding decisions. We evaluate the cumulative profit from DAM arbitrage for 10 repetitions of the naive method (10 scenarios), 1 run with 100 scenarios, naive sampling with clustering, and NPBN sampling with clustering.

Figure 3.4 presents the cumulative profit for the benchmarked approaches in October 2020. The results show the potential of the proposed NPBN approach, where our proposed with 10 scenarios has slightly better performance than the naive approach with 100 scenarios, while both outperform the energy distance clustered naive and the naive with 10 scenarios. By preserving temporal characteristics, the NPBN method constrains the sampling to more realistic scenarios. This proof of concept applies a stochastic objective to formulate a deterministic control plan. Future improvements involve introducing scenario-based control strategies that could further exploit temporal dependencies, allowing each scenario to reflect a unique trajectory for uncertainty evolution.

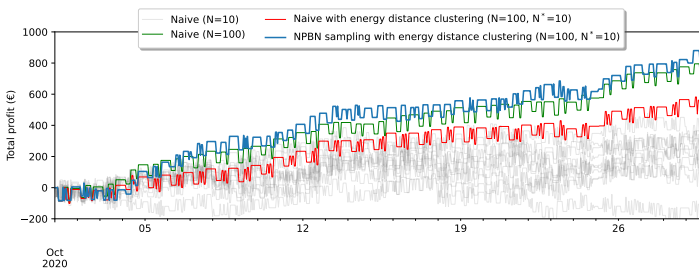


Figure 3.4: Cumulative profit for DAM arbitrage under various approaches of representing price uncertainty. The modelled battery has a usable capacity of 2 MWh, a maximum (dis)charge power of 2.5 MW, and a round-trip efficiency of 98.6%.

3.3. CONCLUSION

This chapter presents methodologies for modelling operational uncertainty, which serves as the cornerstone of the predictive and optimization frameworks throughout this thesis. By introducing the CQRDNN for probabilistic forecasting, we addressed the limitations of traditional quantile regression methods, particularly the issue of crossing quantiles. This advancement ensures consistent quantile estimates, enhancing our ability to capture uncertainties in critical variables such as energy prices and water inflows.

We employed the TPE to optimise regression model performance for simultaneous feature selection and hyperparameter optimization. This dual optimization process fine-tunes models and input data concurrently, leading to improved accuracy and computational efficiency by identifying optimal features and hyperparameters.

We propose the NPBN approach for robust scenario generation, which preserves both marginal distributions and temporal dependencies. This capability is essential for generating realistic multivariate time series scenarios, facilitating informed decision-making in complex systems like energy markets and water management.

Recognizing the computational challenges of handling extensive scenario sets, we explored scenario reduction techniques using energy distance clustering. This method enables the selection of an optimal subset of scenarios that closely approximates the full uncertainty space, which is crucial for applications with limited computational resources by providing a sparse yet statistically representative set of scenarios.

We introduced scenario trees with optimized shapes through a GA to describe the temporal evolution of growing uncertainty. This approach ensures a small complexity representation without compromising the accuracy of uncertainty modelling, effectively modelling the progression of uncertainty over time.

The practical applicability of these methodologies was demonstrated through a proof of concept involving a battery storage system performing DAM arbitrage. The combination of NPBN sampling and energy distance clustering outperformed naive approaches, including a 10 times larger scenario set, underscoring the effectiveness of our methods in optimizing operational decisions under uncertainty.

The methodologies developed in this chapter lay a robust foundation for the subsequent chapters, which will be applied to a real-world case study.

BIBLIOGRAPHY

- [1] Ties van der Heijden, Peter Palensky, and Edo Abraham. “Probabilistic DAM price forecasting using a combined Quantile Regression Deep Neural Network with less-crossing quantiles”. In: *IECON 2021 – 47th Annual Conference of the IEEE Industrial Electronics Society*. 2021, pp. 1–6. DOI: [10.1109/IECON48115.2021.9589097](https://doi.org/10.1109/IECON48115.2021.9589097).
- [2] Ties van der Heijden et al. “Multi-market demand response from pump-controlled open canal systems: an economic MPC approach to pump-scheduling”. In: *Journal of Hydroinformatics* 24 (4 July 2022), pp. 838–855. ISSN: 14651734. DOI: [10.2166/hydro.2022.018](https://doi.org/10.2166/hydro.2022.018).
- [3] Ties van der Heijden et al. “Day Ahead Market price scenario generation using a Combined Quantile Regression Deep Neural Network and a Non-parametric Bayesian Network”. In: *2022 IEEE International Conference on Power Systems Technology (POWERCON)*. 2022, pp. 1–5. DOI: [10.1109/POWERCON53406.2022.9929940](https://doi.org/10.1109/POWERCON53406.2022.9929940).
- [4] Ties van der Heijden et al. “Electricity Price Forecasting in European Day Ahead Markets: A Greedy Consideration of Market Integration”. In: *IEEE Access* 9 (2021), pp. 119954–119966. ISSN: 21693536. DOI: [10.1109/ACCESS.2021.3108629](https://doi.org/10.1109/ACCESS.2021.3108629).
- [5] Roger Koenker and Gilbert Bassett. “Regression Quantiles”. In: *Econometrica* 46.1 (1978), p. 33. ISSN: 00129682. DOI: [10.2307/1913643](https://doi.org/10.2307/1913643).
- [6] J Bergstra, D Yamins, and D D Cox. *Making a Science of Model Search: Hyperparameter Optimization in Hundreds of Dimensions for Vision Architectures*. 2013.
- [7] Jesus Lago, Fjo De Ridder, and Bart De Schutter. “Forecasting spot electricity prices: Deep learning approaches and empirical comparison of traditional algorithms”. In: *Applied Energy* 221. January (2018), pp. 386–405. ISSN: 03062619. DOI: [10.1016/j.apenergy.2018.02.069](https://doi.org/10.1016/j.apenergy.2018.02.069). URL: <https://doi.org/10.1016/j.apenergy.2018.02.069>.
- [8] Miguel Angel Mendoza-Lugo and Oswaldo Morales-Nápoles. “Mapping hazardous locations on a road network due to extreme gross vehicle weights”. In: *Reliability Engineering & System Safety* 242 (2024), p. 109698. ISSN: 0951-8320. DOI: <https://doi.org/10.1016/j.res.2023.109698>. URL: <https://www.sciencedirect.com/science/article/pii/S0951832023006129>.
- [9] Harry Joe. *Multivariate models and multivariate dependence concepts*. CRC press, 1997.
- [10] Anca Hanea, Oswaldo Morales Napoles, and Dan Ababei. “Non-parametric Bayesian networks: Improving theory and reviewing applications”. In: *Reliability Engineering and System Safety* 144 (2015), pp. 265–284. ISSN: 09518320. DOI: [10.1016/j.res.2015.07.027](https://doi.org/10.1016/j.res.2015.07.027). URL: <http://dx.doi.org/10.1016/j.res.2015.07.027>.

- [11] Florian Ziel. “The energy distance for ensemble and scenario reduction”. In: *Philosophical Transactions of the Royal Society A: Mathematical, Physical and Engineering Sciences* 379 (2020), p. 20190431. DOI: [10.1098/rsta.2019.0431](https://doi.org/10.1098/rsta.2019.0431). URL: <https://royalsocietypublishing.org/doi/10.1098/rsta.2019.0431>.
- [12] Gábor J. Székely and Maria L. Rizzo. “Energy statistics: A class of statistics based on distances”. In: *Journal of Statistical Planning and Inference* 143 (8 Aug. 2013), pp. 1249–1272. ISSN: 0378-3758. DOI: [10.1016/J.JSPI.2013.03.018](https://doi.org/10.1016/J.JSPI.2013.03.018).
- [13] N. Grawe-Kuska, H. Heitsch, and Werner Roemisch. *Scenario reduction and scenario tree construction for power management problem*. Vol. 3. July 2003, 7 pp. Vol.3. ISBN: 0-7803-7967-5. DOI: [10.1109/PTC.2003.1304379](https://doi.org/10.1109/PTC.2003.1304379).



4

ELECTRICITY PRICE FORECASTING IN EUROPEAN DAY AHEAD MARKETS

*You're in my system, baby, deep in my system.
You've got me going crazy inside my system.*

Nu:Tone

An ingredient for successfully trading on the energy markets to save costs is the ability to forecast electricity prices. More accurately forecasting electricity prices would allow for better energy planning and management since, in practice, the price is settled after bidding. As explained in Chapter 1, there is a notable trend towards European energy market integration.

In this chapter, we explore European feature importance in Day Ahead Market (DAM) price forecasting models, and apply the knowledge to improve forecasting performance. We propose a greedy algorithm to search over candidate countries for European features to be used in a DAM price forecasting model, that can be applied to several regression and machine learning modelling methodologies. We apply the algorithm to build price forecasting models for the Dutch market, using candidate countries selected through an integrated analysis based on open-source European electricity market data. Feature importance is visualised using an Auto Regressive and Random Forest model, and explained using cross-border flow and DAM price data. Two types of models (LEAR and the Deep Neural Network) are considered as price forecasting models with and without European market features. We show that in the Dutch case, taking European market integration into account improves forecast accuracy with statistical significance.

Parts of this chapter have been published in IEEE Access [1].

4.1. INTRODUCTION

Demand response (DR) is an energy management technique where energy consumers are incentivised to shift their energy use in time [2, 3]. In market based DR, the incentive is economic through variable pricing. The electricity price reflects the availability of (renewable) energy through scarcity of a product. Low prices correspond with an energy surplus and low marginal cost of energy, where high prices correspond with energy scarcity and high marginal cost of energy. The introduction of spot markets allows for a different electricity price in every hour, 30-minutes and even 15-minutes. In Europe, the *Day Ahead Market* (DAM) is the main spot market for trading electricity. On the DAM, energy is traded in hourly blocks with corresponding prices. The DAM is well studied in the context of *Electricity Price Forecasting* (EPF) [4].

The European grid is well connected and the inter-connectivity of countries is expected to increase in the future. In 2002, members of the EU vowed to have 10% of their generation capacity in cross-border transmission capacity [5]. A future "European Supergrid" could even connect the European grid to North Africa [6, 7, 8]. Inter-connectivity of the European grid will help reach greater efficiencies, improve resilience to climate change and will enhance energy flexibility [9]. The development of European infrastructure will improve internal market efficiencies, enhance security of supply and enable *Renewable Energy Sources* (RES) market penetration [5]. Inter-connectivity enables cross-border electricity trading, opening up national electricity markets to foreign demand. These facts already make a strong case for the consideration of European market integration in a DAM price forecasting model. French market features (e.g. load, prices, generation), for example, have been shown to be more important than Belgian features when forecasting the Belgian DAM prices [10]. However, the analysis was limited to one neighbouring country and only a Deep Neural Network (DNN) was applied. Similarly, a study [11] has shown that including *Energy Exchange Austria's* (EXAA) prices as features improves forecast accuracy in all other EU DAM markets, especially in the Dutch and French DAM forecasting models. However, the connection between the Dutch DAM and the EXAA is also shown to be getting weaker over time. Possibly due to the further integration of the Dutch market with the APX UK market. In another study [12], price forecasts of other European markets are used as exogenous input for an Italian DAM forecasting algorithm, significantly improving performance. The effect of European market integration is not only seen in the DAM, but also in the *Intraday Market* (IDM) [13]. In general, the effect of European market integration is understudied in the context of EPF.

Machine Learning (ML) techniques have been shown to be effective at forecasting electricity prices, both in the DAM [4] and the IDM [14, 15]. Specifically, the *MultiLayer Perceptron* (MLP) has been successfully applied to forecast DAM prices in Spain and Pennsylvania-New Jersey-Maryland [16, 17]. The more complex structured *Deep Neural Network* (DNN) was successfully applied in Belgium [18], Nord-Pool markets, Germany, France and Pennsylvania-New Jersey-Maryland [19].

Many other methods have been applied to forecast DAM prices [4]. According to an EPF benchmark study on the Belgian market, a two-layer DNN generally outperforms both statistical and other ML models, given the same features [18]. The *Lasso Estimated Auto Regressive* (LEAR) [19], or fARX-Lasso [20], is the best performing non-ML method and should be considered as a benchmark [19], especially since ML methods have been

shown to not always outperform statistical models [18].

The performance of the different modelling approaches varies over different markets [19], but a recent case-study on the Dutch market is missing in literature. Many statistical methods rely on the calibration of linear relationships. While they can still be powerful modelling approaches, they might not perform well with high-resolution data like hourly prices with high volatility [18]. Price volatility in electricity markets can be pronounced due to the continuous need for balancing supply and demand [21]. It can differ significantly per month, and is subject to external price drivers like energy demand, demand elasticity, congestion, (renewable) energy generation, fuel prices, currency exchange rates and inter-connected electricity markets [22, 21, 23, 10]. With an increasing renewable energy penetration in electricity markets, price volatility is expected to increase due to the intermittent nature of renewables, in the absence of sufficient energy storage [23]. However, effective policy, cooperation between TSO's and intraday trading can presumably prevent a significant increase in price volatility on the DAM [24]. It is possible that as renewable energy penetration increases, price volatility would increase and ML methods would increasingly outperform statistical methods.

To summarize, market integration can be expected to play a large role in price settlement of European Day Ahead Markets. The increasing inter-connectivity may even increase external market influences on national markets. The current state of the art in EPF generally limits market integration features to a single external market, while the inter-connectivity of the grid and different local conditions would make it likely for national markets to be affected by multiple external markets. Also, little clarification is given on the actual market mechanisms that make the markets affect each other. In recent literature, a case study is missing on the Dutch market. And while it is expected that ML methods perform better than statistical methods in times of high price-volatility, this has not been confirmed with statistical significance.

In this chapter we perform an EU wide, data-based analysis of European market feature (e.g. price and load) importance in DAM price forecasting models of European bidding zones. Open-source data from the ENTSO-E transparency platform [25] was used exclusively. Yearly cross-border flows are analysed, after which we apply a *Least Absolute Shrinkage and Selection Operator* (LASSO) [26, 27] estimated Auto Regressive model, and a *Random Forest* [28] model to identify European feature importance (Section 4.4). The results are used to select candidate European countries whose features are to be considered in a Dutch DAM forecasting model. We perform a benchmark using only Dutch features (Section 4.5.2). Then, we propose a greedy approach to search through candidate countries for the best performing combination of features for a DAM forecasting model (Section 4.5.1). We apply two different types of models in the search for market integration features: the LEAR [19, 20] and the DNN. The LEAR is a linear regression model estimated with the LASSO. The DNN will be applied in two different configurations: the *single-market DNN* [18] (SM-DNN) and the *multi-market DNN* [10] (MM-DNN). The SM-DNN [18] forecasts all 24 hourly DAM prices of a bidding zone simultaneously, while the MM-DNN forecasts the 24 hourly prices of multiple bidding zones simultaneously. Temporal variations in relative model forecasting performance will be analysed (Section 4.5.4) using univariate *Diebold-Mariano-tests* (DM-tests) on the hourly forecasts and Kernel Density Estimates DAM prices.

4.2. ELECTRICITY PRICE FORECASTING METHODS

In order to test whether our proposed methodology for including market integration features in a Dutch price forecasting model leads to a performance increase, several benchmarking models are proposed. Using a *naive* forecast as general benchmark, we compare its performance with 4 other Dutch price forecasting models without European features. The *full AutoRegressive* (fAR) and the *fAR with Exogenous variables* (fARX) [29, 20] are compared with the *Lasso Estimated AutoRegressive* (LEAR) [19, 20], consisting of the LASSO- or EN-estimated fARX. In this study we considered both the LASSO- and EN-estimated LEAR, and selected the best performing model based on a preliminary analysis. Since the *Deep Neural Network* (DNN) has recently been shown to be the best performing model in an EPF benchmark for the Belgian market [18], we include it in the benchmark for a Dutch price forecasting model.

The best performing models without European features will be used in the greedy algorithm in order to quantify their performance increase due to the inclusion of European features. The DNN will be included since it has already successfully been applied to improve the accuracy of the Belgian price forecast using French market features [10]. However, we consider two configurations of the DNN. First, we apply the SM-DNN with European features. The SM-DNN is used to forecast the 24 hourly Dutch DAM prices only, while European features are included in the input. Second, we apply and the MM-DNN, where the 24 hourly DAM prices of multiple bidding zones are forecast in the same model [10]. The MM-DNN is depicted in Figure 4.1, where the model is applied to forecast the Dutch and N other bidding zones' hourly DAM prices. We evaluate all models on their forecast accuracy of the Dutch DAM prices only.

4.2.1. LASSO AND ELASTIC-NET

The *Least Absolute Shrinkage and Selection Operator* (LASSO) [26] is a least squares linear regression model, where an additional l_1 -norm penalty is applied to the weights in order to regularise the model and enforce sparsity of the solution. The LASSO solves the optimisation problem

$$\min \frac{1}{2} \|z - \Phi\theta\|_2^2 + \lambda \|\theta\|_1, \quad (4.1)$$

where $z \in \mathbb{R}^{N \times 1}$ is a vector of outputs, $\Phi \in \mathbb{R}^{N \times p}$ is a matrix of features and $\theta \in \mathbb{R}^{p \times 1}$ is a vector of weights. The regularisation parameter $\lambda \in \mathbb{R}$ can be used to control the trade-off between sparsity of the solution and the approximation error.

The *Elastic-Net* (EN) is a linear regression model fit with both an l_1 and l_2 penalty norm on the weights of the model. During model selection, both the penalty gradient on the weights (λ) and the $l_1 l_2$ ratio (ρ) are optimised. A ρ of 0 would result in a Ridge Regression problem, while a ρ of 1 results in a LASSO. The objective function when fitting the EN is:

$$\min \frac{1}{2} \|z - \Phi\theta\|_2^2 + \lambda \rho \|\theta\|_1 + \frac{\lambda(1-\rho)}{2} \|\theta\|_2^2, \quad (4.2)$$

where variables have the same representation as in the LASSO objective (4.1), and ρ represents the $l_1 l_2$ ratio.

RANDOM FOREST

The *Random Forest* (RF) algorithm was developed by Breiman [28]. It is an ensemble classification or regression approach using random regression trees, hence the name Random Forest. The RF is a collection of tree-predictors whose output - in the case of regression - is an unweighted average of the outcomes of the separate trees:

$$\bar{h}(x) = \frac{1}{K} \sum_{k=1}^K h(x; \theta_k), \quad (4.3)$$

where \bar{h} is the averaged output of regression trees $h(x; \theta_k)$ with input x , feature space θ , subspace $\theta_k \subset \theta$ and K regression trees. The RF estimates a feature's importance based on the amount of splits in the trees in comparison to the amount of samples the feature splits. It is also referred to as the 'Gini importance' or the 'mean decrease impurity' [30].

KERNEL DENSITY ESTIMATION

A kernel density is a non-parametric method that can be used to estimate the probability density function (PDF) of a random variable. If (x_1, x_2, \dots, x_n) is a sample from the univariate distribution f , its kernel density estimator is then described by

$$\hat{f}_h(x) = \frac{1}{nh} \sum_{i=1}^n K\left(\frac{x - x_i}{h}\right), \quad (4.4)$$

where K is the kernel (in our case we have applied the Gaussian kernel function) and h is the bandwidth (in our case this has been selected using Scott's method [31]). The KDE has been applied using the Scipy python package [32].

4.2.2. LASSO ESTIMATED AUTO REGRESSIVE MODEL

The *Lasso Estimated Auto Regressive* (LEAR) is a fARX-model estimated using the LASSO (Appendix 4.2.1) [20, 19]. For DAM forecasting considered here, the fARX is given by the following formula:

$$\begin{aligned} p_{d,h} = & \sum_{i=1}^{24} (\beta_{h,i} p_{d-1,i} + \beta_{h,i+24} p_{d-2,i} + \beta_{h,i+48} p_{d-3,i}) \\ & + \beta_{h,73} p_{d-7,h} + \sum_{j=1}^3 (\beta_{h,j} p_{d-j}^{\min} + \beta_{h,j} p_{d-j}^{\max} + \beta_{h,j} p_{d-j}^{\text{avg}}) \\ & + \beta_{h,83} z_{d,h} + \beta_{h,84} z_{d-1,h} + \beta_{h,85} z_{d-7,h} + \sum_{k=1}^7 \beta_{h,85+k} D_k \\ & + \sum_{k=1}^7 \beta_{h,92+k} D_k z_{d,h} + \sum_{k=1}^7 \beta_{h,99+k} D_k p_{d-1,h} + \varepsilon_{d,h}, \end{aligned} \quad (4.5)$$

where $p_{d,h}$ is the price on day d and hour h , β are the weights or coefficients, p_d^{\min} , p_d^{\max} and p_d^{avg} are the minimum, maximum and average price of day d , $z_{d,h}$ is the logarithm of the load for historic data, and the load forecast of day d , D_k are weekday dummies for

all days of the week where holidays are all 0, and ε is the model error. The model can be written more compactly as

$$p_{d,h} = \sum_{i=1}^n \beta_{h,i} X_{d,h,i} + \varepsilon_{d,h}, \quad (4.6)$$

where $X_{d,h,i}$ are the $n = 106$ regressors or features in Equation (4.5).

The model is trained by solving the least-squares estimate of the model, with either an l_1 -norm for the LASSO-estimation or an $l_1 l_2$ -norm for the EN-estimation. With sufficiently large penalty term some weights will become (near) zero [33], effectively performing variable selection. More information on the LASSO- or EN- estimation can be found in Section 4.2.1.

4

4.2.3. DEEP NEURAL NETWORK

A DNN is a feed forward *Artificial Neural Network* (ANN) that is trained using back propagation. It contains a minimum of 3 layers: an input layer, an output layer and at least 1 hidden layers. Following the standard notation in EPFs, we will use the name MLP for ANNs with 1 hidden layer and DNN for ANNs with 1 or more. Although the definition of what is "deep" might be debatable, it is out of the scope of this paper and we simply follow the current standard terminology used in literature [18, 10, 19].

The DNN is trained with the *Adaptive Moment Estimation* (ADAM) [34]. Figure 4.1 shows an MM-DNN with 2 hidden layers (z_1, z_2), where n_f is the number of input features in the input layer x , n_1 and n_2 are the number of nodes in hidden layer 1 and 2, respectively. The output layer (P) consists of 24 nodes for each country included in the forecast, one for each hour of the day (h). In the case of Figure 4.1, the DNN is used to forecast Dutch DAM prices together with a variable number (N) of other bidding zones. In the case of a DNN with one hidden layer, the output layer is fully connected to the first hidden layer.

Features are optimised as hyperparameters similarly to [10], where a single binary choice-option for country load features is added to the search space. In our case these are the historic load, and load forecast of the countries considered in the forecast, which are added or removed through a single binary choice-option per country. Historic prices are always included as model features. The TPE algorithm [35] was applied to efficiently optimize features and hyperparameters.

4.2.4. DIEBOLD-MARIANO TEST

The DM-test is a statistical measure to compare accuracy of two forecast timeseries. Given a target timeseries (y_t) and two forecasts ($\hat{y}_{1t}, \hat{y}_{2t}$), the error timeseries ($e_{i,t}$) are calculated (Equation 4.7a). In this chapter we apply the Mean Absolute Error (MAE) (Equation (4.7b)) as loss function (\mathcal{L}). Based on this, a loss differential timeseries (δ_t) is calculated (Equation 4.7c), which is then used to perform the one-sided DM-test.

$$e_{i,t} = \hat{y}_{i,t} - y_{i,t}, \quad i = 1, 2 \quad (4.7a)$$

$$\mathcal{L}_{i,t} = \|e_{i,t}\|_1, \quad (4.7b)$$

$$\delta_t = \mathcal{L}_{1,t} - \mathcal{L}_{2,t}, \quad (4.7c)$$

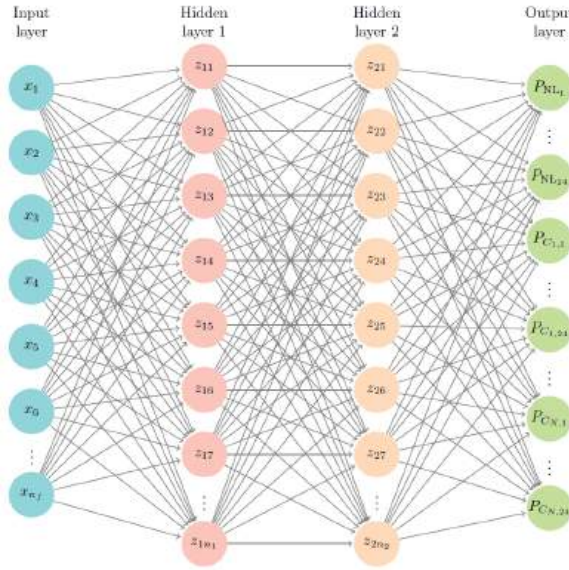


Figure 4.1: Multi-Market Deep Neural Network (MM-DNN) with input layer (x), two hidden layers (z_1, z_2) and output layer (P). The MM-DNN is applied to forecast Dutch DAM prices ($P_{NL,h}$) simultaneously with N other bidding zones' prices ($P_{C_{x,h}}$, with $x \in (1, \dots, N)$ and $h \in (1, \dots, 24)$). If $N = 0$, the DNN forecasts a single market's prices, the Dutch prices, only. If $N = 1$, the dual-market DNN as proposed in [10] results.

The *one-sided DM-test* tests the null hypothesis (H_0) that forecast timeserie 1 is more accurate than or equally accurate as forecast timeserie 2. The alternative hypothesis (H_1) is that forecast 2 is more accurate than forecast 1. In the context of DAM forecasting, the DM-test can be applied to either the full DAM timeseries (e.g. multivariate DM-test) or to evaluate forecasting performance for each hour separately (e.g. univariate DM-test).

$$H_0 : E(\delta_t) \leq 0, \quad (4.8a)$$

$$H_1 : E(\delta_t) > 0 \quad (4.8b)$$

4.2.5. GREEDY ALGORITHM FOR EUROPEAN FEATURE SEARCH

In order to include EU market integration in a bidding zone's DAM forecasting model, we propose a greedy algorithm as defined in Algorithm 2. We apply the algorithm to prevent over-fitting on the large amount of available data by selecting only the relevant features. Starting with a candidate set of features (e.g. Θ_1 contains only Dutch features), a model (\mathcal{M}_i) is trained and its hyperparameters are optimised. The model is evaluated to test its predictive performance (p_i) on the bidding zone of interest's prices, in our case the Dutch bidding zone's, and added to a set (\mathcal{P}_i) together with model performance (p_i) and features (Θ_i) of the current iteration (i). After the first iteration, all candidate countries (Φ) are consecutively added to the latest feature set (Θ_i), to be used in the price forecast-

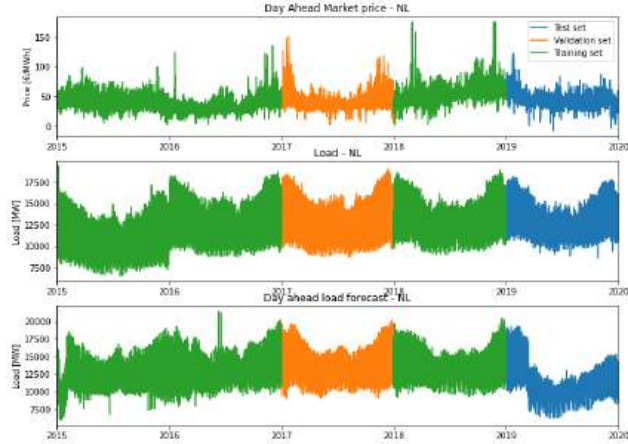


Figure 4.2: Dutch historic price, load and load-forecast with train, validation and test splits indicated for model training.

ing model. The model is trained, its hyperparameters are optimised, and its forecasting performance on the bidding zone of interest (P_j) is evaluated and added to set (P). After all candidate countries are evaluated, the best performing model's features are selected from the set (P). Those features are added to the feature set (Θ_i), while they are removed from the candidate feature set (Φ). The procedure will then be repeated until either performance stops increasing, or all candidate features are added to the model.

The candidate set of features (Φ) was selected using the data analysis described in Section 4.4, where all countries that result from at least one of the analyses (cross-border flow, ARX or RF) are selected. The candidate set of country features used for the Dutch market are summarised in Table 4.1.

Our proposed greedy algorithm can be applied to any model that allows for a large amount of features, and assists with preventing over-fitting. In this chapter we independently apply the algorithm to three different modelling approaches (Section 4.5.3). We perform both hyperparameter optimisation and feature selection on the validation set of the Dutch DAM prices. Finally, all models are evaluated on the test set to evaluate the increase in model performance. No model selection is performed on the test set.

4.3. DATA AND TOOLS

The data used for this study is taken from the ENTSO-E transparency platform [25]. Historic DAM price-series, historic loads and historic day ahead load forecasts are used. The data was split in train-, validation- and test-sets, as depicted in Figure 4.2. Data from 2015-2019 was used, with the year 2019 being used as test data. In order to be able to include the most recent information in training, 2017 was taken as validation data instead of 2018. A single split limits the data leakage that occurs in the first week of the 2018, where data from the validation set is used in the lagged features. There still is no data leakage from the test set.

Algorithm 2: GreedyFeatureSearch(Θ_1, Φ)

```

1  $i \leftarrow 1$ 
2  $\mathcal{P} \leftarrow \emptyset$ 
3  $p \leftarrow \emptyset$ 
4  $\mathcal{M} \leftarrow \emptyset$ 
5  $\mathcal{M}_i \leftarrow \text{TrainModel}(\Theta_i)$ 
6  $p_i \leftarrow \text{EvaluateModel}(\mathcal{M}_i)$ 
7  $\mathcal{P}_i \leftarrow (\Theta_i, p_i, \mathcal{M}_i)$ 
   while ( $p_i \leq p_{i-1} \vee i > I$ )  $\wedge$   $|\Phi| > 0$  do
   | // execute algorithm while performance improves, or until all
   |   country features are included in the model
8    $P \leftarrow \emptyset$ 
9    $M \leftarrow \emptyset$ 
   for  $j = \{1, \dots, |\Phi|\}$  do
   | // train and evaluate the  $i^{\text{th}}$  model by adding a single country's
   |   ( $j$ ) features at a time
10  |  $M_j \leftarrow \text{TrainModel}(\{\Theta_i \cup \Phi_j\})$ 
11  |  $P_j \leftarrow \text{EvaluateModel}(M_j)$ 
   end
12   $j \leftarrow \text{argmin}_j(P)$ 
13   $\Theta_{i+1} \leftarrow \{\Theta_i \cup \Phi_j\}$ 
   | // add best performing country's features ( $\Phi_j$ ) to  $i^{\text{th}}$  model
14   $\Phi \leftarrow \{\Phi \setminus \Phi_j\}$ 
15   $i \leftarrow i + 1$ 
16   $p_i \leftarrow P_j$ 
17   $\mathcal{M}_i \leftarrow M_j$ 
18   $\mathcal{P}_i \leftarrow (\Theta_i, p_i, \mathcal{M}_i)$ 
   end
19 return  $\mathcal{P}$ 

```

The LEAR models are build and trained, and the features were Z-score standardised using the scikit-learn python package [30]. The DNN was made using Tensorflow [36] and trained with the ADAM optimiser [34]. The TPE SMBO algorithm is implemented using the Python Hyperopt package [35]. The DM-tests are performed using the python EPF-toolbox [19].

4.4. EUROPEAN FEATURE IMPORTANCE ANALYSIS

In order to identify possible European features that influence the Dutch market, a EU-wide analysis is performed on cross-border flow data and DAM prices.

European cross-border flow data [25] was analysed to identify trading patterns between countries. Figure 4.3 shows the cross-border flows between countries whose data is available through the ENTSO-E transparency platform. The data shows that France is the largest net exporter of the EU, while Italy is the largest net importer of the EU. The

Nordic markets (FI, SE, DK and NO) seem to be a relatively independent block, mostly trading amongst each other.

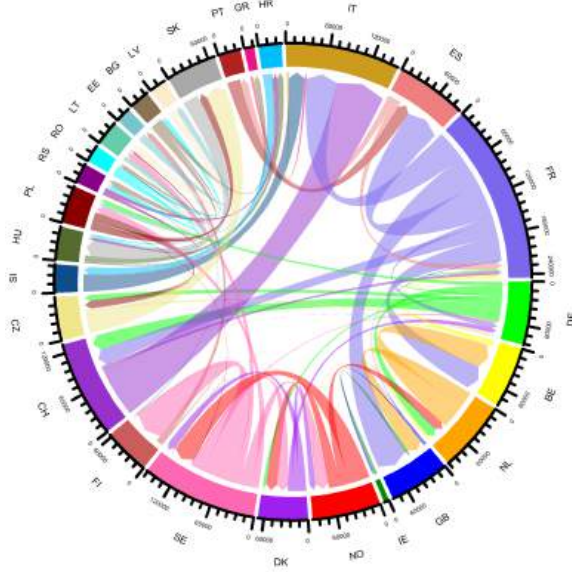


Figure 4.3: Cross-border flows between European countries, units in [MWh/year] based on 2018 data [25]

For each bidding zone, a LASSO-estimated ARX-model is trained and its weights are analysed. The model is estimated by fitting

$$p_{d,h} = \sum_{i=1}^N \beta_i p_{i,d-1,h} + \sum_{j=1}^M \beta_{j+N} z_{j,d,h} + \varepsilon_{d,h}, \quad (4.9)$$

where N is the number of bidding zones, M the number of countries, $p_{i,d,h}$ the price of bidding zone i and $z_{j,d,h}$ the load forecast of country j , on day d and hour h , β are the weights or coefficients, and $\varepsilon_{d,h}$ the model error. The analysis allows us to gain insight in the relative importance of European features with respect to domestic features. The analysis fits the general EPF modelling approach, where historic prices and the load (forecast) are used to forecast next day's price. Figure 4.4a shows the normalised weights resulting from the ARX-models. The incoming arrow width indicates the relative weight of transmitting country features for the receiving country's price forecasting model. For countries containing multiple bidding zones, the weights of the bidding zones are summed. Weights are masked at a minimum of 5% normalised importance.

Since the LASSO estimated ARX is a linear model, it is possible that non-linear relationships are not well reflected in the analysis. To overcome this limitation, a RF-model is applied in similar fashion. The RF is trained to forecast the 24 hourly DAM prices of a bidding zone simultaneously, using the same features as the ARX-model. The RF is able

to capture non-linear relationships, and can similarly show relative features importance. More information on the RF model can be found in Appendix 4.2.1. Figure 4.4b shows the normalised feature importance resulting from the RF-models. The RF seems to give a higher importance to domestic market features compared to the ARX.

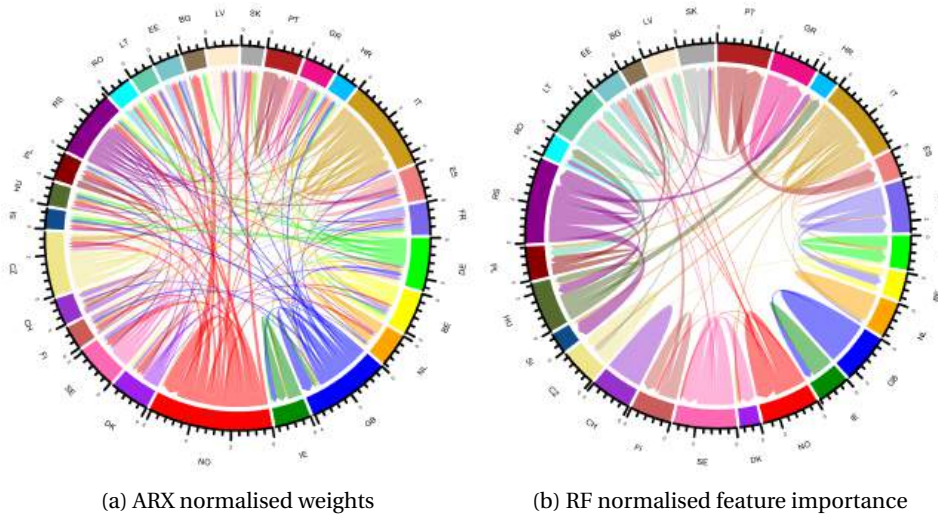


Figure 4.4: Normalised weights for the ARX model (a) and normalised feature importance for the RF model (b) forecasting the DAM prices of day d , using the prices of day $d - 1$ and the load forecast of day d of all European bidding zones and countries. The weights of the load and separate bidding zone's prices are summed for each country.

Both the ARX- and RF-analyses show that Norwegian market features seem to perform well in many other European price forecasting models, while Norwegian models perform well using only Norwegian features. Compared to Sweden, which exports more in an absolute sense, Norwegian features perform well in a large number of forecasting models of other European markets. This could be due to the amount of storage present in the Norwegian system, possibly allowing them to export more dynamically. It would enable them to export at times the merit-order curve in other bidding zones is relatively high and steep, expressing more influence on price settlement. Another explanation could be the relative large transmission losses that come with the overseas cables that connect Norway to many other European markets, making high foreign prices necessary to make up for the transmission losses. Figure 4.5a shows the correlation matrix of Norwegian export and the DAM Prices of the importing markets. The figure shows that Norwegian exports correlates positively with the importing market's DAM prices. The correlation is the strongest in Denmark and Sweden, but is positive for all neighbouring markets. The positive correlation between Norwegian export and Swedish prices is as positive as to other connected market prices. This indicates that the difference between overland- and overseas-connected markets, and as such the possible effect of transmission losses on export behaviour, can't be observed to have an effect on the correlation between Norwegian export and the neighbouring price.

The Spanish and Portuguese markets seem to function as an independent block from the other EU markets, with French features having low importance in their price models. This could partially be explained by the Pyrenees separating them, which makes overland transmission cables relatively expensive [37]. This would result in the relatively low degree of interconnection of Spain with other EU member states [38].

Even though France is the largest net exporter of electricity, its feature importance in neighbouring market models is relatively low. One explanation could be the large share of nuclear power in France, making its export possibilities relatively inflexible. This makes it possible that the information in French features is captured in the historic prices of those markets, and less information from France is needed to quantify its effect on price settlement. Figure 4.5b shows the correlation matrix of French electricity export and the importing market's DAM prices. The figure shows that the correlation between electricity export and DAM prices is weak, and in some cases negative. This can similarly explain the relative low importance of Italian features in other markets' models, regardless of its high net import. Figure 4.6 shows the correlation matrix of Italian import and the transmitting market's DAM prices. Again, only weak correlations are observed. A constant Italian demand in foreign markets (e.g. Slovenian, Swiss and French) could be captured in the historic prices of those markets, and less Italian information is needed to quantify this effect. Although cumulatively, Italian feature importance is relatively high in both the ARX- and RF-models.

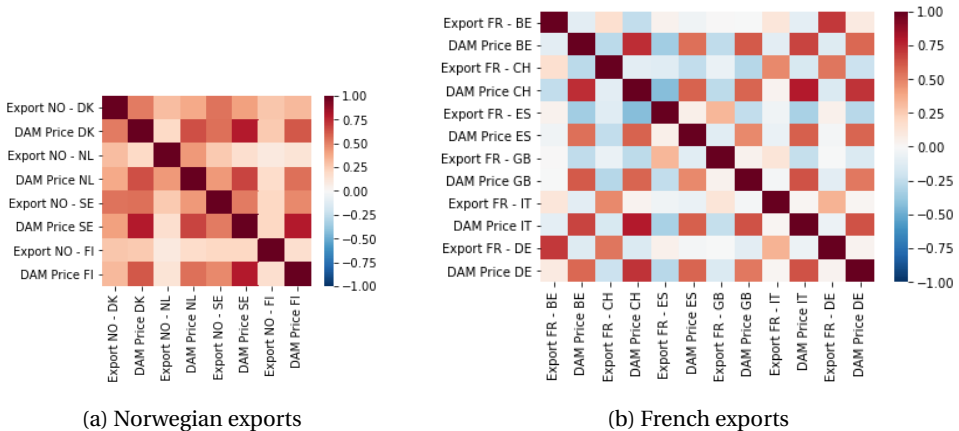


Figure 4.5: Correlation matrices of Norwegian (a) and French (b) electricity exports with importing markets' data. Based on 2018 data.

Germany and Switzerland trade a significant amount of electricity, but their features are not selected each other's price forecasting model. Germany has a large renewable energy share, making constant trading behaviour less likely. However, it could be that a part of the export is from intraday trading. If that is the case, cross-border training would have a smaller effect on DAM prices.

Both the ARX- (Figure 4.4a) and the RF-analyses (Figure 4.4b) show there is no straightforward relationship between cross-border flows and feature importance in a foreign

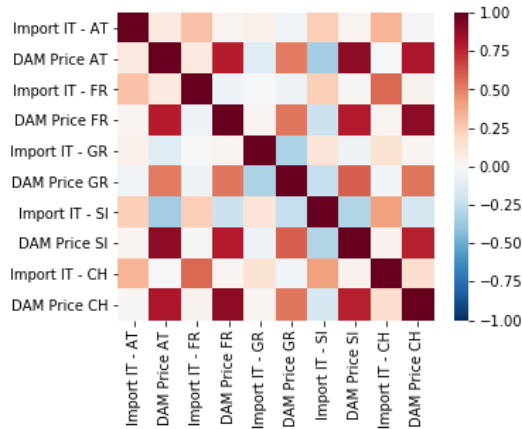


Figure 4.6: Correlation matrix of Italian electricity import and the DAM prices of exporting markets. Based on 2018 data.

price forecasting model. Norwegian features have high importance in many markets, while French feature importance is limited. France exports a lot more electricity than Norway, but their interconnectivity, means of generation and, as such, their inherent flexibility are vastly different. This can also be seen in the correlation matrix of their export and the importing markets' DAM prices. Italian features appear in many ARX-models (Figure 4.4a), but with low importance compared to other markets regardless of its large net import. A possible explanation is the ability of a bidding zone to time its import and export with advantageous prices. However, more research is necessary to conclude this definitely.

For the Dutch price model, Table 4.1 summarises the results of the analysis performed in this section. It stands out that directly connected markets (BE, FR, NO and GB) arise from the ARX- and RF-analyses. The ARX- and RF-models identify second-order market effects through Danish (DK), French (FR) and Italian (IT) features. German features are considered due to the relatively large amount of trading between the two markets. For the Belgian, British and German price forecasting models, Dutch features seem to contain information on their prices as well. However, for the French, Italian, Danish and Norwegian models, Dutch features are not of high importance.

4.5. DUTCH DAM PRICE FORECASTING WITH EU MARKET INTEGRATION

To search for the best combination of European features for several Dutch price forecasting models, we apply the greedy algorithm (Algorithm 2) to three modelling approaches independently. The algorithm will be applied to search over the previously defined candidate countries (Φ). Table 4.1 shows the summarised results for the European feature candidate selection, applied to the Dutch market. For countries containing multiple bidding zones (NO, DK, IT), a single bidding zone (NO-2, DK-1, IT-NORD) is selected for the remaining analysis.

Table 4.1: Candidate countries to be included in the search for Dutch price forecasting features, based on cross-border flows, ARX-, and RF feature importance. A country is selected as candidate when it shows up in at least one of the analyses.

Cross-border flows	LASSO	Random Forest
Germany	Norway	Italy
Norway	Italy	France
Belgium	Belgium	
Great Britain	Denmark	
France	Great Britain	

4.5.1. MODEL TRAINING

For model training of the LEAR and DNN, two slightly different approaches are taken. In the LEAR models, all fARX-variables are considered possible features for the candidate countries. The penalty-factors (λ , ρ) are optimised on the validation set. For the DNN, a feature- and hyperparameter search is performed using the TPE algorithm (Section 4.2.3). The search space (Φ) that we have defined for the DNN's is shown in Table 4.2. The best performing models, evaluated on the validation set, are selected for all modelling approaches.

4.5.2. DUTCH BENCHMARK

In order to be able to say whether the inclusion of European features improves the performance of the Dutch forecast, a benchmark is performed using the Naive, fAR, fARX [29, 20], LEAR [20, 19] and DNN [18] models without European features. For the fAR, fARX and LEAR, a single model is trained for each hour of the day. While the DNN is applied to forecast the 24 prices simultaneously.

The results in Table 4.3 show that the LEAR sets a tough benchmark to beat, outperforming the DNN. Figure 4.7a shows the results of the multivariate DM-test. The test confirms that the LEAR model's forecast is significantly more accurate than all other forecasts using only Dutch features, while the DNN's forecast is significantly more accurate than all others' but the LEAR's.

Table 4.2: TPE search space for the DNN models. Load features are added as a hyperparameter for every country that is considered in the forecast.

Hyperparameter	Variable type	Search space
Number of layers	Integer	[1,2]
Nodes per layer	Integer	Layer 1: 50 - 450 Layer 2: 50 - 250
Dropout rate	Continuous	0 - 0.5
Batch size	Integer	$7^1 - 7^4$
Regularisation (l_2 -norm)	Continuous	$1e^{-5} - 5e^{-2}$
Batch normalisation	Binary	[False, True]
Random seed	Integer	1 - 300
Load features	Binary	[False, True]

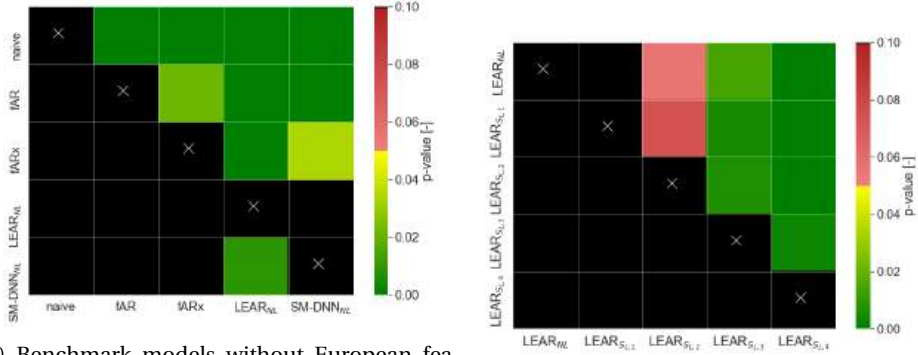
Table 4.3: Performance on the test set (2019) of the benchmark models for Dutch DAM price forecasting.

	Naive	fAR	fARX	LEAR	DNN
MAE [€/MWh]	5.68	4.78	4.63	4.40	4.52
rMAE [-]	1	0.85	0.82	0.78	0.80
sMAPE [%]	14.45	11.91	11.70	11.00	11.36

4.5.3. GREEDY SEARCH FOR EUROPEAN FEATURES

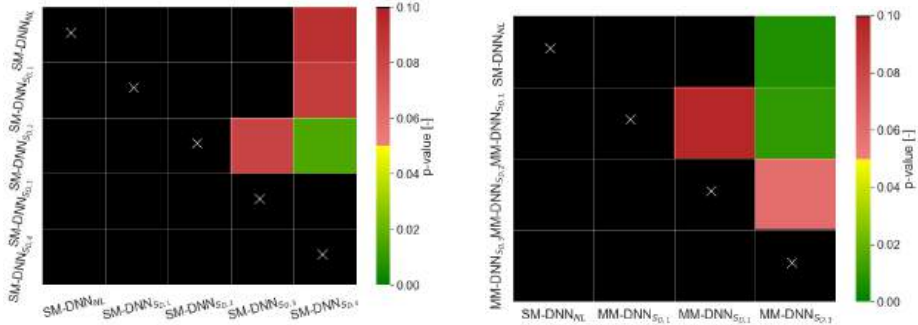
Algorithm 2 is applied to search for the best feature combination in a Dutch DAM forecasting algorithm. The LEAR and DNN models are applied in the search for European features, where the DNN is both applied to forecast the Dutch price only (SM-DNN), and as a multi-market forecasting model (MM-DNN). All models are evaluated for their ability to forecast Dutch DAM prices only. Table 4.4 shows the forecast metrics of the LEAR models, showing an increase in accuracy as features from more countries are included. Model performance stopped increasing after 5 added countries (GB, DK, NO, FR and DE). The largest improvement can be found after the second and fourth iteration, when Danish and French features are included in the model. The uneven increase in performance could mean that there are system effects in price settlement, which are hard to quantify using only two markets. The $LEAR_{S_{all}}$ model using all European features shows similar performance to the LEAR with features from set $S_{L,1}$. It still has improved performance over the LEAR model with only Dutch features. This can be explained by the strong regularisation ability of the LASSO, effectively enforcing sparsity in the solution. However, there is still some degree of over-fitting resulting in a lower loss than most models with less features. Figure 4.7b shows the results of the multivariate DM-test of the forecasts. It shows that as features from more countries are included in the model, the performance increases significantly. This leaves the LEAR with features from set $S_{L,5}$ as statistically significant best performing LEAR-model.

Table 4.5 shows the results from the European feature search applied to the SM-DNN. No significant increase can be seen after the first iteration, where British features are added to the model. After three iterations, test performance increased with respect to



(a) Benchmark models without European features

(b) LEAR models with European features



(c) SM-DNN models with European features

(d) MM-DNN models with European features

Figure 4.7: Multivariate DM-test results of the Dutch DAM benchmark models (a), the LEAR models with European features (b), the SM-DNN models with European features (c), and the MM-DNN models with European features (d). In the figure, the color indicates the p-value (green-yellow: $p \leq 0.05$, light red-dark red: $0.5 > p > 0.1$, black: $p \geq 0.1$) of the one-sided DM-test on whether the forecast of the model on the X-axis is more accurate than the forecast of the model on the Y-axis.

the Dutch-only model. However, the fourth iteration resulted in the model with the lowest test loss. Interestingly, the same countries except Germany are selected as in the LEAR model in different order. Model performance decreased after the second iteration, while the validation loss decreased. This could indicate that relevant market dynamics can change depending on the year. The inclusion of Norway lead to the largest loss decrease, which can possibly be explained by Norway's high feature importance found in Section 4.4. Figure 4.7c shows the results of the multivariate DM-test between the forecasts of the SM-DNN's. It shows little statistical significance in improved forecast accuracy. The model with features from set $S_{D,4}$ does show some significant performance increase. The SM-DNN with features from set $S_{D,4}$ has the most convincing p-values for improved forecast accuracy compared to models with features from sets NL , $S_{D,1}$ and $S_{D,3}$. In general, the forecast error decreased by including more European features.

Even though not all improvements are statistically significant, the final model including features from set $S_{D,4}$ is arguably better than the DNN with only Dutch features. The SM-DNN $_{S_{all}}$ model with all European features shows a large performance decrease, even compared with the SM-DNN using only Dutch features. This indicates that even though the degree of l_2 regularisation is taken as a hyperparameter, the model is hard to train with this amount of features.

Table 4.6 shows the performance of the models generated in the European feature search for the MM-DNN. The model is trained by minimizing the MAE of the price forecasts over all countries included in the model. Naturally, trade-offs are made between, for example, Dutch and French price forecasting accuracy. This could both lead to a performance decrease due to trade-offs, or to a performance increase by preventing overfitting. The greedy algorithm select the same markets in the same order as the single market DNN, but stops one iteration sooner.

The MM-DNN with features from $S_{D,2}$ and $S_{D,3}$ outperform the single market DNN with the same features. Indicating that forecasting prices of multiple markets could indeed lead to better single-market performance. Forecast accuracy generally improved with the inclusion of more European features. The MM-DNN with countries from set $S_{D,3}$ is significantly better than all other MM-DNN models and the DNN using only Dutch features. Although the significance of the improvement from $S_{D,2}$ to $S_{D,3}$ is debatable. The MM-DNN $_{S_{all}}$ model with all European features shows a large performance decrease. The rMAE larger than 1 shows the forecast performance is lower than the naive model. The larger performance decrease in the MM-DNN could be explained by a trade-off between target accuracy's. The loss function while training the model combines the losses for all bidding zones, which could result in a trade-off between price forecasting performance in the Dutch and other bidding zones.

Table 4.7 shows the countries whose features are added in every iteration and for all applied modelling approaches. Table 4.8 shows the improvements of the applied modelling approaches when European market integration features are included in the model. All approaches show improvements with an increasing number of market integration features. For the Netherlands, the first countries whose features are included by the greedy algorithm are Great Britain and Denmark for all modelling approaches. French features are included in all modelling approaches, and in some cases Norwegian and German features are included as well. The third country added by the greedy algorithm differs between the LEAR and the DNN's. In the LEAR, Norway is chosen as third external market, while in the DNN French features are included. This could indicate that the relationship between the Norwegian market and Dutch prices are more linearly approachable than the relationship between the Dutch price and French market. A possible explanation is that the effect of the dynamics between the French and British market on the Dutch price, are better captured in the DNN's.

The largest improvements are found in the MM-DNN, but it doesn't perform better than the LEAR. The large relative improvement of the MM-DNN could mean that market integration dynamics are better captured by non-linear relationships, resulting in a larger possible improvement in non-linear models in comparison to linear models.

The SM-DNN doesn't perform as well as the MM-DNN, which could be explained by two factors: during training, it is possible that the MM-DNN's were able to overcome

local optima when different features are included. This would result in improvements in accuracy that are not due to the information in the data, but due to the training process. Another factor could be the prevention of over-fitting by generalizing tasks [10]. However, extensive optimisation of the DNN-type model performance was not within the scope of the research. Meaning that it is possible that other DNN configurations or other training methods could result in DNN models that outperform the LEAR.

Table 4.4: Dutch DAM LEAR models with European features. Notation: $S_{L,1} = \{NL, GB\}$, $S_{L,2} = \{S_{L,1}, DK\}$, $S_{L,3} = \{S_{L,2}, NO\}$, $S_{L,4} = \{S_{L,3}, FR\}$, $S_{L,5} = \{S_{L,4}, DE\}$, S_{all} includes all European features in the model.

	NL	$S_{L,1}$	$S_{L,2}$	$S_{L,3}$	$S_{L,4}$	$S_{L,5}$	S_{all}
MAE [€/MWh]	4.40	4.39	4.35	4.33	4.29	4.26	4.38
rMAE [-]	0.78	0.77	0.77	0.77	0.76	0.75	0.77
sMAPE [%]	11.00	11.02	10.89	10.85	10.76	10.69	10.92

Table 4.5: Single-market DNN forecasting models with European features. Notation: $S_{D,1} = \{NL, GB\}$, $S_{D,2} = \{S_{D,1}, DK\}$, $S_{D,3} = \{S_{D,2}, FR\}$, $S_{D,4} = \{S_{D,3}, NO\}$, S_{all} includes all European features in the model.

	NL	$S_{D,1}$	$S_{D,2}$	$S_{D,3}$	$S_{D,4}$	S_{all}
MAE [€/MWh]	4.52	4.52	4.58	4.49	4.43	5.61
rMAE [-]	0.80	0.80	0.81	0.79	0.78	0.99
sMAPE [%]	11.36	11.31	11.47	11.26	11.08	13.79

Table 4.6: Multi-market DNN forecasting models, evaluated on Dutch price forecasting performance only. Notation: $S_{D,1} = \{NL, GB\}$, $S_{D,2} = \{S_{D,1}, DK\}$, $S_{D,3} = \{S_{D,2}, FR\}$, S_{all} includes all European features in the model.

	NL	$S_{D,1}$	$S_{D,2}$	$S_{D,3}$	S_{all}
MAE [€/MWh]	4.52	4.53	4.45	4.36	6.29
rMAE [-]	0.80	0.80	0.79	0.77	1.11
sMAPE [%]	11.36	11.38	11.19	10.95	15.33

Table 4.7: Countries whose features are selected by the greedy algorithm for every iteration and per model type.

	LEAR	SM-DNN	MM-DNN
Iteration 1	GB	GB	GB
Iteration 2	DK	DK	DK
Iteration 3	NO	FR	FR
Iteration 4	FR	NO	-
Iteration 5	DE	-	-

Table 4.8: Performance increase of the applied modelling approaches due to the inclusion of market integration features.

	LEAR	DNN	MM-DNN
Δ MAE [%]	3.1	2.0	3.5
Δ rMAE [%]	3.85	2.5	3.75
Δ sMAPE [p.p.]	0.31	0.29	0.41

4.5.4. TEMPORAL VARIATION IN PERFORMANCE

While the multivariate DM-tests give a good relative representation of forecast accuracy, electricity prices are known to be more volatile in some hours than others. Figure 4.8 shows the Kernel Density Estimates (see Appendix 4.2.1) of the Dutch DAM prices in August and October 2019. It can be seen that the DAM price behaves differently throughout the day, with low price volatility in the early morning and late evening, and more volatile prices during midday. Figure 4.9 shows the univariate DM-test of LEAR model with features from $S_{L,5}$ against the benchmark LEAR and DNN, $DNN_{S_{D,4}}$ and $MM-DNN_{S_{D,3}}$. It can be seen that the LEAR forecasts are more accurate than the DNN models' forecasts mostly at hours with low price volatility. Figure 4.10 shows the same DM-test but applied to model $MM-DNN_{S_{D,3}}$. It can be seen that the MM-DNN forecasts are more accurate than the LEAR type model forecasts at times with some degree of volatility, but not when it is too high. These months have been chosen for the sake of simplicity, the results can also be seen in other months. Renewable energy generation forecasts are not included as features, but could assist with forecasting highly volatile prices. The analysis indicates that as prices are becoming more volatile, stochastically trained non-linear models start outperforming mathematically optimised and regularised linear models. This makes the DNN modelling approach worth considering for the future Dutch DAM forecast, as it is possible that electricity prices will become more volatile in the future [23].

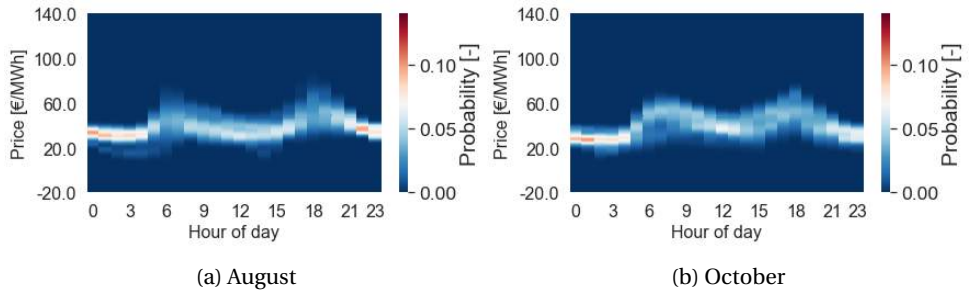


Figure 4.8: Kernel density estimates of Dutch DAM prices in August (a) and October (b) 2019. The X-axis shows the hours of the day, the Y-axis shows the price in [€/MWh], and the color shows the probability of occurrence [-].

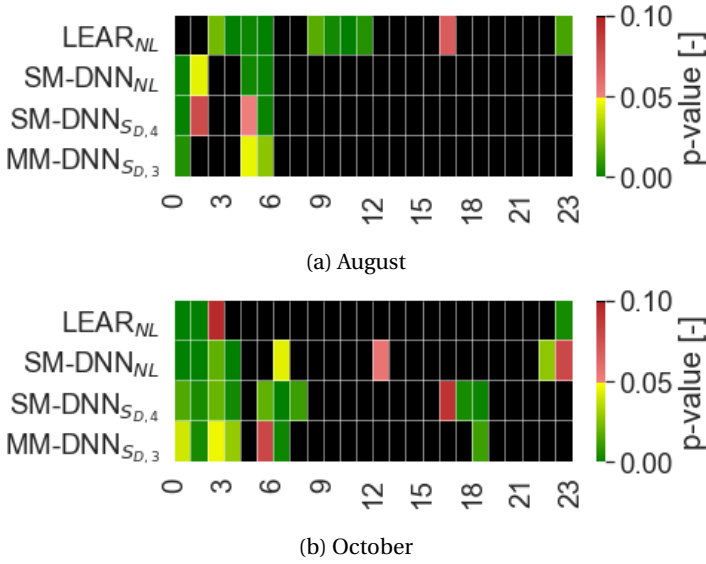


Figure 4.9: Univariate DM-test of LEAR_{SL,5} model's hourly forecasts in August (a) and October (b), being more accurate than the hourly forecasts of the models on the Y-axis.

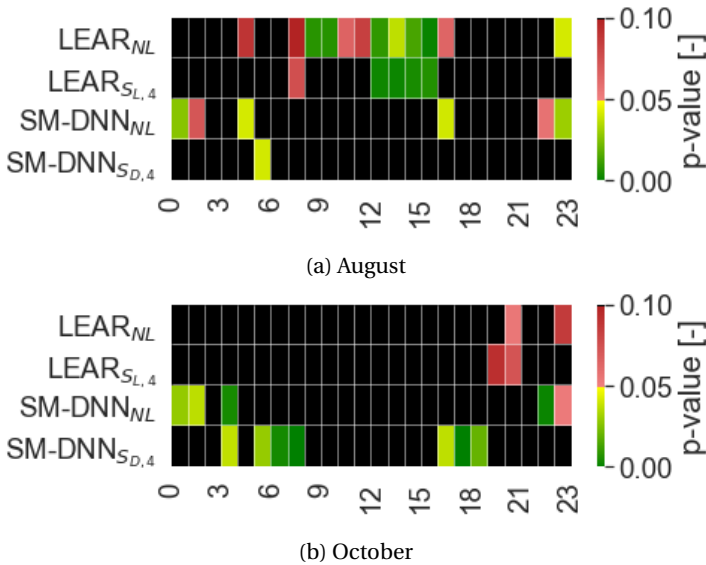


Figure 4.10: Univariate DM-test of MM-DNN_{S_D,3} model's hourly forecasts in August (a) and October (b), being more accurate than the hourly forecasts of the models on the Y-axis.

4.6. CONCLUSION

In this chapter, we propose a method for searching optimal combinations of European features in DAM price forecasting models. By using the Dutch market as a case study, we show that taking European market integration into account in regression and machine learning models can improve the forecasting performance of the best performing DAM models. We identify and visualize European feature importance, showing that flexibility in the energy system might affect a country's feature importance. This is confirmed by the correlation between electricity export and DAM prices. We have proposed a greedy algorithm to search for European features in a DAM price forecasting model, using candidate countries resulting from an analysis on before-mentioned feature importances. The proposed greedy algorithm improved forecasting performance of all proposed modelling approaches with statistical significance.

4

The algorithm was applied to the Dutch market, using three different modelling approaches: the LEAR [20, 19], the SM-DNN [18] and the MM-DNN [10]. A benchmark was performed using the LEAR and DNN including only Dutch features. The algorithm was able to identify features while preventing over-fitting on the data, which did happen in the models when including all European features. The greedy algorithm first chose British and Danish market features, after which either Norwegian or French were included in the model, differing between the LEAR and the DNN's. The LEAR model, which is known to have good regularisation properties, performed best when features from 5 other countries are included in the model. The SM-DNN model performed best with features from 4 other countries, and the MM-DNN performed best with features from 3 other countries. The largest improvement was found in the MM-DNN, which can be explained by either the training process (as discussed in Section 4.5.3) or the non-linear nature of market dynamics. However, in the Dutch case the LEAR model with market integration features is the overall best performing model. Temporal variations in model performance are shown, and a relationship between price volatility and relative model performance was found. The LEAR generally performs better than the DNN during hours with low volatility, while the DNN-type models show some improved performance over the LEAR in hours with high volatility. This could indicate that as prices are expected to become more volatile in the future [23], non-linear models could outperform linear models. The LEAR model performed relatively well using all European features, which can be explained by its strong regularisation properties. The DNN type models that used all European features showed a decrease in performance, also with respect to using only Dutch features. The MM-DNN showed the largest performance decrease, which could be due to the multi-market loss function. This could result in trade-offs between price forecasting performance on the Dutch market and other bidding zones. In future work, other modelling approaches could be used in the proposed greedy algorithm. Also, different lengths of the training data could be used, other hyperparameter configurations of the DNN could be set, and model ensembles could be made, in order to optimise forecasting performance. More features could be used, like renewable energy generation forecasts. Weights could be added to the MM-DNN loss function to optimize Dutch price forecasting performance. Other years of data can be used to train and test the models, allowing the investigation of temporal changes in market dynamics. Also, the analysis could be applied to different European markets to test

the sensitivity of a certain market's model accuracy to market integration features. This would also allow for an extended analysis on the relative performance of linear and non-linear models under different scenarios of price volatility.

BIBLIOGRAPHY

- [1] Ties van der Heijden et al. “Electricity Price Forecasting in European Day Ahead Markets: A Greedy Consideration of Market Integration”. In: *IEEE Access* 9 (2021), pp. 119954–119966. ISSN: 21693536. DOI: [10.1109/ACCESS.2021.3108629](https://doi.org/10.1109/ACCESS.2021.3108629).
- [2] European Commission. *2050 low-carbon economy roadmap*. Tech. rep. European Commission, 2016. URL: https://ec.europa.eu/clima/policies/strategies/2050%5C_en (visited on 06/13/2018).
- [3] A. Rezaee Jordehi. “Optimisation of demand response in electric power systems, a review”. In: *Renewable and Sustainable Energy Reviews* 103.July 2018 (2019), pp. 308–319. ISSN: 18790690. DOI: [10.1016/j.rser.2018.12.054](https://doi.org/10.1016/j.rser.2018.12.054). URL: <https://doi.org/10.1016/j.rser.2018.12.054>.
- [4] Rafał Weron. “Electricity price forecasting: A review of the state-of-the-art with a look into the future”. In: *International Journal of Forecasting* 30.4 (2014), pp. 1030–1081. ISSN: 01692070. DOI: [10.1016/j.ijforecast.2014.08.008](https://doi.org/10.1016/j.ijforecast.2014.08.008). URL: <http://dx.doi.org/10.1016/j.ijforecast.2014.08.008>.
- [5] European Commission. *Achieving the 10% electricity interconnection target*. Tech. rep. 9. European Commission, 2015. URL: https://ec.europa.eu/energy/sites/ener/files/publication/FOR%20WEB%20energy%20union%20interconnections%7B%5C_%7DEN-1.pdf.
- [6] Werner Platzer and Fraunhofer ISE. *SUPERGRID – Approach for the integration of renewable energy in Europe and North Africa*. Tech. rep. Fraunhofer institute, 2016, p. 38. URL: <https://www.ise.fraunhofer.de/en/publications/veroeffentlichungen-pdf-dateien-en/studien-und-konzeptpapiere/study-supergrid-fraunhofer-ise.pdf>.
- [7] House of Commons, London. *A European Supergrid*. Tech. rep. February. Department of Energy and Climate, 2011. URL: <http://www.publications.parliament.uk/pa/cm201314/cmselect/cmenergy/194/194we03.htm%7D>.
- [8] Mokhtar Benasla et al. “The transition towards a sustainable energy system in Europe: What role can North Africa’s solar resources play?” In: *Energy Strategy Reviews* 24.August 2018 (2019), pp. 1–13. ISSN: 2211467X. DOI: [10.1016/j.esr.2019.01.007](https://doi.org/10.1016/j.esr.2019.01.007). URL: <https://doi.org/10.1016/j.esr.2019.01.007>.
- [9] European Commission. *An Energy Policy for Europe*. Tech. rep. European Commission, 2007.
- [10] Jesus Lago et al. “Forecasting day-ahead electricity prices in Europe: The importance of considering market integration”. In: *Applied Energy* 211.July 2017 (2018), pp. 890–903. ISSN: 03062619. DOI: [10.1016/j.apenergy.2017.11.098](https://doi.org/10.1016/j.apenergy.2017.11.098). arXiv: [1708.07061](https://arxiv.org/abs/1708.07061). URL: <https://doi.org/10.1016/j.apenergy.2017.11.098>.

- [11] Florian Ziel, Rick Steinert, and Sven Husmann. “Forecasting day ahead electricity spot prices: The impact of the EXAA to other European electricity markets”. In: *Energy Economics* 51 (2015), pp. 430–444. ISSN: 01409883. DOI: [10.1016/j.eneco.2015.08.005](https://doi.org/10.1016/j.eneco.2015.08.005). arXiv: 1501.00818. URL: <http://dx.doi.org/10.1016/j.eneco.2015.08.005>.
- [12] Ioannis P. Panapakidis and Athanasios S. Dagoumas. “Day-ahead electricity price forecasting via the application of artificial neural network based models”. In: *Applied Energy* 172 (2016), pp. 132–151. ISSN: 03062619. DOI: [10.1016/j.apenergy.2016.03.089](https://doi.org/10.1016/j.apenergy.2016.03.089). URL: <http://dx.doi.org/10.1016/j.apenergy.2016.03.089>.
- [13] Christopher Kath. “Modeling intraday markets under the new advances of the cross-border Intraday Project (XBID): Evidence from the German intraday market”. In: *Energies* 12.22 (2019), pp. 1–35. ISSN: 19961073. DOI: [10.3390/en12224339](https://doi.org/10.3390/en12224339).
- [14] Michał Narajewski and Florian Ziel. “Ensemble Forecasting for Intraday Electricity Prices: Simulating Trajectories”. In: *Applied Energy* 279. April (2020), p. 115801. ISSN: 03062619. DOI: [10.1016/j.apenergy.2020.115801](https://doi.org/10.1016/j.apenergy.2020.115801). arXiv: 2005.01365. URL: <http://arxiv.org/abs/2005.01365>.
- [15] Claudio Monteiro et al. “Short-term price forecasting models based on artificial neural networks for intraday sessions in the Iberian electricity market”. In: *Energies* 9.9 (2016). ISSN: 19961073. DOI: [10.3390/en9090721](https://doi.org/10.3390/en9090721).
- [16] Dogan Keles et al. “Extended forecast methods for day-ahead electricity spot prices applying artificial neural networks”. In: *Applied Energy* 162 (2016), pp. 218–230. ISSN: 03062619. DOI: [10.1016/j.apenergy.2015.09.087](https://doi.org/10.1016/j.apenergy.2015.09.087).
- [17] P. M.R. Bento et al. “A bat optimized neural network and wavelet transform approach for short-term price forecasting”. In: *Applied Energy* 210. October 2017 (2018), pp. 88–97. ISSN: 03062619. DOI: [10.1016/j.apenergy.2017.10.058](https://doi.org/10.1016/j.apenergy.2017.10.058). URL: <http://dx.doi.org/10.1016/j.apenergy.2017.10.058>.
- [18] Jesus Lago, Fjo De Ridder, and Bart De Schutter. “Forecasting spot electricity prices: Deep learning approaches and empirical comparison of traditional algorithms”. In: *Applied Energy* 221. January (2018), pp. 386–405. ISSN: 03062619. DOI: [10.1016/j.apenergy.2018.02.069](https://doi.org/10.1016/j.apenergy.2018.02.069). URL: <https://doi.org/10.1016/j.apenergy.2018.02.069>.
- [19] Jesus Lago et al. “Forecasting day-ahead electricity prices: A review of state-of-the-art algorithms, best practices and an open-access benchmark”. In: *Applied Energy* 293 (2021), p. 116983. ISSN: 0306-2619. DOI: <https://doi.org/10.1016/j.apenergy.2021.116983>. URL: <https://www.sciencedirect.com/science/article/pii/S0306261921004529>.
- [20] Bartosz Uniejewski, Jakub Nowotarski, and Rafal Weron. “Automated variable selection and shrinkage for day-ahead electricity price forecasting”. In: *Energies* 9.8 (2016). ISSN: 19961073. DOI: [10.3390/en9080621](https://doi.org/10.3390/en9080621).

- [21] Michele Benini et al. “Day-ahead market price volatility analysis in deregulated electricity markets”. In: *Proceedings of the IEEE Power Engineering Society Transmission and Distribution Conference 3.SUMMER* (2002), pp. 1354–1359. DOI: [10.1109/pess.2002.1043596](https://doi.org/10.1109/pess.2002.1043596).
- [22] Shadi Goodarzi, H. Niles Perera, and Derek Bunn. “The impact of renewable energy forecast errors on imbalance volumes and electricity spot prices”. In: *Energy Policy* 134.June (2019), p. 110827. ISSN: 03014215. DOI: [10.1016/j.enpol.2019.06.035](https://doi.org/10.1016/j.enpol.2019.06.035). URL: <https://doi.org/10.1016/j.enpol.2019.06.035>.
- [23] Stephanía Mosquera-López and Anjali Nursimulu. “Drivers of electricity price dynamics: Comparative analysis of spot and futures markets”. In: *Energy Policy* 126.October 2018 (2019), pp. 76–87. ISSN: 03014215. DOI: [10.1016/j.enpol.2018.11.020](https://doi.org/10.1016/j.enpol.2018.11.020). URL: <https://doi.org/10.1016/j.enpol.2018.11.020>.
- [24] Abdolrahman Khoshrou, André B. Dorsman, and Eric J. Pauwels. “The evolution of electricity price on the German day-ahead market before and after the energy switch”. In: *Renewable Energy* 134 (2019), pp. 1–13. ISSN: 18790682. DOI: [10.1016/j.renene.2018.10.101](https://doi.org/10.1016/j.renene.2018.10.101).
- [25] ENTSO-E. *ENTSO-E Transparency Platform*. 2018. URL: <https://transparency.entsoe.eu/>.
- [26] Robert Tibshirani. “Regression Shrinkage and Selection Via the Lasso”. In: *Journal of the Royal Statistical Society: Series B (Methodological)* 58.1 (1996), pp. 267–288. ISSN: 0035-9246. DOI: [10.1111/j.2517-6161.1996.tb02080.x](https://doi.org/10.1111/j.2517-6161.1996.tb02080.x).
- [27] Sunil L. Kukreja, Johan Löfberg, and Martin J. Brenner. “a Least Absolute Shrinkage and Selection Operator (Lasso) for Nonlinear System Identification”. In: *IFAC Proceedings Volumes* 39.1 (2006), pp. 814–819. ISSN: 14746670. DOI: [10.3182/20060329-3-au-2901.00128](https://doi.org/10.3182/20060329-3-au-2901.00128).
- [28] L. Breiman. “Random Forests”. In: *Machine Learning* 45.1 (2001), pp. 5–32. ISSN: 1098-6596. DOI: [10.1023/A:1010933404324](https://doi.org/10.1023/A:1010933404324). arXiv: [arXiv:1011.1669v3](https://arxiv.org/abs/1011.1669v3).
- [29] Adam Misiorek, Stefan Trueck, and Rafal Weron. “Point and interval forecasting of spot electricity prices: Linear vs. non-linear time series models”. In: *Studies in Nonlinear Dynamics and Econometrics* 10.3 (2006). ISSN: 15583708. DOI: [10.2202/1558-3708.1362](https://doi.org/10.2202/1558-3708.1362).
- [30] F. Pedregosa et al. “Scikit-learn: Machine Learning in Python”. In: *Journal of Machine Learning Research* 12 (2011), pp. 2825–2830.
- [31] D.W. Scott. *Multivariate Density Estimation: Theory, Practice, and Visualization*. John Wiley & Sons, New York, Chichester, 1992.
- [32] Pauli Virtanen et al. “SciPy 1.0: Fundamental Algorithms for Scientific Computing in Python”. In: *Nature Methods* 17 (2020), pp. 261–272. DOI: [10.1038/s41592-019-0686-2](https://doi.org/10.1038/s41592-019-0686-2).
- [33] T. Hastie, R. Tibshirani, and M. Wainwright. *Statistical Learning with Sparsity: The Lasso and Generalizations*. Vol. 84. CRC Press, 2016, pp. 156–157. DOI: [10.1111/insr.12167](https://doi.org/10.1111/insr.12167).

- [34] Diederik Kingma and Jimmy Ba. “Adam: A Method for Stochastic Optimization”. In: *International Conference on Learning Representations*. Dec. 2014.
- [35] J Bergstra, D Yamins, and D D Cox. *Making a Science of Model Search: Hyperparameter Optimization in Hundreds of Dimensions for Vision Architectures*. 2013.
- [36] Martín Abadi et al. *TensorFlow: Large-Scale Machine Learning on Heterogeneous Systems*. Software available from tensorflow.org. 2015. URL: <http://tensorflow.org/>.
- [37] David Elliott. “Emergence of European supergrids - Essay on strategy issues”. In: *Energy Strategy Reviews* 1.3 (2013), pp. 171–173. ISSN: 2211467X. DOI: [10.1016/j.esr.2012.04.001](https://doi.org/10.1016/j.esr.2012.04.001). URL: <http://dx.doi.org/10.1016/j.esr.2012.04.001>.
- [38] Javier Serrano González and César Álvarez Alonso. “Industrial electricity prices in Spain: A discussion in the context of the European internal energy market”. In: *Energy Policy* 148.October 2020 (2021). ISSN: 03014215. DOI: [10.1016/j.enpol.2020.111930](https://doi.org/10.1016/j.enpol.2020.111930).



5

INCORPORATING RISK IN OPERATIONAL WATER RESOURCES MANAGEMENT

*There's no room in the ring for overbearing pride.
Closing your mind to the prospect of failure will only ensure your defeat.*

Master Roshi

This chapter presents an innovative approach to risk-aware decision-making in water resource management. Recognizing the limitations of deterministic methods in the face of weather and energy system uncertainty, we propose a stochastic Model Predictive Control framework incorporating probabilistic forecasting, scenario generation, and stochastic optimal control. The multi-market Demand Response strategy for the Noordzeekanaal–Amsterdam-Rijnkanaal (NZK-ARK), as described in Chapter 2, is extended to include operational uncertainty of incoming discharge, outgoing sea water level, and the Day Ahead and Intraday hourly electricity prices. We propose using Combined Quantile Regression Deep Neural Networks (Section 3.1 and Non-parametric Bayesian Networks to generate scenarios with realistic temporal dependencies (Section 3.2). Key to our approach is the use of Exceedance Risk (ER) constraints on water level bounds within the Model Predictive Control, enabling a more nuanced and risk-aware decision-making process.

We simulate historical multi-market participation with real water system and electricity price data, where the control of the NZK-ARK system is simulated under uncertainty in a receding horizon fashion over multiple years. We show that incorporating uncertainty significantly reduces operational costs – by up to 44 percent-point compared to a deterministic approach. We show that our proposed ER constraint formulation leads is effective in reducing energy cost and maintaining safe water levels.

Parts of this chapter have been submitted for publication in Water Resources Research.

5.1. INTRODUCTION

The Netherlands, facing unique geographical challenges, has developed significant expertise in water management. Much of its land is below sea level, requiring methods to manage precipitation and groundwater levels. In the past, pumping stations with rule-based or deterministic model predictive control (MPC) have been central to these management efforts. However, as climate change can lead to more unpredictable weather, the limits of deterministic approaches are being reached. This situation incentivised a move towards adaptive strategies, leveraging real-time data and probabilistic forecasts in the optimization process. These advances allow for better adaptation to climate variations and changes in water catchment areas [1, 2, 3].

Stochastic MPC approaches can employ chance constraints to ensure that certain conditions are met with a predefined probability level [4]. However, their inherent binary nature, indicating that they either meet the conditions or don't, overlooks the potential magnitude or likelihood of constraint violations, which is critical in applications such as water management. Additionally, while robust optimization techniques aim to handle uncertainty by considering the worst-case scenarios, they can also be overly conservative, leading to suboptimal or overly cautious operational decisions that may not capitalize on potential opportunities or efficiencies. In stochastic MPC, uncertainty can be considered explicitly by expressing the uncertain variables as parametric PDF, or implicitly through scenarios sets. In recent literature, the main focus has been on implicit approaches, possibly due to their ability to include model uncertainty or the possibility to condense scenarios sets into tree-shapes to reduce computational complexity [2]. Generally, explicit approaches do not account for autocorrelation in disturbances or forecast errors [1, 5], which can relatively easily be implicitly taken into account in scenario sets.

Adapting to the unpredictability of weather and its impact on water levels requires sophisticated forecasting methods. The integration of probabilistic forecasts not only enhances prediction accuracy but also enhances dynamic responses such as Demand Response (DR) in the energy sector to achieve a necessary balance between supply and demand. DR refers to the changes in electric usage by end-use customers from their normal consumption patterns. These signals are achieved through prices that reflect scarcity of supply and marginal cost of production. The variable supply of renewables leads to changing electricity prices over time, and induces lower electricity use at times of high market prices. By enabling dynamic adjustments of demand, DR contributes to the electricity grid's stability, reduces the need for peak generation capacity, and optimizes energy costs for consumers. In DR, inaccuracies in forecasting can significantly impact system efficiency, leading to both operational challenges and financial consequences for consumers and producers. With the increasing reliance on renewable energy sources, accurately forecasting energy production has become more complex. This unpredictability and complexity call for enhanced predictive models that adequately reflect the operational uncertainty given the latest information. Moreover, integrating stochastic optimization methods into energy management strategies can mitigate the risks associated with operational uncertainty. These methods enable the consideration of multiple possible future scenarios in the decision-making process, thus providing a more comprehensive strategy that accounts for a wide range of outcomes. By adopting a probabilistic approach to forecasting and optimization, stakeholders can better pre-

pare for and adapt to the inherent volatility associated with Renewable Energy Sources and demand fluctuations and the operational risk involved in their processes [6, 7, 8], inspiring research in uncertainty estimation in forecasting and making it an increasingly present industry requirement [9, 10, 11]. However, ensemble forecasts have become a standard in hydro-meteorological forecasting as well, due to their ability to capture forecast uncertainty [2, 12].

Central to this study are the uncertainties faced in operational water resources management, from variable discharges to dynamic seawater levels influenced by tides and winds. The inherent volatility of energy spot markets, combined with real-time supply-demand dynamics, and the integration of renewable energy, exemplify the need for advanced forecasting methodologies. This motivated our exploration into probabilistic methodologies, such as the Combined Quantile Regression Deep Neural Network [10] (CQRDNN) and the Non-parametric Bayesian network [13] (NPBN). Our framework integrates probabilistic forecasting, scenario generation, and reduction approaches. We further extend the scenario-based MPC approach into Tree-based MPC (TB-MPC) [14, 15] formulations for improved and sometimes necessary computational efficiency in large uncertainty representations.

Our approach emphasizes risk-based constraints, inspired by the Conditional-Value-at-Risk (CVaR) approach, also known as the mean excess loss [16]. CVaR represents the tightest convex formulation of a chance constraint [17], while its linear formulation leads to reduced computational complexity. Unlike traditional chance constraints or robust optimization methods, CVaR represents the tail distribution of potential outcomes, revealing worst-case scenarios and associated risks. We propose the use of Exceedance Risk (ER) constraints that are formulated similarly to CVaR, but are tailored for the application in operational water resources management. In the Dutch water sector, risk-awareness is key to system design and policy-making. Our work considers probabilistic risk of exceedances for water levels in real-time operational control. We formulate a stochastic MPC problem, where the states are stochastic variables driven by uncertain disturbances and parameters, and the objective and constraints are formulated as expectation of cost and probabilistic constraint violations, respectively. As such, the optimal control problem of the MPC requires solving stochastic optimization problems via a scenario-based approach. We also specifically consider CVaR-type stochastic problems to model water-level exceedance risks.

In response to the societal challenges posed by climate variability and the energy transition on water management systems, this chapter introduces several novel methodologies to capture dependencies between weather, markets, and control decisions, and shows how to exploit these in control for our case study area, the drainage canal Noordzeekanaal–Amsterdam–Rijnkanaal (NZK-ARK). Firstly, we have developed a Combined Quantile Regression Deep Neural Network (CQRDNN) (Section 3.1.1), which leverages deep learning to provide probabilistic forecasts of water levels and energy demands. Unlike traditional models, CQRDNN incorporates a quantile-based approach that inherently manages forecast uncertainty, offering a range of potential outcomes that are crucial for effective decision-making under uncertainty. Secondly, we introduce a Non-parametric Bayesian network (NPBN) (Section 3.2.1) for generating dependent scenarios that respect the temporal dynamics of water systems and energy markets. This method

allows for a more realistic simulation of future states, enhancing the strategic planning capabilities of water resource managers. This approach not only improves computational efficiency—critical for real-time operational adjustments—but also incorporates advanced risk-based constraints tailored for water management. We further propose a scenario-tree generation method (Section 3.2.3) to further reduce the computational complexity of the optimization problem, allowing for TB-MPC. Finally, we propose novel Exceedance Risk (ER) (Section 5.3) constraints, allowing our framework to mitigate potential risks more effectively than traditional methods, which often overlook the magnitude of violations.

By examining the operational flexibility of electric pumping stations and their role in the broader energy system, this chapter aims to contribute to a more sustainable and integrated approach to managing the interdependencies between water and energy in the Netherlands. The presented innovations collectively enhance the ability of water management systems to operate efficiently in the face of uncertainty, optimizing both water usage and energy expenditure. The integration of these methodologies not only addresses the immediate needs of operational control but also sets a foundation for future research and application in sectors grappling with similar variability and uncertainty, notably in the context of energy flexibility and DR.

5.2. DEMAND RESPONSE IN THE NETHERLANDS: CASE STUDY IJMUIDEN

In this section, we describe the case study for our proposed framework. First, we describe the water system; the NZK-ARK, located in IJmuiden, the Netherlands (Section 5.2.1). Then we describe the Dutch electricity markets that are considered for DR services which recent studies have shown to offer significant flexibility and cost reduction potential [18] (Section 5.2.2).

5.2.1. THE NOORDZEEKANAAL-AMSTERDAM-RIJNKANAAL

The NZK-ARK is an intricate open canal system. It's equipped with multiple undershot gates and has a pumping station at IJmuiden, which aids in consistently directing water into the North Sea, regardless of the sea's variable water levels. Water from four regional water boards flows into the NZK-ARK, helping redirect excess rainwater. This water is methodically channelled or pumped out to the North Sea. A detailed representation of this water system, focusing on the inflow and outflow mechanisms, is provided in Figure 1.5a. A simplified schematic of the system is presented in Figure 5.1.

The operations at the IJmuiden pumping station highlight the complexities in decision-making caused by the presence of operational uncertainty. IJmuiden is not only Europe's largest pumping station, but also plays a key role in managing ship traffic, controlling saltwater intrusion, and working with four local water authorities. The complexity of its operations is further amplified with the possible addition of Demand Response (DR) and energy trading in the spot market. Previous work has shown that a control strategy that taps into varying electricity prices from the Day Ahead Market (DAM) and the Intraday Market (IDM) could prove more cost-effective than the current method, especially as the penetration of renewable energy grows. [18] However, that analysis was based on perfect

foresight and did not consider operational uncertainty. The interaction between water management and energy usage in pumping stations is increasingly significant within the context of the water-energy nexus [19, 20, 21]. Despite this significance, the opportunity to optimize pump schedules with regard for the energy markets is still largely untapped in practice.

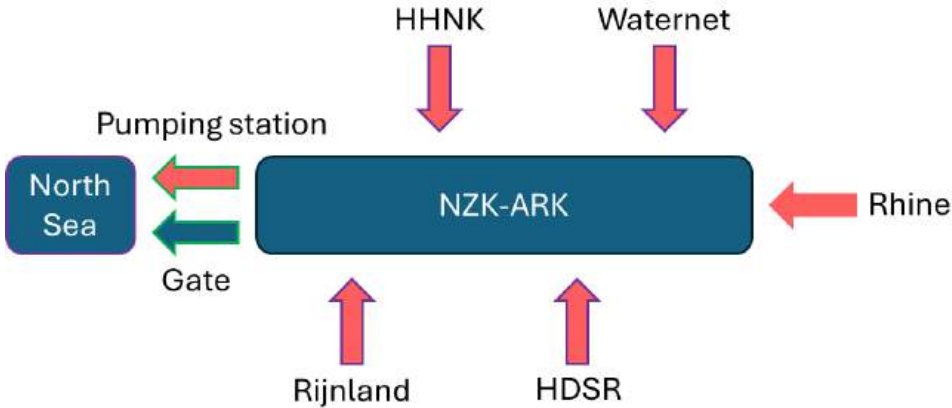


Figure 5.1: The Netherlands, Noordzeekanaal–Amsterdam–Rijnkanaal. (a) The water management area of different local water authorities are shown by color. Pumping stations owned by local water authorities are shown by red diamond, gate structures with red rectangles, and the IJmuiden gate- and pumping station with a yellow diamond. (b) The water level regime of the NZK-ARK showing target ranges and warning/emergency levels. (c) NZK-ARK schematic for control, where the purple-outlined items indicate forecast variables, and the green-outlined items indicate control variables.

Within the MPC's internal model, the canal is depicted as a linear reservoir with pre-defined surface area. This approach is consistent with the current control system of the NZK-ARK. Owing to the canal's considerable depth and width, water movement occurs at reduced speeds, ensuring that friction remains minimal [22]. The primary sources of water inflow come from the water board discharges and water from the Rhine directed through Maarsse, the outflow is directed towards the North Sea.

At IJmuiden, the gate operations are dictated by specific water level differentials. They can be activated when there's a 16 cm water level difference and deactivated at 12 cm. This modulation is necessary to account for the contrasting densities of salt and freshwater, along with inherent system friction [23]. With automated controls in place, these gates have a maximum discharge rate of $500 \text{ m}^3 \text{ s}^{-1}$, a precaution to protect the foundation of the gate complex. The IJmuiden station incorporates six distinct pumps, with a combined maximum power consumption nearing 5 MW. For modelling convenience, the MPC represents these multiple pumps as a singular entity, merging their unique attributes. Even though there are six individual pumps, an integrated approach is adopted, utilizing various Q–dH curves to represent the pumping station's overall dis-

charge ability. Another composite representation is designed to represent the pumping station's energy use in a single equivalent PQH-curve, encapsulating pump energy consumption in relation to discharge levels and the pump head. A comprehensive description of these modelling techniques is available in [18].

At present, the IJmuiden pumping station operates using MPC, focusing on energy efficiency by drawing power from the Futures market with fixed-price contracts. It works with a 24-hour prediction, ensuring water levels stay within set limits. To better fit the needs of energy trading on the DAM, we've expanded the prediction horizon to 48-hours. This change allows for a detailed look at the cost-saving potential of energy cost optimization over flexible energy markets for the NZK-ARK system, and aligns the control system with DAM rules. We've considered uncertainties in sea water levels, incoming discharge from local water authorities, and electricity prices. While sea water levels and discharge, which directly impact system limits, are exhaustively combined, electricity prices are evaluated on their own, focusing on reducing expected costs without needing more decision points.

5

5.2.2. ENERGY MARKETS IN THE NETHERLANDS

The energy trading landscape in the Netherlands is predominantly facilitated through the DAM and the IDM. On the DAM, energy transactions are made a day in advance, with consumers placing bids for the upcoming day in hourly blocks. By 12:00 CET each day, bids are collected on the Amsterdam Power Exchange (APX)-Endex. The market then establishes a price equilibrium where demand meets supply. These two markets are the main markets for trading renewable energy in Europe and reward the exploitation of energy flexibility through DR services.

In contrast, the IDM offers a more dynamic trading environment, allowing participants to continuously buy or sell energy in quarterly, half-hourly, or hourly segments, sometimes up to just 5 minutes before the actual delivery time. Due to this flexible nature, individual buy and sell orders set varying contract prices. This study utilizes the volume-weighted price over the three hours leading up to delivery, termed the ID3-price. However, in real-world scenarios, every transaction could exhibit a distinct price. The IDM serves as a platform to adjust day-ahead plans and sidestep potential imbalances. Given its adaptability, many speculate that the IDM is poised to become the primary trading platform for renewable energy in the near future [24], a hypothesis that is being confirmed by the yearly doubling of traded volume.

Both DAM and IDM incentivise participants to tailor their energy schedules in response to price signals that echo supply scarcity and production costs. By adhering to such price-sensitive DR strategies, there's potential for shifts in energy consumption patterns in correspondence with price changes [25]. Figure 5.2 shows a 2-Dimensional *Kernel Density Estimate* (KDE) that sheds light on the evolving trends of DAM and IDM prices in the Netherlands. Interestingly, Dutch prices have demonstrated more pronounced fluctuations over the years, which might be attributed to various factors, including the maturity of the market, changing consumption patterns in the COVID pandemic, the lack of nuclear base-load in France, and the Russian invasion of Ukraine leading to a reduced gas and oil supply to Europe, and increased prices due to embargos. This caused spot market fluctuations to increase from around 0 - 75 [€/MWh] in 2019 to -200

- +600 [€/MWh] in 2022. Interestingly, the relative ID₃ price seems normally distributed around the DAM price and has stayed in a similar range since 2020.

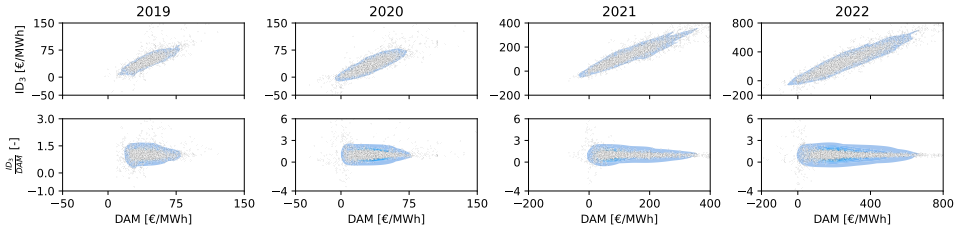


Figure 5.2: 2D-KDE of top: the Dutch IDM electricity prices over the DAM prices, bottom: the relative IDM prices over the DAM prices (2019-2022). Blue indicates the empirical probability where darker colors indicate a higher empirical probability. Dots represent the individual samples.

While the Futures market provides long-term or base-load trading opportunities, its fixed pricing model doesn't facilitate the intermittent nature of renewable energy. As energy supply becomes more uncertain, it is expected that fixed-price contracts will carry higher risk premiums, giving flexibility a business case. Energy users might turn to the Futures market to hedge against risks, and producers find it useful to guarantee consistent sales. However, its inherent rigidity with predetermined prices makes it less suited for strategies that aim to exploit energy flexibility.

In the following sections, we extend the multi-market approach as defined in [18] to incorporate operational uncertainty. The proposed strategy combines both DAM and IDM, optimizing the strengths of each. Combining multiple markets promises to amplify the efficacy of market-based DR initiatives [26]. With the rising prominence of renewable energy sources, the roles of DAM and IDM are set to further magnify in order to keep supply and demand in balance.

5.3. RISK-AWARE OPTIMAL CONTROL

In this section, we describe the control model and methods that we propose to optimize the gate and pump schedule for IJmuiden with regard for uncertainty. We start with an introduction to stochastic MPC and our justification for the use of ER constraints (Section 5.3.1), continued by the water system constraints (Section 5.3.2) and the multi-market trading objective (Section 5.3.3). The full MPC control problem is formulated in Section 5.3.4.

5.3.1. STOCHASTIC MODEL PREDICTIVE CONTROL

Stochastic MPC is a powerful extension to Deterministic MPC for control problems in the presence of uncertainties [4]. It leverages mathematical optimization to make optimal control decisions based on probabilistic information about system dynamics and disturbances. The key idea behind stochastic MPC is to formulate the control problem as a stochastic optimization problem, where the objective is to find a control policy that minimizes an expected cost while considering the constraints and uncertainties in the

system. In addition to handling uncertainties in a single time step, stochastic MPC can be extended to multi-stage scenarios, where the uncertainty evolves over the prediction horizon. This extension enables the controller to make decisions that take into account the changing nature of uncertainties over time. By making use of real-time updated information and probabilistic forecasts in the optimization, stochastic MPC can help water systems cope with changes in the climate or catchment, and mitigate impacts of extreme hydrological events [1].

Robust optimization techniques play a significant role in stochastic MPC by addressing uncertainties and maintaining system performance under worst-case scenarios. Scenario-robust optimization aims to find control policies that can withstand uncertainties by optimizing over a range of possible scenarios or uncertainty realizations. By considering the most unfavorable outcomes in the scenario set, scenario-robust optimization provides assurances regarding system stability and performance, even when uncertainties deviate from their nominal distributions. In stochastic MPC, scenario-robust optimization techniques are integrated into the optimization framework, enabling controllers to account for uncertainties while minimizing the potential impact of worst-case scenarios on system behavior. By explicitly considering worst-case scenarios and their associated constraints or objectives, scenario-robust optimization provides a reliable control framework. This approach is particularly valuable in safety-critical systems or applications where deviations from nominal conditions can have severe consequences, such as the NZK-ARK where constraint violation can lead to flooding.

Robustness in MPC can extend to both constraints and objectives. In scenario-robust constraint formulation, constraint violation will not be tolerated in the whole range of uncertainty realizations. Scenario-robust optimization ensures that the system remains within predefined safety bounds under all considered scenarios, providing a reliable control strategy. Although in most cases, subjecting to constraints even in the most unlikely considered scenarios can be considered conservative. The authors hypothesize that this robustness in control has a price when put in context of DR.

We propose the use of CVaR-inspired constraints for managing risk by controlled relaxing of robustness in decision-making, while minimizing the expected value of the energy cost by trading over multiple markets. Unlike traditional measures like chance constraints that focus solely on a probability threshold or variance constraints that constrain a variance around the expectation, CVaR considers the size of the tail of the distribution beyond the threshold. By capturing the tail of the risk, CVaR provides a more comprehensive measure of the risk associated with the system's outcomes while being the tightest convex approximation of the chance constraint [17].

The constraint can be formulated as a linear constraint with a slack variable, while being a coherent risk measure [27]. Consider the optimization problem

$$\min_x \mathbb{E}[C(x, \mathcal{W})] \quad (5.1)$$

$$\text{s.t. CVaR}_\alpha[C(x, \mathcal{W})], \quad (5.2)$$

where x represents the control variable, and \mathcal{W} represents the set of possible uncertainty realizations. The cost function $C(x, \mathcal{W})$ captures the system's cost under control variable x and uncertainty set \mathcal{W} . The CVaR_α constraint ensures that the Conditional Value at Risk of the cost function remains below a certain threshold γ with confidence level α . This constraint can be discretely approximated by introducing a slack variable and two linear constraints [28]

$$\zeta + (1 - \alpha)^{-1} \sum_{w \in \mathcal{W}} p[w] \cdot z[w] \leq \gamma, \quad (5.3)$$

$$z[w] \geq C[x, w] - \zeta \quad \forall w \in \mathcal{W}, \quad (5.4)$$

where ζ represents the VaR, α the confidence level, w an uncertainty realization in set \mathcal{W} with probability set p , γ the CVaR upper bound, C the cost function, and z the newly introduced slack variable representing the cost exceeding the VaR.

Operational water resources management, however, generally requires the risk measure to reflect the risk of water level bound exceedance and, therefore, the tail should be calculated with respect to a fixed threshold. As a fixed threshold would not always equal the VaR, we call this reformulation *Exceedance Risk* (ER) constraints. This constraint imposes a limit on the risk associated with the constraint violation (i.e. violation of the upper bound on the water level in the canal), ensuring that the system operates within acceptable bounds with confidence level α . By incorporating ER_α constraints, the optimization algorithm ensures that the system satisfies the constraint with predefined statistical confidence. As γ approaches the threshold and α approaches 1, the constraint converges towards a scenario-robust constraint where no constraint violation is allowed in any of the considered uncertainty realizations.

5.3.2. WATER SYSTEM CONSTRAINTS

In this section, we describe the constraint formulation of the stochastic MPC based on the already published deterministic model [18]. The constraints describe the water balance on the linear reservoir model (Eq. (5.5a)), and constraints on gate discharge formulated as big-M constraints (Eq. (5.5c), (5.5d)) using binary indicator variable z_g , which is 1 when the gate discharge is actuated, and gate discharge curve (Eq. (5.5e)). The physical constraints for pump discharge are similarly formulated with big-M constraints (Eq. (5.5f), (5.5g)) using binary indicator variable z_p and the pump discharge curve (Eq. (5.5h)), the lower bound constraint on the water level (Eq. (5.5i)), and a quadratic constraint on a new variable to make the pump energy use in the objective bi-linear (Eq. (5.5j)).

$$h_{nzk}[t, w] = h_{nzk}[t-1, w] + (q_{in}[t-1, w] - q_g[t-1, w] - q_p[t-1, w]) \cdot \frac{\Delta t}{A_{nzk}} \quad \forall t \in T \text{ and } w \in \mathcal{W}_{q \times h}, \quad (5.5a)$$

$$dh[t, w] := h_{nzk}[t, w] - h_{NS}[t, w], \quad (5.5b)$$

$$dh[t, w] - dh_g^- + (1 - z_g[t, w]) \cdot M_g \geq 0 \quad \forall t \in T \text{ and } w \in \mathcal{W}_{q \times h}, \quad (5.5c)$$

$$dh[t, w] - dh_g^- - z_g[t, w] \cdot M_g \leq 0 \quad \forall t \in T \text{ and } w \in \mathcal{W}_{q \times h}, \quad (5.5d)$$

$$q_g[t, w] \leq (a_g \cdot dh[t, w] + b_g) \cdot z_g[t, w] \quad \forall t \in T \text{ and } w \in \mathcal{W}_{q \times h}, \quad (5.5e)$$

$$-dh[t, w] - dh_p^- + (1 - z_p[t, w]) \cdot M_p \geq 0 \quad \forall t \in T \text{ and } w \in \mathcal{W}_{q \times h}, \quad (5.5f)$$

$$-dh[t, w] - dh_p^- - z_p[t, w] \cdot M_p \leq 0 \quad \forall t \in T \text{ and } w \in \mathcal{W}_{q \times h}, \quad (5.5g)$$

$$q_p[t, w] \leq z_p[t, w] \cdot \sum_{i=1}^6 (a_p[i] \cdot -dh[t, w] + b_p[i]) \quad \forall t \in T \text{ and } w \in \mathcal{W}_{q \times h}, \quad (5.5h)$$

$$h_{nzk}[t, w] \geq h^- \quad \forall t \in T \text{ and } w \in \mathcal{W}_{q \times h}, \quad (5.5i)$$

$$H[t, w] = (h_{NS}[t-1, w] - h_{nzk}[t-1, w])^2 \quad \forall t \in T \text{ and } w \in \mathcal{W}_{q \times h}, \quad (5.5j)$$

with time steps $t \in [0, T]$, prediction horizon T , sea water level uncertainty realization set \mathcal{W}_h , incoming discharge uncertainty realization set \mathcal{W}_q , their exhaustively combined set $\mathcal{W}_{q \times h} = (\mathcal{W}_q \times \mathcal{W}_h)$, the water level of the NZK-ARK $h_{nzk,t}^w$ with probabilities $p_q \cdot p_h$, the outgoing gate discharge scenarios $q_{g,t}^w$ with probabilities $p_q \cdot p_h$, the outgoing pump discharge scenarios $q_{p,t}^w$ with probabilities $p_q \cdot p_h$, incoming discharge scenarios $q_{in,t}^w \in \mathcal{W}_q$ with probabilities p_q , and the North Sea water level scenarios $h_t^w \in \mathcal{W}_h$ with probabilities p_h .

The upper bound constraint on the water level is formulated as a ER_α constraint (Eq. (5.6a),(5.6b)) or as scenario-robust constraint (Eq. (5.7)). The ER_α constraints are formulated to represent the expectation of the water level exceeding the given bound; we formulate linear ER constraints inspired by the CVaR formulation proposed in [28], described in Equation (5.3) and (5.4). By introducing slack variable $z_{wl} \in [0, \infty)$ for all scenarios and time steps, the constraint can be efficiently formulated as

$$h^+ + (1 - \alpha)^{-1} \cdot \sum_{w \in \mathcal{W}^*} z_{wl}[t, w] \cdot p[w] \leq \gamma \quad \forall t \in T, \quad (5.6a)$$

$$z_{wl}[t, w] \geq h_{nzk}[t, w] - h^+ \quad \forall t \in T \text{ and } w \in \mathcal{W}_{q \times h}, \quad (5.6b)$$

where h^+ is the water level threshold after which we consider violations for which we use the currently applied target water level (-0.4m+NAP), z_{wl} is the slack variable measuring the upper bound violation of the water level in the NZK for each uncertainty realization w and timestep $t \in T$, α the confidence level, and γ the upper bound on the acceptable ER_α expressed in water level of the NZK (m+NAP) (i.e. the expectation of the scenarios that violate h^+ with confidence level α).

In this formulation, the slack variable z_{wl} represents the water level exceedance of a scenario and timestep with respect to h^+ . The sum of the probability-weighted exceedances over all scenarios is the expected water level violation at each timestep, making the formulation a discrete approximation of the conditional expectation of water level bound violation, given that the water level in that scenario is higher than h^+ .

As α approaches 1, conditionalising the expectation of the exceedance towards the h^+ will increase and become tighter. When $\gamma = h^+$, the constraints in Equations (5.6) become scenario-robust (i.e. allow no constraint violation in any of the considered uncertainty realizations) and are reformulated as

$$h_{nzk}[t, w] \leq h^+ \quad \forall t \in T \text{ and } w \in \mathcal{W}_{q \times h}, \quad (5.7)$$

where h^+ is applied as upper bound constraint on the water level over all timesteps, taking all uncertainty realizations into considerations. The continuous decision-variables in this problem are water level h_{nzk} , gate discharge q_g , pumped discharge q_p , slack variable describing water level violations z_{wl} and the quadratic pump head H . Two binary variables, z_g and z_p are present to describe pump- and gate opportunities due to the water level variations between the NZK-ARK and the North Sea.

5.3.3. MULTI-MARKET TRADING OBJECTIVE

To create a cost-effective pump schedule, we minimize the expected energy cost over all possible control actions over the combined uncertainty of waterboard discharge and water level of the North Sea, and all possible Intraday and Day Ahead market prices.

$$J_{IDM} := \min_{w_1, w_2} \mathbb{E} | \Delta E_{t, w_1} \cdot c_{t, w_2}^{ID} |, \quad \forall t \in T_{IDM} \text{ and } w_1 \in \mathcal{W}_{q \times h} \text{ and } w_2 \in \mathcal{W}_{idm|dam}, \quad (5.8)$$

$$J_{DAM} := \min_{w_1, w_3} \mathbb{E} | E_{t, w_1} \cdot c_{t, w_3}^{DA} |, \quad \forall t \in T_{DAM} \text{ and } w_1 \in \mathcal{W}_{q \times h} \text{ and } w_3 \in \mathcal{W}_{dam}, \quad (5.9)$$

with the set of possible DAM price realizations \mathcal{W}_{dam} and the set of possible intraday price realizations that is conditionalised to the observed DAM prices of that day $\mathcal{W}_{idm|dam}$.

The difference between the actual energy use and the energy bought on the Day Ahead Market $\Delta E_{t,w_1}$ and the intraday price c_{t,w_2}^{ID} are used for intraday trading in J_{IDM} . The energy consumption E_{t,w_1} and the Day Ahead price c_{t,w_2}^{DA} are as used for Day Ahead trading in J_{DAM} ,

5.3.4. FULL MPC CONTROL PROBLEM

The full MPC control problem is defined as

$$J_{IDM} := \min \mathbb{E} | \Delta E_{t,w_1} \cdot c_{t,w_2}^{ID} |, \quad \forall t \in T_{IDM} \text{ and } w_1 \in \mathcal{W}_{q \times h} \text{ and } w_2 \in \mathcal{W}_{idm|dam}, \quad (5.10)$$

$$J_{DAM} := \min \mathbb{E} | E_{t,w_1} \cdot c_{t,w_3}^{DA} |, \quad \forall t \in T_{DAM} \text{ and } w_1 \in \mathcal{W}_{q \times h} \text{ and } w_3 \in \mathcal{W}_{dam}, \quad (5.11)$$

subject to

$$h_{nzk}[t, w] = h_{nzk}[t-1, w] + (q_{in}[t-1, w] - q_g[t-1, w] - q_p[t-1, w]) \cdot \frac{\Delta t}{A_{nzk}} \quad \forall t \in T \text{ and } w \in \mathcal{W}_{q \times h}, \quad (5.12a)$$

$$dh[t, w] := h_{nzk}[t, w] - h_{NS}[t, w], \quad (5.12b)$$

$$dh[t, w] - dh_g^- + (1 - z_g[t, w]) \cdot M_g \geq 0 \quad \forall t \in T \text{ and } w \in \mathcal{W}_{q \times h}, \quad (5.12c)$$

$$dh[t, w] - dh_g^- - z_g[t, w] \cdot M_g \leq 0 \quad \forall t \in T \text{ and } w \in \mathcal{W}_{q \times h}, \quad (5.12d)$$

$$q_g[t, w] \leq (a_g \cdot dh[t, w] + b_g) \cdot z_g[t, w] \quad \forall t \in T \text{ and } w \in \mathcal{W}_{q \times h}, \quad (5.12e)$$

$$-dh[t, w] - dh_p^- + (1 - z_p[t, w]) \cdot M_p \geq 0 \quad \forall t \in T \text{ and } w \in \mathcal{W}_{q \times h}, \quad (5.12f)$$

$$-dh[t, w] - dh_p^- - z_p[t, w] \cdot M_p \leq 0 \quad \forall t \in T \text{ and } w \in \mathcal{W}_{q \times h}, \quad (5.12g)$$

$$q_p[t, w] \leq z_p[t, w] \cdot \sum_{i=1}^6 (a_p[i] \cdot -dh[t, w] + b_p[i]) \quad \forall t \in T \text{ and } w \in \mathcal{W}_{q \times h}, \quad (5.12h)$$

$$h_{nzk}[t, w] \geq h^- \quad \forall t \in T \text{ and } w \in \mathcal{W}_{q \times h}, \quad (5.12i)$$

$$H[t, w] = (h_{NS}[t-1, w] - h_{nzk}[t-1, w])^2 \quad \forall t \in T \text{ and } w \in \mathcal{W}_{q \times h}, \quad (5.12j)$$

$$h^+ + (1 - \alpha)^{-1} \cdot \sum_{w \in \mathcal{W}^*} z_{wl}[t, w] \cdot p[w] \leq \gamma \quad \forall t \in T, \quad (5.12k)$$

$$z_{wl}[t, w] \geq h_{nzk}[t, w] - h^+ \quad \forall t \in T \text{ and } w \in \mathcal{W}_{q \times h}, \quad (5.12l)$$

$$(5.12m)$$

where

$$E_{t,w} := a_p \cdot q_p[t, w]^2 + b_p \cdot H[t, w] \cdot q_p[t, w] + c_p \cdot q_p[t, w] \cdot -dh[t, w] \cdot \Delta t, \quad (5.12n)$$

$$\Delta E_{t,w} := E_{t,w} - E_{bid}, \quad (5.12o)$$

where decision variables h_{nzk} (water level of the NZK-ARK), q_g (gate discharge), q_p (pump discharge), z_g (binary indicator for gate discharge opportunities), z_p (binary indicator for pump discharge opportunities), H (quadratic constraint for dh^2 in the objective), and z_{wl} (the slack variable used for the ER constraint) are optimized to minimize the expected energy cost of pumping under uncertainty.

5.4. RESULTS AND DISCUSSION

In this section, we describe the results of the proposed framework applied to the case study area; the NZK-ARK. We simulate historical multi-market participation with the real water system and electricity price data, where the optimal control of the NZK-ARK system is simulated under uncertainty in a receding horizon fashion over multiple years and months. We first describe the probabilistic forecasting of incoming discharge from four local water authorities into the canal, the water level of the North Sea, and the DAM prices using the methodology described in Sections 3.1.1 and 3.1.2. We then describe how scenarios are generated and reduced to optimal subsets using the method described in Section 3.2.1, 3.2.2 and 3.2.3. Finally, we perform closed-loop simulations for several months in 2019, 2020, and 2021 in Section 5.4.4. We analyse the difference between the deterministic (perfect forecasts and deterministic 'point' forecast), and stochastic MPC. We vary the stochastic MPC with different numbers of scenarios and risk-acceptance settings, including ER and scenario-robust constraints. Figure 5.3 depicts the workflow that is applied in this manuscript. It describes the steps that are take to model operational uncertainty in each source, and what study is performed to evaluate performance.

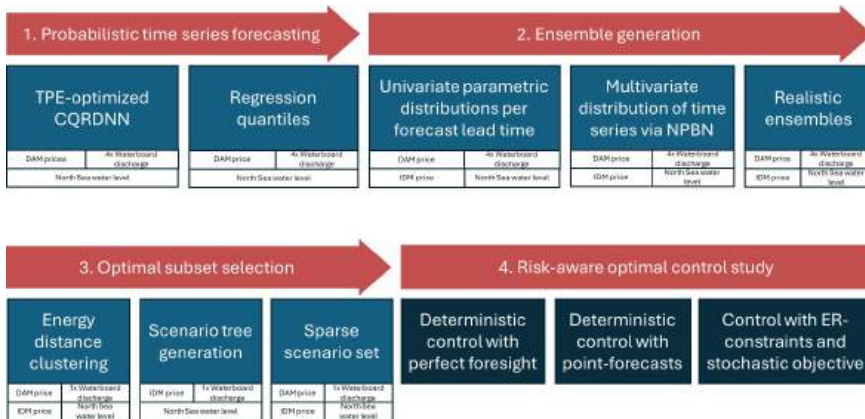


Figure 5.3: The applied workflow in this manuscript, describing what steps were taking to model operational uncertainty for each variable.

5.4.1. PROBABILISTIC FORECASTING

The system, as depicted in Figure 5.7, is schematized as depicted in Figure 5.1. We forecast the pumped discharge into the NZK-ARK and the adjacent water level of the North Sea, as depicted with purple outlines in the Figure, where green outlines depict control variables. The Rhine discharge is taken as known since the same authority regulates the incoming water as the pumping station; Rijkswaterstaat. To train and optimize a CQRDNN to forecast pumped discharge by the four local water authorities, the sea water level of the North Sea, and the DAM electricity prices, we apply the same hyperparameter search space for all modelling tasks while changing the feature search space. The feature and hyperparameter search space applied in this work can be found in Table 5.1. Model selection is performed based on the combined pinball loss (Equation (3.1)) and an independent validation dataset. All results shown in this work are from independent test datasets. In the case of the DAM, we retrain the model every week to cope with the effects of COVID and the fast-changing energy system on the market. Figure 5.4a shows example operational forecasts for the considered sources of uncertainty.

Table 5.1: Feature and hyperparameter search space dimensions for the optimization of the CQRDNN in several forecasting tasks. ²Sea water level is only included in the feature search space for waterboards that have the option to discharge into the North Sea directly.

Hyperparameters	Waterboard discharge	North Sea water level	DAM price
N layers	Discharge lag range	Lagged water level range	Lagged price range
Neurons per layer	Lagged wind data range	Lagged wind data range	Include prices of d-7
Dropout rate	Rolling window size	Rolling water level window size	Load data
Regularization	Include precipitation window	Include hourly wind data	Lagged load range
Batch normalization	Include evaporation window	Include 10min wind data	Include load of d-7
Random seed	Include temperature window	Include wind direction data	Include load forecast for targets
	Include discharge window	Include day of the year	Include onshore wind generation data
	Include wind forecast	Include hour of the day	Include offshore wind generation data
	Include precipitation forecast		Include solar generation data
	Include sea water level ¹		Market integration

We had access to data from the beginning of 2014 to January 2021. Data from 2019 - 2021 is used as test set, data from 2016 was used as validation set to optimize features and hyperparameters, while the remaining data was used to train the models. The validation year was selected based on a preliminary analysis of discharge rates in order to select an average year. In essence, the CQRDNN is trained to model a rainfall-runoff system affected by human influences through the control of pumps. We optimize a 'rolling window' where we take the sum of the fluxes over a variable window length (rolling window size in Table 5.1). Besides optimizing the window size, we also optimize for the features to include (i.e. precipitation, evaporation) with a binary search space. Waterboards Rijnland and HHNK have the option to discharge directly into the North Sea. Therefore, we include the sea water level and wind as optional features too since these determine possibility of direct discharge to the sea. This approach works best for the waterboard Waternet, possibly due to the relatively low amount of storage present in the Waternet system. The NZK-ARK is used as a drainage canal (in Dutch: 'boezem'), where most waterboards have an intermediate drainage canal with higher storage capacity. This could make Waternet's system less influenced by human behaviour. In the case of Rijnland, the main pumping stations are not variable speed pumps, leading to discrete pump modes that CQRDNN regression seems to have difficulties with. It could also indicate that pump

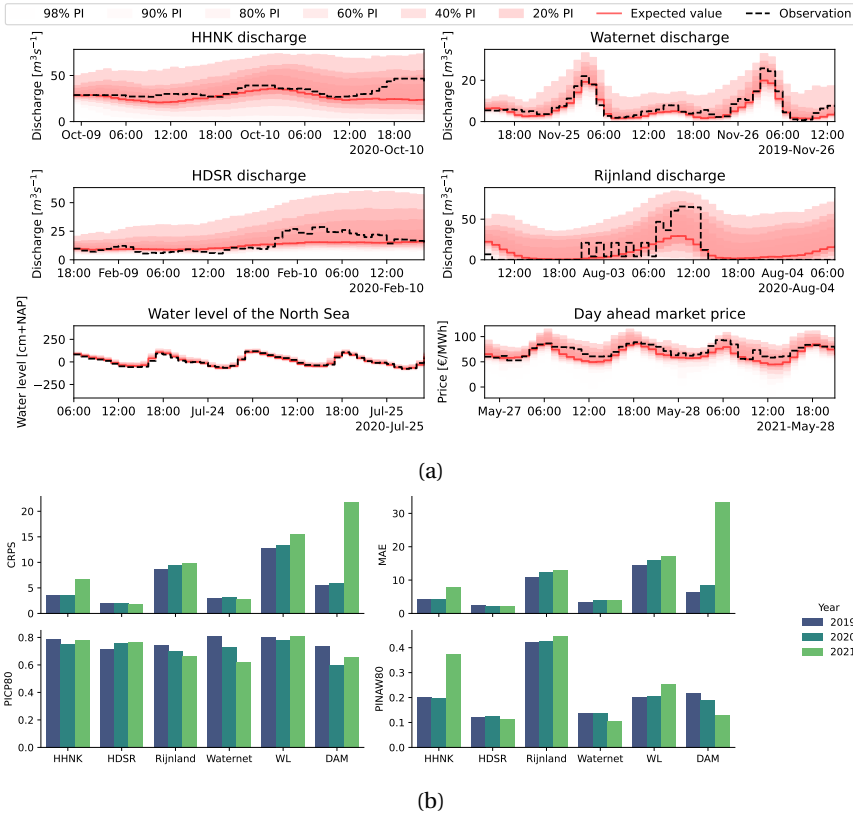


Figure 5.4: Operational forecast examples (a) discharge from the four local water authorities (HHNK, Rijnland, HDSR, and Waternet), the water level of the North Sea, and the DAM electricity price. Performance metrics of the forecasting models (b), where the metrics are averaged over the 48h lead time for all years in the receding horizon simulations.

scheduling can't be forecast based on the current feature data only, leading to high upper quantiles due to the inability to time the actual pumping.

The model forecasting the water level of the North Sea seems to perform well in stable conditions. A model was trained with perfect foresight for the wind forecast since historic meteorological forecasts are not easily accessible, and fully optimizing for the best model is out of the scope of this work. For the North Sea water level model, we used 2016 and 2017 data as training set, 2018 data as validation set, and 2019 - 2021 as test set.

The Day Ahead price forecasting model is based on the methodology presented in [10], and we had access to data from 2015 onward. The search space, however, was expanded to include renewable energy data. Due to the unstable markets during the time of simulation, the model was retrained on a weekly basis to be able to learn from the most recent data. In general, the model represents the curve of the price profile well but tends to miss

the most extreme cases.

Figure 5.4b shows some averaged performance metrics over the lead time of the models. The CRPS shows the Continuous Ranked Probability Score, which is a combined score for all quantiles in the forecast and is expressed in the unit of the forecast variable. The MAE is the Mean Absolute Error calculated with the 50th percentile of the forecasts. The PICp80 stands for the Prediction Interval Coverage Percentage at the 80% confidence interval, representing how many observations were between the 90th and 10th percentile. The PINAW80 stands for Prediction Interval Normalized Average Width at the 80% confidence interval. Some models show some performance decrease over the length of the test sets, which would be especially visible in the decrease of PICP and therefore the validity of confidence intervals.

The models could be optimized further in order to improve performance but seem to perform well on average. Every model can be optimized for performance, especially if performance evaluation is purely metric-based. We test model goodness based on operational performance, to be measured in constraint violation and energy cost - compared to perfect foresight. In this work, we focus on the probabilistic control framework and closed-loop simulation testing; the aim is not the exhaustive optimization of each single model based on classical time-series forecast metrics.

5

5.4.2. SCENARIO GENERATION AND REDUCTION

To generate scenarios with realistic temporal dependency, we first fit parametric distributions, as available in the Scipy [29] python package, on the quantile forecasts, to be used in an NPBN with pre-defined structure as depicted in Figure 5.5a. For all variables that are forecast using the CQRDNN, we apply the same NPBN structure.

Forecasting electricity prices on the IDM requires renewable energy production data that is updated during the day. ENTSO-E's open database [30] is of insufficient quality to accurately model the IDM. Therefore, we model IDM price uncertainty using an NPBN that conditionalizes the IDM price to the DAM price and already observed IDM prices, as depicted in Figure 5.5b. We use the distributions of the relative ID₃ price (e.g. $\frac{ID_3}{DAM}$) to model and infer IDM prices.

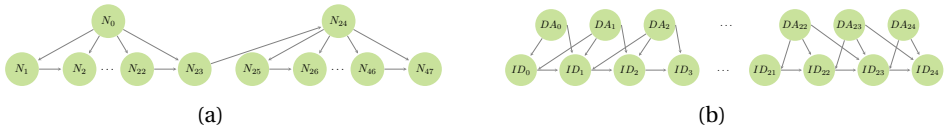


Figure 5.5: Non-parametric Bayesian Network structures for uncertainty modelling of (a) DAM prices, incoming discharge, and the water level of the North Sea (adopted from [13]), and (b) IDM prices. N_i represents the i -th hour forecast lead time, DA_i and ID_i represent the DAM and IDM prices for the i -th hour of the day.

In order to sufficiently represent the uncertainty space, we sample 1000 timeseries from the BN for each variable. This number was selected a posteriori based on a trade-off between the computational feasibility of the optimization problem and the completeness of the uncertainty representation. We then apply Algorithm 1 to select an optimal

subset with new weights. To transform the scenario set into a fan, we cluster the root node to a single scenario. We select a root node size of three hours, which corresponds with the time when the IDM has the most liquidity. To reduce computational complexity, we also consider scenario trees. A scenario tree can significantly reduce the amount of decision variables necessary to describe the optimization problem. We apply a GA as described in Section 3.2.3 to reduce the selected subset to a scenario tree and constrain a minimum 50% reduction in tree complexity. Figure 5.6 shows an example reduced scenario subset, a scenario fan, and a scenario tree, for the water level of the North Sea.

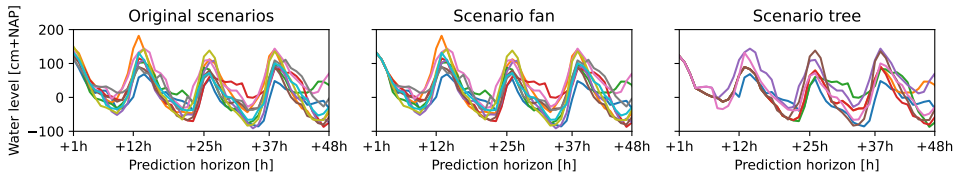
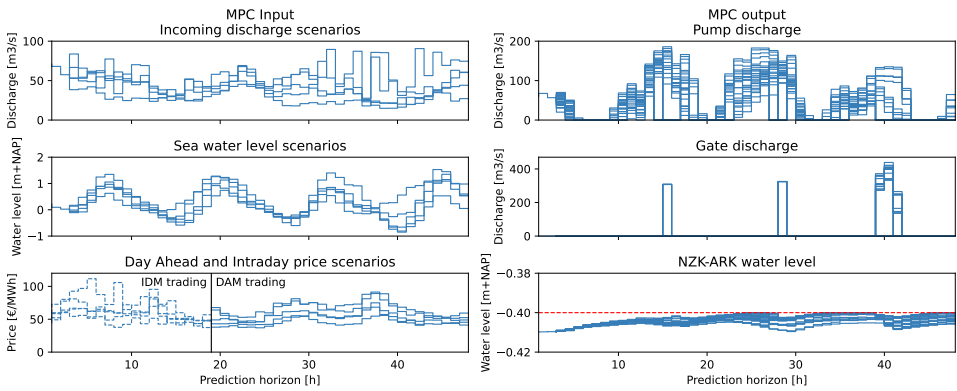


Figure 5.6: The energy-distance optimal scenario subset of size 10, and the constructed scenario fan and scenario tree with 50% complexity reduction for North Sea water level at a single simulation timestep.

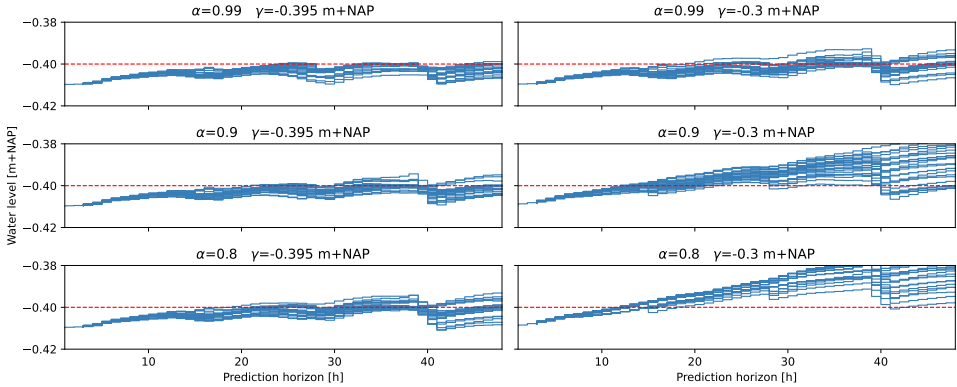
5.4.3. STOCHASTIC MPC

To investigate the effect of the variations in risk-acceptance on the water level, we explore the output of the MPC's internal model. Within the internal MPC model, there is a pump discharge, gate discharge, and water-level decision variable for each timestep and all scenario combinations. However, since we need a single implementable output for control, a root node of 3h is maintained where the values of the energy-distance optimal scenario are used, leading to a deterministic pump- and gate schedule for the coming three hours.

Figure 5.7b shows the water level in the internal MPC model for a single control timestep of the simulation with receding horizon implementation. We can see how, as the ER α and γ change, the output water level changes, effectively translating ER parameters into operational consequences.



(a)



(b)

Figure 5.7: (a) The MPC model input and output from the internal model with constraints that are robust towards to the worst case in the reduced set, and (b) the output water level from MPCs with different ER α and γ constraint settings and the same input.

5.4.4. CLOSED-LOOP SIMULATION TESTING

We perform closed-loop simulations of energy market participation for January, April, July, and October for 2019 and 2020, and January for the year 2021 (due to data availability). The months are simulated separately due to the framework’s runtime resulting from the computational demands of the optimisation problem. The simulations were run on Snellius, the Dutch National Supercomputer [31], and a single month of simulation still took 22.5h to run on average. The MPC problem was solved using Gurobi [32] with the relative MIPGap set to 0.01, the absolute MIPGap to €1, the NonConvex parameter set to 2, and a time limit of 15min if a solution was found, else the optimization would continue until the first feasible solution was found.

We perform a sensitivity analysis on the amount and shape of the scenarios, where we consider 1 (e.g. a deterministic forecast with deterministic constraints), 3, and 5 scenarios per source of uncertainty in either a fan or tree shape, and where all scenarios are selected based on the energy distance subset selection method described in Algorithm 1. We then compare a scenario-robust approach with several ER settings ($\alpha \in \{0.99, 0.9, 0.8\}$, $\gamma \in \{-0.395, -0.3\}$), and we compare all simulated scenarios and energy costs with a simulation using a deterministic perfect forecast. Figure 5.8 shows the relative yearly cost of the simulations of market participation compared to the perfect forecast.

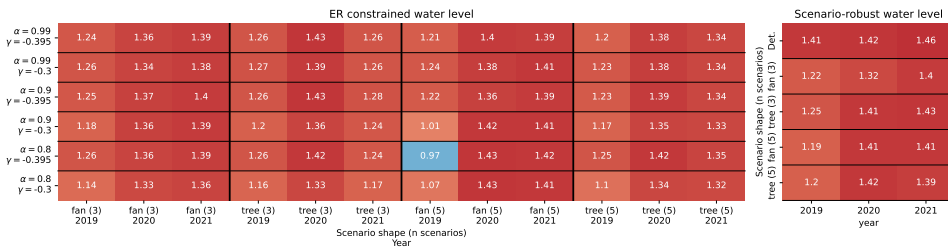


Figure 5.8: Relative yearly cost of the simulated months compared to the simulations with a perfect forecast. The left figure shows the relative cost for the simulations with ER-constrained water levels, while the right figure shows the relative cost of the simulations with scenario-robust control. Scenario-robust with one scenario is the same as a deterministic problem and is depicted as ‘Det.’. Red indicates that the simulated costs were higher than the cost for the simulation with perfect forecasts, while blue indicates the cost were lower.

Figure 5.8 shows a clear value in a probabilistic approach compared to a deterministic (i.e. scenario-robust with 1 scenario) approach, especially in 2019. All considered probabilistic approaches result in lower energy costs than the deterministic approach. However, large variations in relative performance can be seen over the years. The lowest performance increase was seen in 2020 when the COVID pandemic hit. One possible explanation is that the difficulty of forecasting electricity prices increased in 2020 and 2021, leading to suboptimal operational uncertainty estimation.

When comparing ER approaches with scenario-robust approaches, the figure shows that, on average, ER approaches result in lower energy cost than scenario-robust approaches. ER approaches with low α and high γ are notable exceptions. ER approaches

seem to perform worse than the scenario-robust approaches, which a lack of intervention can explain. As the future probability of a high water level becomes more tolerable, the scenario will become more likely at some point, activating the upper-bound constraint. Suppose this happens too close to the execution time. In that case, more energy has to be traded on the IDM since the DAM is already closed, limiting the economic potential of multi-market trading.

Increasing the size of the scenario set does not always lead to better results. When the MPC problem is hard to solve, the optimal solution would not be reached within the cut-off time. A more scarce scenario-tree representation, therefore, generally performs better with 5 scenarios. In 2021, which only consists of January, the difference between a fan- or tree uncertainty representation is the largest. January 2021 was a wet month, with an average simulation runtime for the 5-scenario fan approach was 58h, while the average simulation runtime for the 5-scenario tree approach was 27h. This is consistent with our hypothesis that time constraints can affect the optimal scenario set size for uncertainty representation.

In one simulation with actual forecasts, we observe a lower cost than in the perfect forecast scenario. This can be explained by a forecast error at the right time when IDM prices were advantageous. Even with the perfect forecast, IDM prices are only known after DAM closure, leading to the absence of speculation on IDM prices. This could lead to more profitable energy on the IDM, even though the initial DAM bid was suboptimal. The portfolio could be further optimized if IDM and DAM prices were available for the optimization problem at the same time. However, that would increase the complexity of the optimisation problem and might not be practically feasible using the same problem formulation.

In general, it can be seen that the benefits of the proposed stochastic method vary over the years. The year 2019, when electricity prices were easiest to forecast, seemed to have the most optimal results with up to 44 p.p. cost savings compared to the deterministic forecast, and even contained a simulation with lower cost than the perfect forecast scenario. In 2020, when the COVID pandemic just started, the profitability of the proposed strategy decreased, but the stochastic method still allows 10 p.p. cost savings compared to a deterministic approach. We also see that the value of taking risks decreases in 2020, while that benefit is present in 2019 and 2021 when the electricity markets were relatively calm compared to 2020.

Figure 5.9 shows the probability distributions of the observed water levels of the NZK-ARK and a set of simulated water levels. The figure shows that a deterministic forecast can lead to a sharp distribution around the target water level. This is possibly caused by forecast inaccuracies, causing the control system to correct when water levels rise. This is consistent with the higher energy cost since flexibility can't be exploited well. The difference between scenario-robust and ER constraints can be seen in the figure. While both strategies have a similar distribution shape, ER constraints allow for a shift of the distribution and a slight flattening of the shape. When the complexity of the problem is lower, it seems like there is slightly more constraint violation occurring, as depicted by the distribution of the simulated water level with a tree-shaped uncertainty representation. None of the strategies will lead to a significant added risk compared with the observed water levels. Arguably, there can be a large difference between modelled and

actual water levels, but we believe the main conclusions stand. When comparing the distributions with the regime depicted in Figure 1.5b, we conclude that a lot of flexibility is left unexploited and that having less conservative control could well benefit both the energy transition as Rijkswaterstaat, the operator of the IJmuiden pumping station.

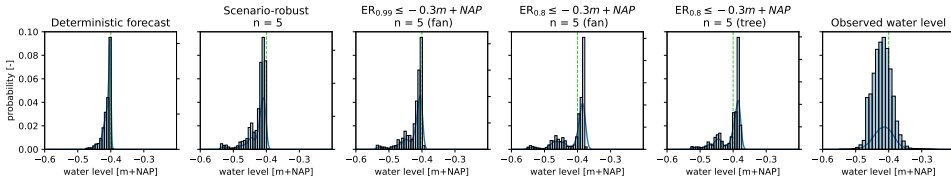


Figure 5.9: Histogram and KDEs of the simulated and observed water levels in the NZK-ARK. From left to right, the figure shows the distribution of the simulated water level with an optimization using deterministic forecasts, scenario-robust optimization with 5 scenario forecasts, two optimization problems with ER-constrained water level, and the observed water level in the NZK-ARK.

5.5. SUMMARY AND CONCLUSION

This chapter has presented a framework for incorporating risk into the operational management of water resources, focusing on the Netherlands' unique water management challenges. Our approach centred around the NZK-ARK system and effectively integrates probabilistic forecasting and optimal control strategies in a real-world setting, integrating uncertainty from various sources.

In our proposed framework, we apply a *Combined Quantile Regression Deep Neural Network* (CQRDNN) to estimate operational uncertainty, while a *Non-Parametric Bayesian Network* (BN) was applied to model auto-temporal relationships of forecast variables. Our methodology for scenario reduction, employing the Energy distance metric, has shown that it is feasible to distil a comprehensive set of scenarios into an optimal subset, while closed-loop performance does seem to be partially dependent on the number of scenarios in the subset.

By formulating *Stochastic Model Predictive Control* (MPC) with *Exceedance Risk* (ER) constraints, we provide an advancement over traditional deterministic MPC approaches. ER constraints allow for nuanced risk management by modulating the control response based on the severity and likelihood of upper-bound violations of water levels. This novel approach not only manages risks more effectively but also provides a mechanism for adjusting risk preferences dynamically, illustrated by our ability to warp and shift the distribution of the simulated water levels as shown in Figure 5.9. Besides leading to a nuanced description of risk, the constraints are formulated linearly, giving considerable computational advantages compared to integer programming.

We use 'historical simulations' with real water system and electricity market data to demonstrate the advantages of multi-market participation under uncertainty. The optimal control of the NZK-ARK system, simulated over several years, revealed that stochastic MPC could yield substantial energy cost savings compared to deterministic strate-

gies. These savings highlighted the effectiveness of our approach in adapting to variabilities in climate and market conditions, thereby providing a more resilient and economically efficient operational framework that can potentially be applied in many fields. Furthermore, our results show the utility of employing larger scenario sets for enhancing decision-making optimality, although we noted the practical constraints of optimization under tight time frames. The use of scenario trees are shown to be an effective strategy under these circumstances, facilitating more manageable computations while minimizing compromising the quality of outcomes.

In examining water levels, our simulated results stayed within acceptable ranges, indicating the operational viability of our approach. While there are observable differences between simulated and actual water levels, our findings also show that adjusting the ER parameters effectively modifies risk profiles, offering avenues for further refinement in future applications.

To conclude, this research advances the field of operational water resource management by delivering a robust, adaptable, and economically viable framework capable of managing the uncertainty and variability inherent in weather and electricity price conditions. This framework not only supports Rijkswaterstaat in optimizing energy costs but also enhances the safety and reliability of water and energy systems. While our study focused on the Dutch context, the methodologies and findings are applicable globally, offering valuable insights for regions facing similar challenges. The proposed methods also extend beyond water resources, possibly benefiting any application facing similar uncertainty and risk.

BIBLIOGRAPHY

- [1] Andrea Castelletti, Francesca Pianosi, and Rodolfo Soncini-Sessa. “Integration, participation and optimal control in water resources planning and management”. In: *Applied Mathematics and Computation* 206 (1 Dec. 2008), pp. 21–33. ISSN: 00963003. DOI: [10.1016/j.amc.2007.09.069](https://doi.org/10.1016/j.amc.2007.09.069).
- [2] Andrea Castelletti et al. “Model Predictive Control of water resources systems: A review and research agenda”. In: *Annual Reviews in Control* 55 (Jan. 2023), pp. 442–465. ISSN: 13675788. DOI: [10.1016/j.arcontrol.2023.03.013](https://doi.org/10.1016/j.arcontrol.2023.03.013).
- [3] M. Giuliani et al. “A State-of-the-Art Review of Optimal Reservoir Control for Managing Conflicting Demands in a Changing World”. In: *Water Resources Research* 57.12 (2021). DOI: <https://doi.org/10.1029/2021WR029927>. eprint: <https://agupubs.onlinelibrary.wiley.com/doi/pdf/10.1029/2021WR029927>.
- [4] Ali Mesbah. “Stochastic Model Predictive Control: An Overview and Perspectives for Future Research”. In: *IEEE Control Systems Magazine* 36.6 (Dec. 2016), pp. 30–44. ISSN: 1941-000X. DOI: [10.1109/MCS.2016.2602087](https://doi.org/10.1109/MCS.2016.2602087).
- [5] F. Pianosi and R. Soncini-Sessa. “Real-time management of a multipurpose water reservoir with a heteroscedastic inflow model”. In: *Water Resources Research* 45.10 (2009). DOI: <https://doi.org/10.1029/2008WR007335>. eprint: <https://agupubs.onlinelibrary.wiley.com/doi/pdf/10.1029/2008WR007335>. URL: <https://agupubs.onlinelibrary.wiley.com/doi/abs/10.1029/2008WR007335>.
- [6] Christian Pape. “The impact of intraday markets on the market value of flexibility — Decomposing effects on profile and the imbalance costs”. In: *Energy Economics* 76 (2018), pp. 186–201. ISSN: 01409883. DOI: [10.1016/j.eneco.2018.10.004](https://doi.org/10.1016/j.eneco.2018.10.004). URL: <https://doi.org/10.1016/j.eneco.2018.10.004>.
- [7] Conor Sweeney et al. “The future of forecasting for renewable energy”. In: *WIREs Energy and Environment* 9.2 (2020), e365. DOI: <https://doi.org/10.1002/wene.365>. eprint: <https://wires.onlinelibrary.wiley.com/doi/pdf/10.1002/wene.365>. URL: <https://wires.onlinelibrary.wiley.com/doi/abs/10.1002/wene.365>.
- [8] Reetik Kumar Sahu and Dennis B. McLaughlin. “An Ensemble Optimization Framework for Coupled Design of Hydropower Contracts and Real-Time Reservoir Operating Rules”. In: *Water Resources Research* 54.10 (2018), pp. 8401–8419. DOI: <https://doi.org/10.1029/2018WR022753>. eprint: <https://agupubs.onlinelibrary.wiley.com/doi/pdf/10.1029/2018WR022753>. URL: <https://agupubs.onlinelibrary.wiley.com/doi/abs/10.1029/2018WR022753>.

- [9] Ricardo J. Bessa et al. “Towards Improved Understanding of the Applicability of Uncertainty Forecasts in the Electric Power Industry”. In: *Energies* 10.9 (2017). ISSN: 1996-1073. DOI: [10.3390/en10091402](https://doi.org/10.3390/en10091402). URL: <https://www.mdpi.com/1996-1073/10/9/1402>.
- [10] Ties van der Heijden, Peter Palensky, and Edo Abraham. “Probabilistic DAM price forecasting using a combined Quantile Regression Deep Neural Network with less-crossing quantiles”. In: *IECON 2021 – 47th Annual Conference of the IEEE Industrial Electronics Society*. 2021, pp. 1–6. DOI: [10.1109/IECON48115.2021.9589097](https://doi.org/10.1109/IECON48115.2021.9589097).
- [11] Spyros Makridakis et al. “The M5 uncertainty competition: Results, findings and conclusions”. In: *International Journal of Forecasting* 38.4 (2022). Special Issue: M5 competition, pp. 1365–1385. ISSN: 0169-2070. DOI: <https://doi.org/10.1016/j.ijforecast.2021.10.009>. URL: <https://www.sciencedirect.com/science/article/pii/S0169207021001722>.
- [12] Pengcheng Zhao et al. “Which precipitation forecasts to use? Deterministic versus coarser-resolution ensemble NWP models”. In: *Quarterly Journal of the Royal Meteorological Society* 147.735 (2021), pp. 900–913. DOI: <https://doi.org/10.1002/qj.3952>. eprint: <https://rmets.onlinelibrary.wiley.com/doi/pdf/10.1002/qj.3952>. URL: <https://rmets.onlinelibrary.wiley.com/doi/abs/10.1002/qj.3952>.
- [13] Ties van der Heijden et al. “Day Ahead Market price scenario generation using a Combined Quantile Regression Deep Neural Network and a Non-parametric Bayesian Network”. In: *2022 IEEE International Conference on Power Systems Technology (POWERCON)*. 2022, pp. 1–5. DOI: [10.1109/POWERCON53406.2022.9929940](https://doi.org/10.1109/POWERCON53406.2022.9929940).
- [14] L. Raso et al. “Short-term optimal operation of water systems using ensemble forecasts”. In: *Advances in Water Resources* 71 (2014), pp. 200–208. ISSN: 03091708. DOI: [10.1016/j.adwatres.2014.06.009](https://doi.org/10.1016/j.adwatres.2014.06.009).
- [15] J. M. Maestre et al. “Distributed tree-based model predictive control on a drainage water system”. In: *Journal of Hydroinformatics* 15.2 (2013), pp. 335–347. ISSN: 14647141. DOI: [10.2166/hydro.2012.125](https://doi.org/10.2166/hydro.2012.125).
- [16] R Tyrrell Rockafellar and Stanislav Uryasev. “Optimization of Conditional Value-at-Risk”. In: *Journal of Risk* 2 (3 2000), pp. 21–41. DOI: [10.21314/JOR.2000.038](https://doi.org/10.21314/JOR.2000.038). URL: [http://www.gloriamundi.org/..](http://www.gloriamundi.org/)
- [17] Janani Venkatasubramanian, Vahab Rostampour, and Tamas Keviczky. “Stochastic MPC for energy management in smart grids with conditional value at risk as penalty function”. In: vol. 2020-October. IEEE Computer Society, Oct. 2020, pp. 309–313. ISBN: 9781728171005. DOI: [10.1109/ISGT-Europe47291.2020.9248769](https://doi.org/10.1109/ISGT-Europe47291.2020.9248769).
- [18] Ties van der Heijden et al. “Multi-market demand response from pump-controlled open canal systems: an economic MPC approach to pump-scheduling”. In: *Journal of Hydroinformatics* 24 (4 July 2022), pp. 838–855. ISSN: 14651734. DOI: [10.2166/hydro.2022.018](https://doi.org/10.2166/hydro.2022.018).

- [19] Minh Dang Doan et al. “A distributed accelerated gradient algorithm for distributed model predictive control of a hydro power valley”. In: *Control Engineering Practice* 21 (11 Nov. 2013), pp. 1594–1605. ISSN: 09670661. DOI: [10.1016/j.conengprac.2013.06.012](https://doi.org/10.1016/j.conengprac.2013.06.012).
- [20] K. Horváth et al. “Potential of model predictive control of a polder water system including pumps, weirs and gates”. In: *Journal of Process Control* 119 (Nov. 2022), pp. 128–140. ISSN: 09591524. DOI: [10.1016/j.jprocont.2022.10.003](https://doi.org/10.1016/j.jprocont.2022.10.003).
- [21] Fatemeh Karimi Pour et al. “A two-layer control architecture for operational management and hydroelectricity production maximization in inland waterways using model predictive control”. In: *Control Engineering Practice* 124 (July 2022). ISSN: 09670661. DOI: [10.1016/j.conengprac.2022.105172](https://doi.org/10.1016/j.conengprac.2022.105172).
- [22] A Goedbloed. “Kwaliteitsanalyse Beslissingen Ondersteunend Systeem Noordzeekanaal / Amsterdam-Rijnkanaal”. MA thesis. TU Delft, 2006.
- [23] H. Janssen. *Effect selectieve onttrekking IJmuiden op waterbeheer*. Tech. rep. Rijkswaterstaat, 2017. URL: https://www.platformparticipatie.nl/binaries/Effect%5C%20selectieve%5C%20onttrekking%5C%20IJmuiden%5C%20op%5C%20waterbeheer%5C_tcm117-377563.pdf.
- [24] Jacques De Jong et al. *Improving the Market for Flexibility in the Electricity Sector*. Tech. rep. Centre for European Policy Studies, 2017, p. 30. URL: http://aei.pitt.edu/92294/1/CEPS%7B%5C_%7DTRFR%7B%5C_%7DFlexibility%7B%5C_%7DElectricity%7B%5C_%7DMarkets.pdf.
- [25] A. Rezaee Jordehi. “Optimisation of demand response in electric power systems, a review”. In: *Renewable and Sustainable Energy Reviews* 103 (July 2018 (2019)), pp. 308–319. ISSN: 18790690. DOI: [10.1016/j.rser.2018.12.054](https://doi.org/10.1016/j.rser.2018.12.054). URL: <https://doi.org/10.1016/j.rser.2018.12.054>.
- [26] Daniel Schwabeneder et al. “Business cases of aggregated flexibilities in multiple electricity markets in a European market design”. In: *Energy Conversion and Management* 230 (August 2020 (2021)), p. 113783. ISSN: 01968904. DOI: [10.1016/j.enconman.2020.113783](https://doi.org/10.1016/j.enconman.2020.113783). URL: <https://doi.org/10.1016/j.enconman.2020.113783>.
- [27] Antonio J. Conejo, Miguel Carrión, and Juan M. Morales. *Decision Making Under Uncertainty in Electricity Markets*. Springer New York, NY, 2010. Chap. 4.3. DOI: <https://doi.org/10.1007/978-1-4419-7421-1>.
- [28] Pavlo Krokhmal, Jonas Palmquist, and Stan Uryasev. “Portfolio Optimization With Conditional Value-at-Risk Objective and Constraints”. In: *Journal of Risk* 4 (May 2003). DOI: [10.21314/JOR.2002.057](https://doi.org/10.21314/JOR.2002.057).
- [29] Pauli Virtanen et al. “SciPy 1.0: Fundamental Algorithms for Scientific Computing in Python”. In: *Nature Methods* 17 (2020), pp. 261–272. DOI: [10.1038/s41592-019-0686-2](https://doi.org/10.1038/s41592-019-0686-2).
- [30] ENTSO-E. *ENTSO-E Transparency Platform*. 2018. URL: <https://transparency.entsoe.eu/>.

- [31] Surf Cooperation. *Snellius: The National Supercomputer*. <https://www.surf.nl/en/services/snellius-the-national-supercomputer>. 2023.
- [32] Gurobi Optimization, LLC. *Gurobi Optimizer Reference Manual*. Tech. rep. Gurobi Optimization, LLC, 2018. URL: <http://www.gurobi.com>.



6

RAYCAST: A SATELLITE-BASED QUANTILE REGRESSION IRRADIANCE NOWCAST

*Space age!
Forget the glock and cock the laser back.*

Camo & Krooked, Jeru The Damaja

As the integration of solar energy in the energy system continues, electricity grid management is becoming an increasingly difficult task. As grid operators need to innovate in managing congestion, the uncertainty in incoming radiation is becoming a large obstacle in operational grid management.

In this chapter, we introduce RayCast: a spatially distributed quantile regression solar irradiance nowcasting model to assist operational management of electricity grids under meteorological fluctuations. Utilizing data from meteorological stations and satellite-derived cloud characteristics from Meteosat Second Generation across the Netherlands, the model proficiently predicts irradiance quantiles, spatially representing the related uncertainties for up to 6 hours ahead at a 15-minute temporal resolution and 4x6km spatial resolution. The model is validated through an analysis of spatial and temporal variations in performance using several deterministic and probabilistic forecasting metrics. Subsequently, the model is validated in an operational context, where it is applied in a net-load forecasting model for a transformer station near Eelde, characterized by significant solar generation capacity. In this real-world use case, we show that our proposed model increases the ability of a net-load forecasting model to show the possibility of extreme loads by up to 20 percent-point.

Parts of this chapter are under review for publication in IEEE Transactions on Sustainable Energy.

6.1. INTRODUCTION

Solar energy has become a serious component in the energy mix of the Netherlands. Years of advantageous subsidies for consumers have, high electricity prices, and a stubborn net-metering policy, lifted the country to hold the second-highest adoption rate for rooftop PV in the world, surpassed only by Australia [1]. Over the past decade, the Netherlands has significantly augmented its renewable energy resources, especially solar power, to reduce its national carbon footprint and navigate risks showcased by the recent energy crises, such as the Russian invasion of Ukraine. The installed solar generation capacity grew from 2.5 GW in 2018 to 14.9 GW in 2022 [2], with an ambitious target set at 125 GW by 2050 [3].

However, this rapid expansion presents unique challenges, especially for *Distribution System Operators* (DSOs). The inherent variability of solar energy, driven by dynamic weather conditions like fluctuating cloud cover and changing atmospheric humidity, leads to unpredictable grid fluctuations [4, 5]. These variations introduce volatility in *photovoltaic* (PV) production, affecting the stability and management of the utility grid. Accurate nowcasts (short-term, high-resolution forecasts) are essential to effectively manage these abrupt changes. This chapter builds on existing probabilistic approaches and aims to enhance the precision and utility of solar irradiance forecasts for grid management by implementing a *Quantile Regression* (QR) irradiance nowcast that considers multiple cloud characteristics [6].

Addressing these uncertainties has led to the development of various methodologies, ranging from traditional radar observations to advanced machine-learning models. Notably, the utilization of sky camera images, artificial intelligence techniques, and short-term forecasting has paved the way for anticipating disturbances hours in advance, benefiting efficient electricity distribution and energy trading [6, 7, 8, 9, 10]. The application of QR does not merely show forecast uncertainty, but opens up new risk-aware decision-making tools for the DSO. Furthermore, recent advancements in nowcasting, particularly through deep generative models, machine learning, and integration of *numerical weather prediction* (NWP) models, have significantly enhanced weather forecasting accuracy, informing our approach [11, 12, 13, 14, 15, 16].

As the electrification of transportation, heating, and other sectors continues and consequent demand on the distribution system grows, facilitating the transport of substantial solar energy to end-users, particularly through ageing or capacity-limited parts of the grid, becomes a challenge. Instances such as the spatial disconnect between generation and consumption in locations like the historic center of Amsterdam, or the installation of large solar generation plants in scarcely populated areas have caused local congestion issues and subsequent waiting lists for new grid connections [17].

In this chapter, we explore the implementation of QR for nowcasting solar irradiance in the Netherlands, using satellite data derived cloud characteristics from *Meteosat Second Generation* (MSG) [18]. We focus on nowcasting *Cloud Top Height* (CTH) and *Cloud Optical Thickness* COT, which we hypothesise to have the highest influence on irradiance compared to the other available MSG Cloud Physical Properties. COT acts as a surrogate metric for the amount of solar irradiance that would be able to penetrate clouds, while the CTH is a measure of how well the cloud can reflect irradiance originating from the Earth. An AENN [19] is utilized to convert the derived cloud parameters into a proba-

bility distribution of solar irradiance with a CQRDNN [20] (Chapter 3) for the coming 6 hours at 4x6km spatial resolution. Through a case study with Dutch DSO Alliander, we validate our model, demonstrating its operational utility in forecasting congestion issues. This is done by analysing the hit rate and false alarm rate for a QR net-load forecast at a transformer station with a high penetration of solar energy. We compare our irradiance model with Harmonie [21], the model developed by the *Dutch Royal Meteorological Institute* (KNMI) that is currently being applied by the DSO, and confirm that our approach contributes to the forecasting of congestion issues, an important step towards improving grid stability and reliability.

6.2. METHODOLOGY

In this section we describe our methodology. First, we explain the algorithms applied to nowcast cloud characteristics, after which we explain the CQRDNN and the model validation techniques.

6.2.1. ADVERSARIAL EXTRAPOLATION NEURAL NETWORK

Adversarial Extrapolation Neural Networks (AENN), as depicted in Figure 6.1a, leverage adversarial learning principles to enhance the extrapolation capabilities of neural networks. AENN consists of two types of neural networks: a generator-type network and a discriminator-type network. The generator network is trained to produce outputs that resemble the input data, while the discriminator network is trained to distinguish between the generated outputs and the original input data. The training process of AENN is similar to that used in *Generative Adversarial Networks* (GANs). In this approach, we condition the generator solely on historic satellite observations, eliminating the use of latent variables. Furthermore, we define a reconstruction loss with respect to the target variables CTH and COT.

The AENN generator losses are defined as

$$\mathcal{L}_{\text{gen}}(\mathbf{y}, \hat{\mathbf{y}}) = \alpha \cdot \mathcal{L}_{\text{rec}}(\mathbf{y}, \hat{\mathbf{y}}) + (1 - \alpha) \cdot (\beta \cdot \mathcal{L}_{\text{adv},f}(\hat{\mathbf{y}}) + (1 - \beta) \cdot \mathcal{L}_{\text{adv},s}(\hat{\mathbf{y}})), \quad (6.1)$$

$$\mathcal{L}_{\text{rec}}(\mathbf{y}, \hat{\mathbf{y}}) := \frac{1}{N} \sum_{i=1}^N \|\mathbf{y}_i - \hat{\mathbf{y}}_i\|, \quad (6.2)$$

$$\mathcal{L}_{\text{adv},f}(\hat{\mathbf{y}}) := \frac{1}{N} \sum_{i=1}^N \log(1 - D(\hat{\mathbf{y}}_i)), \quad (6.3)$$

$$\mathcal{L}_{\text{adv},s}(\hat{\mathbf{y}}) := \log(1 - D(\hat{\mathbf{y}})), \quad (6.4)$$

where, i is the time index of a spatial forecast, \mathcal{L}_{rec} represents the reconstruction loss, $\mathcal{L}_{\text{adv},f}$ denotes the adversarial loss for the generated outputs, and $\mathcal{L}_{\text{adv},s}$ indicates the adversarial loss for the original input data. The generator-loss \mathcal{L}_{gen} combines these losses, and the hyperparameters α and β control their contributions.

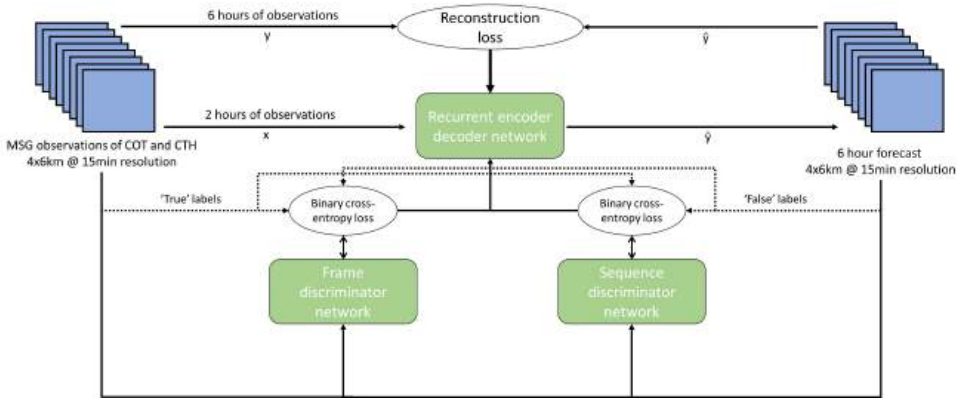
The reconstruction loss $\mathcal{L}_{\text{rec}}(\mathbf{y}, \hat{\mathbf{y}})$ measures the dissimilarity between the ground truth target variables \mathbf{y} and the generated outputs $\hat{\mathbf{y}}$. It is computed as the average of the element-wise absolute differences over all considered pixels.

The adversarial losses, $\mathcal{L}_{adv,f}(\hat{\mathbf{y}})$ and $\mathcal{L}_{adv,s}(\hat{\mathbf{y}})$, assess the generator network's ability to produce outputs that are indistinguishable from the original input data. One discriminator is used to classify single forecast frames as fake or real, while the other discriminator is employed to classify sequences of forecasts as fake or real. The discriminators are trained with loss

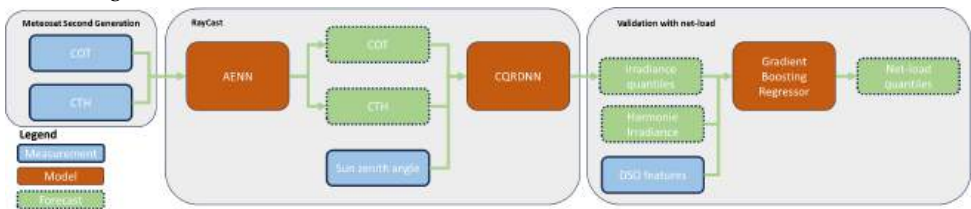
$$\mathcal{L}_{dis}(\mathbf{y}, \hat{\mathbf{y}}) = -\log(D(\mathbf{y})) - \log(1 - D(\hat{\mathbf{y}})), \tag{6.5}$$

where in each iteration, the generator network strives to minimize these losses, $D(\hat{\mathbf{y}})$, by generating outputs that deceive the discriminator networks. The discriminator networks aim to accurately distinguish between the generated outputs and the original input data.

By optimizing the generator-loss, \mathcal{L}_{gen} , which combines the reconstruction loss $\mathcal{L}_{rec}(\mathbf{y}, \hat{\mathbf{y}})$, and the adversarial losses $\mathcal{L}_{adv,f}(\hat{\mathbf{y}})$ and $\mathcal{L}_{adv,s}(\hat{\mathbf{y}})$, the AENN method trains the generator network to produce outputs that both closely reconstruct the target variables and successfully deceive the discriminator networks. This combination of losses enables the AENN to enhance the extrapolation capabilities of neural networks.



(a) Training schematic of the AENN.



(b) Schematic of the model chain from MSG input data of COT and CTH, to the forecast of irradiance quantiles, to validation with a net-load forecasting model.

Figure 6.1: RayCast schematics for the training of the AENN (a) and the total model chain from input data to the validation with a net-load forecast (b).

In our specific case, the AENN models receive a 2-channel input consisting of CTH and COT as obtained from the MSG satellite product. The models utilize 8 historic observations, spanning 2 hours, to forecast the next 24 frames, covering 6 hours. These

timeframes were chosen based on a pragmatic trade-off between forecast accuracy and usability. MSG is a geostationary optical satellite and can therefore give an updated image of cloud characteristics every 15 minutes while having a spatial resolution of 4x6km in the Netherlands, but will also have a significant amount of time without data due to the lack of sunlight, limiting the amount of historic observations that can be used in a forecast. When more than 2h of historic observations are used, the first operational forecasts can only be generated after more than 2h of sunlight.

The AENN is trained and validated on 7 years (2011-2018) of MSG data at 15-min resolution. Two years (2015 and 2017) were used as validation set in order to optimize the hyperparameters of the model. These years were selected in order to create a diverse set of COT and CTH combinations in both the training and validation data. The test set is comprised of the years 2019 and 2020, the most recent data available to the authors.

To summarize, the AENN method combines adversarial learning principles with neural networks to enhance the extrapolation capabilities of neural networks. By training a generator network to produce outputs similar to the input data and utilizing discriminator networks to differentiate between generated and original data, the AENN achieves improved performance in extrapolation tasks. The generator-loss, which includes the reconstruction loss and the adversarial losses, allows for flexible trade-offs between reconstruction fidelity and adversarial similarity. This versatility makes the AENN an effective approach for enhancing neural network extrapolation capabilities.

6.2.2. STUDY SET-UP

In this study, we train the CQRDNN to estimate 13 quantiles of KNMI measured solar irradiance based on the AENN forecasts in the validation set and the calculated Sun zenith angle (the angle of the Sun with respect to the vertical). This allows the CQRDNN to learn to estimate forecast uncertainty based on 1) uncertainty in the cloud measurement, 2) pixel uncertainty due to the KNMI measured irradiance being a point measurement in a cell, and 3) forecast uncertainty of the AENN since the model is trained on historic forecasts. By having a representation of the forecast uncertainty, the uncertainty can be propagated to forecasting congestion, improving the DSO's ability to apply risk-aware decision-making strategies for grid operations.

The *Tree Parzen Estimator* (TPE) [22] algorithm was utilized for combined feature and hyperparameter optimization.

6.2.3. HYPERBAND PRUNING

Hyperband pruning [23] is a technique employed in hyperparameter optimization to efficiently allocate computational resources and expedite the search for optimal hyperparameter configurations. It combines a multi-armed bandit strategy with early stopping to identify and discard unpromising hyperparameter settings early in the optimization process.

The algorithm comprises multiple iterations known as brackets. Each bracket involves training multiple models with different hyperparameter configurations while utilizing limited training resources. The models are trained for a fixed number of iterations or epochs, and at the end of each iteration, a fraction of poorly performing models is eliminated based on their intermediate validation performance. In our case we quantify

performance with the \mathcal{L}_{rec} rather than the \mathcal{L}_{gen} , since we want to prevent optimizing for weak discriminators by rewarding the inability of the discriminator to correctly label generated and original clouds.

Hyperband pruning effectively balances exploration (evaluating a wide range of hyperparameter configurations) and exploitation (allocating more resources to the most promising configurations). By swiftly discarding poor configurations and allocating additional resources to potentially superior ones, Hyperband pruning facilitates efficient hyperparameter optimization and expedites the search for optimal configurations. By intelligently allocating resources and selectively pruning unpromising configurations, Hyperband pruning can significantly reduce the computational burden associated with hyperparameter optimization, making it an especially valuable technique for the optimization of large neural networks that need large amount of resources to be trained. In this work, we apply Hyperband pruning combined with the TPE algorithm to efficiently optimize the AENN hyperparameters.

6.2.4. MODEL VALIDATION

To assess the effectiveness of our proposed model, we employ two evaluation approaches. Initially, we conduct an analysis of the model's performance by comparing its forecasts against actual irradiance measurements taken at various KNMI locations across the Netherlands. This involves examining both deterministic and probabilistic metrics across different lead times to gauge the accuracy of the model. However, since these metrics alone may not fully reflect real-world applicability, we continue our validation process through a real-world use-case provided by Alliander, a Dutch DSO. We develop net-load QR forecasting models based on the provided data and perform a comparative analysis of feature importance, contrasting our model's irradiance forecasts with those generated by Harmonie [21], a forecasting model developed by KNMI that is currently being applied by the DSO, to demonstrate our model's practical utility and efficacy. Further validation using KNMI's Harmonie model is not feasible due to limited data availability.

METRIC-BASED EVALUATION

In order to analyze model performance, we quantify the spatial and temporal variation in model performance with probabilistic and deterministic metrics

$$\text{MAE}(y, \hat{y}) = \frac{1}{N} \sum_{i=1}^N |y - \hat{y}|, \quad (6.6)$$

$$\text{RMSE}(y, \hat{y}) = \sqrt{\frac{1}{N} \sum_{i=1}^N (y - \hat{y})^2}, \quad (6.7)$$

$$\text{CRPS}(\mathbf{y}, \hat{\mathbf{y}}) = \frac{1}{N} \sum_{\tau \in T} \max(\tau \cdot (\hat{y}_{\tau} - y), (\tau - 1) \cdot (\hat{y}_{\tau} - y)), \quad (6.8)$$

$$\text{PICP}_{\tau_0:\tau_1}(y, \hat{\mathbf{y}}) = \frac{1}{N} \sum_{i=1}^N \mathbb{1}_{\hat{y}_{\tau_0} \leq y \leq \hat{y}_{\tau_1}}, \quad (6.9)$$

$$\text{PINAW}_{\tau_0:\tau_1}(\mathbf{y}, \hat{\mathbf{y}}) = \frac{\hat{y}_{\tau_1} - \hat{y}_{\tau_0}}{y_{\max} - y_{\min}}, \quad (6.10)$$

where y is the observation, \hat{y} the expected value of the QR nowcast, and \hat{y}_τ the τ -quantile of the QR nowcast. The MAE and RMSE depict an image of the error of the expected value of the quantile forecast, the *Continuous Ranked Probability Score* (CRPS) is a combined weighted metric for the quantile-errors, the *Prediction Interval Coverage Percentage* (PICP) shows the amount of observations that fall within a *predefined prediction interval* (PI) (e.g. the 80% PI should cover 80% of the observations), and the *Prediction Interval Normalized Average Width* (PINAW) depicts the normalized width of a predefined PI. An ideal 80% PI should therefore have a low PINAW but a PICP of exactly 80%. In order to construct a spatially distributed image of the derived forecast metrics, inverse distance weighting [24] was applied to interpolate model performance between KNMI weather stations spatially.

REAL-WORLD USE-CASE EVALUATION

To evaluate the practical applicability of the developed nowcasting model, we conducted an investigation into quantile coverage of extreme net-loads of a net-load forecasting model, utilizing data from a transformer station located near Eelde, the Netherlands, characterized by significant solar production. Net-load is the consumption minus the generation and will be negative when there is a generation surplus. We looked at hit- and false alarm rates for certain forecast quantiles of the net-load (i.e. 0.1, 0.3, 0.5, 0.7, 0.9), and observed load quantiles. For the purpose of forecasting net-load quantiles, we employed a Gradient Boosting Regressor [25, 26], applying the data that is practically utilized by the DSO, as depicted in Figure 6.1b.

The dataset provided encompasses a complete year (2020) of data, recorded at 15-minute intervals, comprising local weather features derived from the KNMI Harmonie model (e.g. temperature, humidity, irradiance, ...), temporal features (e.g. the hour of the day), load profiles as developed by the DSO, and the target variable, namely the net load as measured at the transformer station. Additionally, we incorporated the irradiance quantiles obtained through our proposed methodology for fixed lead times.

To optimize hyperparameters (e.g. number of estimators, max depth, learning rate), a 10-fold Cross-Validation (CV) was performed on the whole dataset, employing the TPE search algorithm and stratifying the folds based on the hours of the day. For each candidate set of hyperparameters, 10 models are trained with a different subset of the data being the validation set. No feature selection was performed to optimize model performance, but the same features that are applied in practice were used. The same setup was applied for all raycast lead times and for the reference without raycast (but with Harmonie).

6.3. SPATIOTEMPORAL MODELLING OF CLOUD CHARACTERISTICS

In this chapter, we apply the AENN (Section 6.2.1) to simultaneously forecast CTH and COT on a 4x6km spatial and 15min temporal resolution. By modelling COT and CTH simultaneously, the model can learn the relationship between the two characteristics, possibly leading to more accurate nowcasts. The AENN takes 8 historical observations (2h) of COT and CTH to forecast the next 24 observations (6h). The use of 8 historical

observations was decided on based on a pragmatic trade-off between forecast accuracy and forecast length. The AENN's conditional generator consists of an encoder, a ConvLSTM [15], and a decoder. The discriminators comprise multiple convolutional layers and a fully connected layer (e.g. an MLP layer). For more information about the network architecture, we refer the reader to the original manuscript [19].

Figure 6.2 shows the model output over the Netherlands for several lead times. The blurriness of the forecast increased over the lead time, which can be explained by increased uncertainty leading to a more averaged output through the reconstruction loss. By training the subsequent CQRDNN on the validation dataset, the irradiance quantiles are theorized to be estimated wider for large lead times due to this uncertainty.

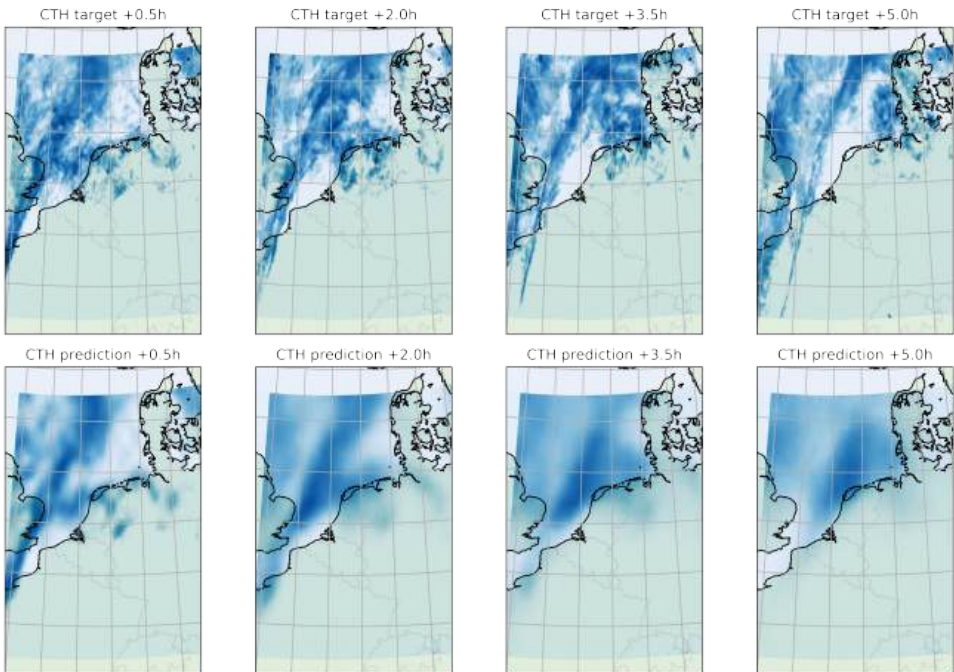
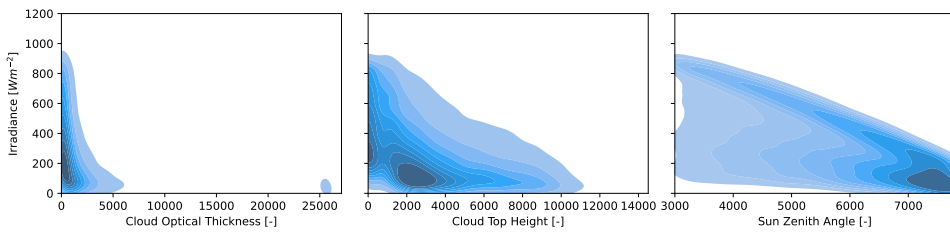


Figure 6.2: The Cloud Top Height as forecast by the AENN (bottom) and the observed target (top) for several lead times.

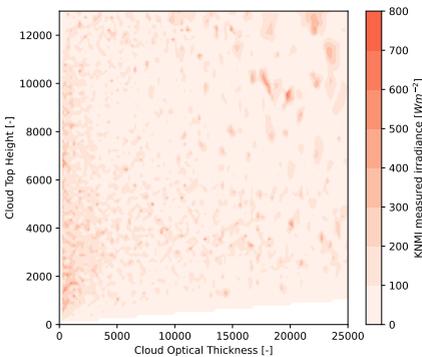
6.4. TRANSLATING CLOUD CHARACTERISTICS TO IRRADIANCE QUANTILES

In order to estimate irradiance on the Earth's surface, we sample the forecast COT and CTH from the validation set at the locations of meteorological stations, calculate the sun zenith angle, and use these as features to construct irradiance quantiles based on measurements with the CQRDNN (Section 3.1.1). Figure 6.3a shows the 2D Kernel Density Estimates (KDE) of the applied features with the measured irradiance at KNMI stations.

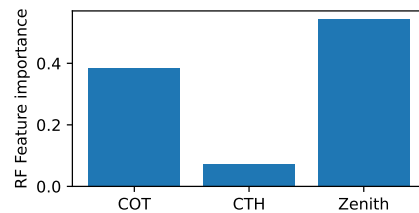
The angle of the sun has direct impact on the theoretical maximum amount of energy arriving at the Earth's surface. The COT can be used to estimate the amount of radiation that can penetrate the clouds, while the CTH can account for indirect radiation that possibly bounces back. Figure 6.3b depicts the non-linearity of the relationship between measured irradiance and cloud characteristics. The irradiance is highest with low COT and low CTH, possibly due to the penetration of irradiance through the clouds (low COT) while also scattering back after irradiance bounced from the Earth (CTH). With a high COT and CTH there are still possibilities for high irradiance, possibly due to the irradiance going underneath the clouds under an angle, making it possible to reach the Earth's surface regardless of clouds. This confirms the value of a probabilistic representation of irradiance, since some combined characteristics at a single pixel can lead to different outcomes in irradiance, especially when the irradiance comes under an angle. Figure 6.3c shows the feature importance of a Random Forest Regressor [27] translating the proposed features into irradiance as measured by the KNMI, confirming that the proposed features are of importance in irradiance modelling. It is noteworthy that we don't apply a Random Forest Regressor, but a CQRDNN (Section 3.1.1) to model irradiance quantiles.



(a) 2D-Kernel Density Estimate of COT (left), CTH (middle), and the Sun zenith angle (right) with measured irradiance at KNMI stations.



(b) Combined occurrences of COT, CTH, and irradiance as measured by the KNMI.



(c) Random Forest feature importance for estimating irradiance based on the proposed features.

Figure 6.3: Feature analysis for the translation of cloud characteristics to irradiance quantiles.

6.5. RESULTS AND DISCUSSION

In this section we show the results for the irradiance nowcast and discuss their implications. First, we analyze final model performance in irradiance nowcasting using forecast metrics, after which we will apply the output in a real-world use case provided by Alliander.

6.5.1. MODEL OUTPUT

For a sense of what the model output looks like to users, Figure 6.4 shows the forecast irradiance quantiles at KNMI station Eelde for random dates in the test set where the forecast for the coming six hours is shown over the x-axis. Generally, the model gives a reasonable representation of the irradiance with growing uncertainty over the lead times (over the x-axis). When the forecast error is large, the quantiles tend to widen, indicating an increase in forecast uncertainty. The plots indicate that the quantiles are somewhat conservative, which is exemplified by the number of times the observation is out of the extreme PIs.

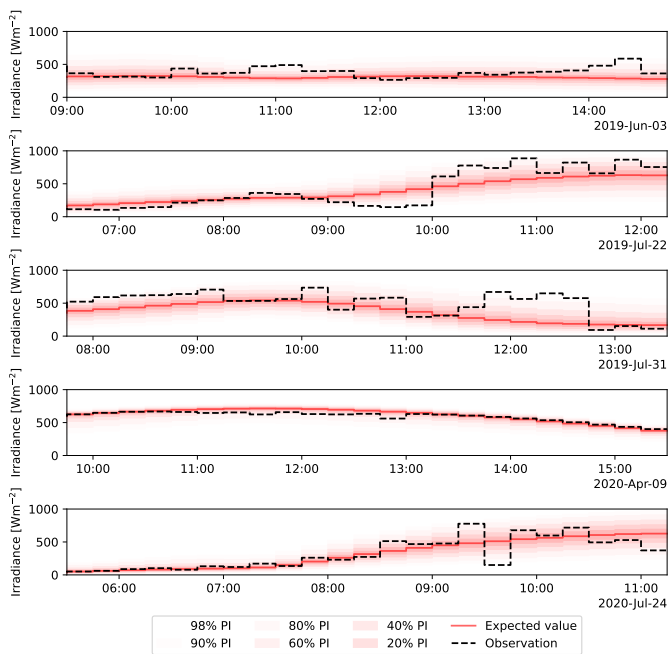


Figure 6.4: Operational forecast plots for random dates in the test set at a KNMI station in Eelde with increasing lead time over the x-axis. The dark line indicates the measurement at the weather station, the red line indicates the expected value of the forecast. The 98%, 90%, 80%, 60%, 40%, and 20% PIs are indicated with red planes around the expected value.

6.5.2. SPATIALLY DISTRIBUTED PERFORMANCE METRICS

Figure 6.5 depicts the spatial variation in model performance for a 1h lead time. Due to limited data availability, no comparison can be made with KNMI's Harmonie model in this analysis. The figures show that model performance tends to be slightly higher in the West of the Netherlands, possibly due to a slightly higher concentration of KNMI stations. This effect is especially clear in the CRPS of the nowcasts. The PICP, however, shows a more equally distributed image of performance with a notable difference in the North- and South-West, as exemplified in Figure 6.4. The 80% PIs have on average a 79.5% coverage percentage, which near to the ideal 80%. The PICP manages to perform well over the lead time, but with higher CRPS indicating wider PIs, as confirmed by the PINAW.

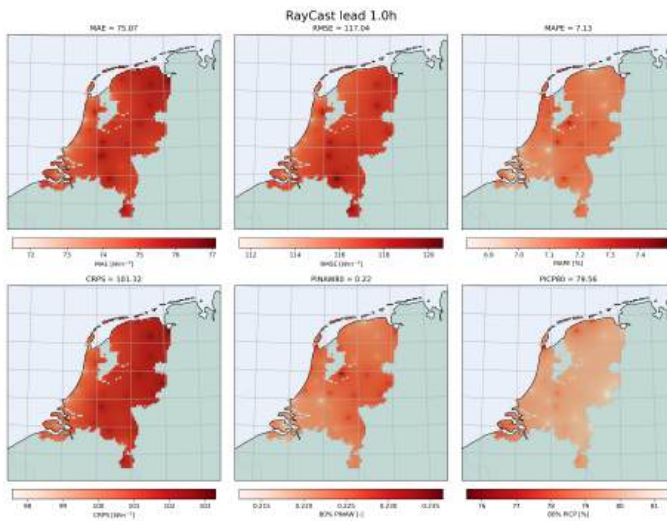


Figure 6.5: Inverse distance weighted spatially distributed performance metrics based on observations on KNMI weather stations. Metrics are calculated based on the nowcast with a lead time of 1 hour. Metrics are interpolated over the Netherlands using inverse-distance weighting. Note the inverted scale for PICP, since a higher rate is desirable.

6.5.3. TEMPORAL VARIATION IN MODEL PERFORMANCE

Figure 6.6 shows the difficulty of analyzing generalized model performance, which is expected to degrade over the lead time. However, in the case of solar irradiance nowcasting, in the begin and end of the day the forecast is relatively easy due to the low amount of irradiance, which would lead to small errors. The nowcast is most critical when solar irradiance is high, which is during the middle of the day. This inconsistency in forecast difficulty skews metrics when not properly taken into account.

Interestingly, model performance seems to peak at a 2h lead time. This could be explained by the beformentioned difference in forecast task. However, it can also indicate that initial cloud movement is hard to forecast.

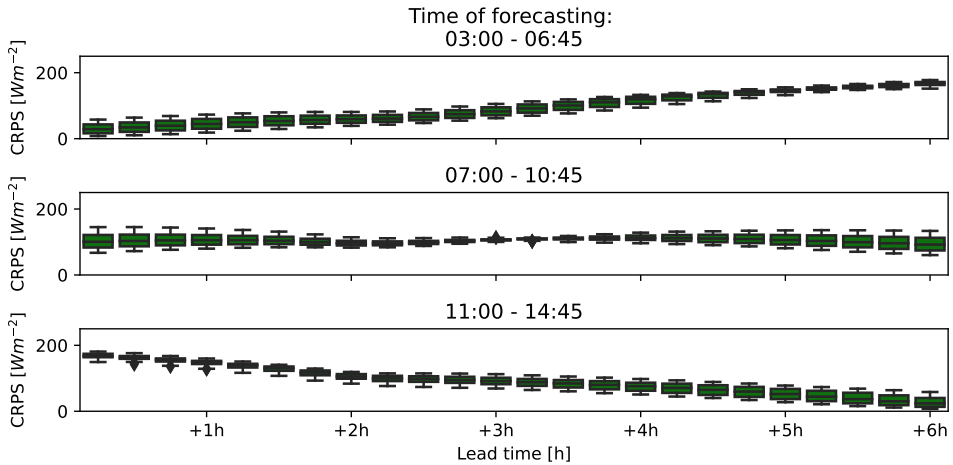


Figure 6.6: Boxplot of the CRPS for different times of forecasting and leadtimes, with confidence intervals based on the different KNMI stations.

6

Figure 6.7 shows more clearly that there is a large variation in forecasting and evaluation difficulty. A small absolute error can lead to significant relative error in the MAPE, leading to a more evenly distributed MAPE in comparison to the other metrics. This exemplifies the value of testing the model in a real-world setting, instead of validating models purely based on metrics.

6.5.4. MODEL VALIDATION WITH DSO DATA

We apply the features (the irradiance quantiles) generated by our proposed approach in a net-load forecasting model with data provided by Alliander. The net-load is defined as the differential between demand and generation, where a negative net-load means a generation surplus. Figure 6.8 depicts the Kernel Density Estimates of the observed net-load and the expected value of RayCast (left) and Harmonie (right) during the daytime (with non-zero irradiance). The stronger (spearman) correlation of our proposed methodology and the net-load indicates a possible added value in the forecast task. The net-load seems to be more widely distributed over Harmonie irradiance, than it is over the RayCast irradiance. The correlation seems stronger for the high load and irradiance values, indicating that the RayCast irradiance might be more useful when it comes to forecasting extremes. The most occurring net-load is still positive and with relatively low irradiance, showing that irradiance features, while helpful, aren't the only important predictors for the net-load. In this work, however, we focus on irradiance only while keeping the other features as they are currently being used by the DSO.

Figure 6.9 shows the output for the models generated in each fold of the cross-validation for a lead time of 2h. To quantify the added value of our approach, we look at times when an extreme value was foreseen by a net-load forecast quantile with and without our proposed model features. Figure 6.10 shows heatmaps with the net-load forecast quantiles'

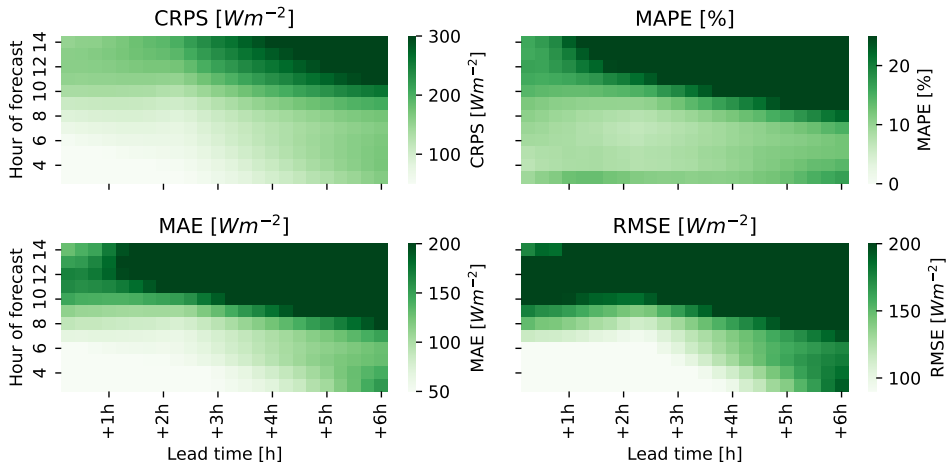


Figure 6.7: The CRPS, MAE, RMSE, and MAPE of the irradiance nowcast splitted by the hour of the forecast and lead time.

hit- and false alarm rate on the validation set. The figure shows that for extremely low load observations (observed load quantiles 0.05 and 0.1), Raycast' features tend to increase the hit rate of the net-load forecast quantile over most lead times and net-load forecast quantiles with up to 20 per cent points. Although less consistent, the increased hit rate also applies to high loads with little irradiance, possibly due to better forecasting of sudden clouds by Raycast. The false alarm rate seems to increase slightly by using our proposed irradiance features. However, that is to be expected for extreme forecast quantiles.

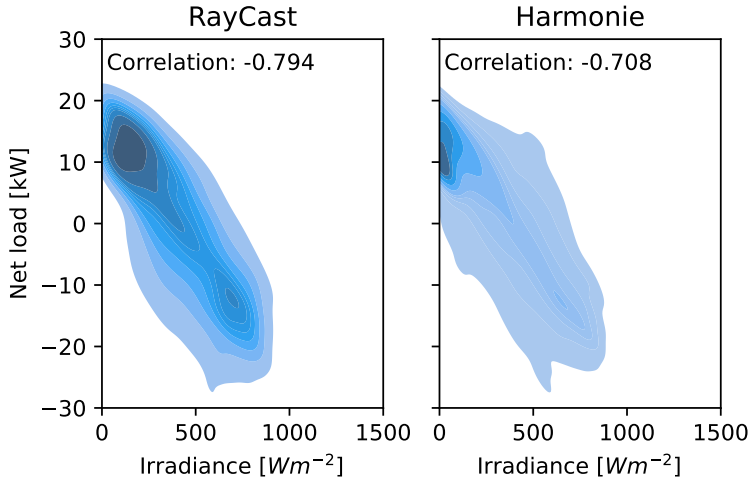


Figure 6.8: Kernel Density Estimate of the observed net-load and the expected value for a raycast forecast with lead time of 1h (left) and the harmonie forecast (right). The correlation depicted is the Spearman correlation.

6

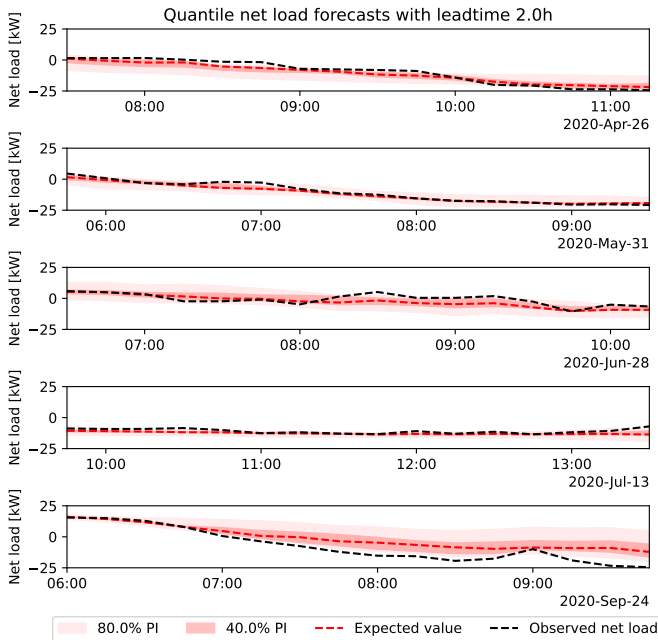


Figure 6.9: The output of the quantile net load forecasting models at a 2h lead time for a transformer station with a large penetration of solar energy. The colors indicate the prediction interval, the expected value, and the observed net load.

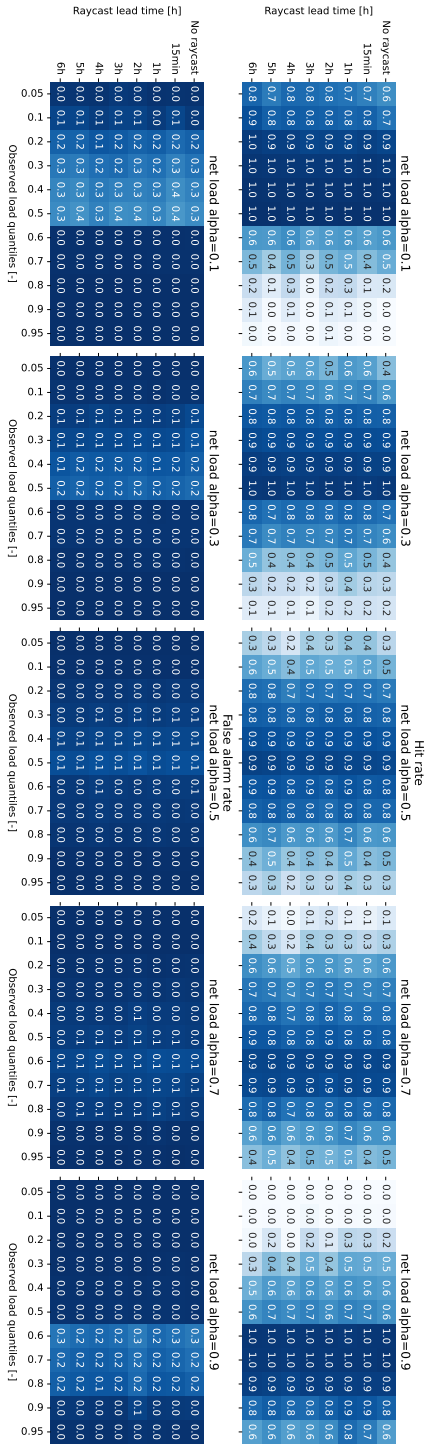


Figure 6.10: Heatmaps depicting the hit- (upper row) and false alarm (lower row) rate for certain load forecast quantiles (columns) and quantile threshold values based on the observed load. The x-axis shows the load-threshold quantile for which the rates are calculated, and the y-axis shows what raycast lead time was applied or if it wasn't included in the model. The color scale goes from blue (perfect) to white (bad). For the observed load quantiles lower or equal to 0.5, a hit is defined as both the forecast quantile and the observation being lower than the quantile value. A false alarm is a forecast quantile being lower than the quantile value, but the observation was higher. For the observed load quantiles higher than 0.5, hits and false alarms are based on higher values than the quantile value.

6.6. CONCLUSION

In this chapter, we have combined the best of spatiotemporal regression (the AENN) with probabilistic forecasting, leading to a novel approach to dealing with the inherent uncertainty and variability of solar power generation. The representation of forecast uncertainty would improve the DSO's ability to apply risk-aware decision-making strategies to protect infrastructure from extreme loads. Our model demonstrated a practical performance, evidenced by the quantile representation of irradiance with growing uncertainty over the lead time. Some spatial variability in model performance was seen, possibly due to geographical and meteorological variabilities, leaving room for improving performance across the considered area and beyond.

Additionally, our analysis shed light on temporal variations in the model's performance, giving insights into the impact of different times of day on forecasting proficiency. There is a variation in model performance over the time of forecasting, which could be caused by variable difficulty in the forecast task. Opportunities for future work might lie in improving the forecasting performance over the lead time and time of forecast.

Applying the model on real data through a net-load forecasting model for a transformer station near Eelde, the Netherlands, confirmed its practicality and relevance in a realistic operational context. We highlighted the added value of our approach compared to the irradiance features currently applied by the DSO through hit- and false alarm-rate analyses. We show that our proposed irradiance nowcast improves the ability of a net-load forecast to capture extreme events by up to 20 percentage points (p.p.), with consistent improvements over the forecast lead times. The interplay between deterministic and probabilistic forecasts was investigated, showing that probabilistic forecast features lead to performance increases, especially for the extreme quantiles of the net load. The false alarm rate also went up for the extreme forecast quantiles, which is to be expected since a 0.9 forecast quantile should exceed observations most of the time by definition.

We show a direction for additional inquiries and advancements in irradiance nowcasting, where the intersection between machine learning, meteorology, renewable energy forecasting, and operational grid management needs further exploration. Future studies might focus on rectifying the identified limitations of the present model, such as addressing the conservativeness of prediction intervals and enhancing forecast skill by incorporating more weather features, such as wind direction and speed or atmospheric pressure. Furthermore, explorations into the model's applicability in varied geographical and infrastructural contexts promise to unfold additional dimensions of its utility and versatility.

BIBLIOGRAPHY

- [1] W. Hemetsberger, M. Schmela, and R. Lopes Saaia. *Global Market Outlook For Solar Power 2022 - 2026*. Tech. rep. Solar Power Europe, 2022.
- [2] ENTSO-E. *ENTSO-E Transparency Platform*. 2018. URL: <https://transparency.entsoe.eu/>.
- [3] Marijke Kelner et al. *Het Energiesysteem van de Toekomst*. Tech. rep. 2021. URL: <https://www.netbeheernederland.nl/dossiers/toekomstscenarios-64>.
- [4] M. Trigo-González et al. “Photovoltaic power electricity generation nowcasting combining sky camera images and learning supervised algorithms in the Southern Spain”. In: *Renewable Energy* 206 (2023), pp. 251–262. DOI: [10.1016/j.renene.2023.01.111](https://doi.org/10.1016/j.renene.2023.01.111).
- [5] Jessica Wojtkiewicz et al. “Hour-Ahead Solar Irradiance Forecasting Using Multivariate Gated Recurrent Units”. In: (2019). DOI: [10.3390/en12214055](https://doi.org/10.3390/en12214055). URL: www.mdpi.com/journal/energies.
- [6] B. Nouri et al. “Probabilistic solar nowcasting based on all-sky imagers”. In: *Solar Energy* 253 (2023), pp. 285–307. DOI: [10.1016/j.solener.2023.01.060](https://doi.org/10.1016/j.solener.2023.01.060).
- [7] Frank P.M. Kreuwel et al. “Forecasting day-ahead 1-minute irradiance variability from numerical weather predictions”. In: *Solar Energy* 258 (July 2023), pp. 57–71. ISSN: 0038-092X. DOI: [10.1016/J.SOLENER.2023.04.050](https://doi.org/10.1016/J.SOLENER.2023.04.050).
- [8] Ruiyuan Zhang et al. “Photovoltaic Nowcasting With Bi-Level Spatio-Temporal Analysis Incorporating Sky Images”. In: *IEEE TRANSACTIONS ON SUSTAINABLE ENERGY* 12 (3 2021). DOI: [10.1109/TSTE.2021.3064326](https://doi.org/10.1109/TSTE.2021.3064326). URL: <https://www.ieee.org/publications/rights/index.html>.
- [9] Mitsuru Kakimoto et al. “Probabilistic Solar Irradiance Forecasting by Conditioning Joint Probability Method and Its Application to Electric Power Trading”. In: *IEEE Transactions on Sustainable Energy* 10.2 (2019), pp. 983–993. DOI: [10.1109/TSTE.2018.2858777](https://doi.org/10.1109/TSTE.2018.2858777).
- [10] Mahdi Khodayar et al. “Convolutional Graph Autoencoder: A Generative Deep Neural Network for Probabilistic Spatio-Temporal Solar Irradiance Forecasting”. In: *IEEE Transactions on Sustainable Energy* 11.2 (2020), pp. 571–583. DOI: [10.1109/TSTE.2019.2897688](https://doi.org/10.1109/TSTE.2019.2897688).
- [11] Chang Hoo Jeong et al. “Enhancing the Encoding-Forecasting Model for Precipitation Nowcasting by Putting High Emphasis on the Latest Data of the Time Step”. In: (2021). DOI: [10.3390/atmos12020261](https://doi.org/10.3390/atmos12020261). URL: <https://doi.org/10.3390/atmos12020261>.

- [12] Suman Ravuri et al. “Skillful precipitation nowcasting using deep generative models of radar”. In: *Nature* 597 (2021). DOI: [10.1038/s41586-021-03854-z](https://doi.org/10.1038/s41586-021-03854-z). URL: <https://doi.org/10.1038/s41586-021-03854-z>.
- [13] Seppo Pulkkinen et al. “Pysteps: an open-source Python library for probabilistic precipitation nowcasting (v1.0)”. In: *Geoscientific Model Development* 12 (10 Oct. 2019), pp. 4185–4219. ISSN: 1991-9603. DOI: [10.5194/gmd-12-4185-2019](https://doi.org/10.5194/gmd-12-4185-2019). URL: <https://gmd.copernicus.org/articles/12/4185/2019/>.
- [14] Ruben O. Imhoff et al. “Scale-dependent blending of ensemble rainfall nowcasts and numerical weather prediction in the open-source pysteps library”. In: *Quarterly Journal of the Royal Meteorological Society* 149.753 (2023), pp. 1335–1364. DOI: <https://doi.org/10.1002/qj.4461>. eprint: <https://rmets.onlinelibrary.wiley.com/doi/pdf/10.1002/qj.4461>. URL: <https://rmets.onlinelibrary.wiley.com/doi/abs/10.1002/qj.4461>.
- [15] Xingjian Shi et al. “Convolutional LSTM Network: A Machine Learning Approach for Precipitation Nowcasting”. In: *Advances in Neural Information Processing Systems*. Ed. by C. Cortes et al. Vol. 28. Curran Associates, Inc., 2015. URL: https://proceedings.neurips.cc/paper_files/paper/2015/file/07563a3fe3bbe7e3ba84431ad9d055af-Paper.pdf.
- [16] Remi Lam et al. “Learning skillful medium-range global weather forecasting”. In: *Science* 0.0 (2023), eadi2336. DOI: [10.1126/science.adi2336](https://doi.org/10.1126/science.adi2336). eprint: <https://www.science.org/doi/pdf/10.1126/science.adi2336>. URL: <https://www.science.org/doi/abs/10.1126/science.adi2336>.
- [17] Netbeheer Nederland. *Netbeheerders publiceren landelijke capaciteitskaart voor producenten duurzame energie*. Apr. 2021. URL: <https://www.netbeheernederland.nl/nieuws/netbeheerders-publiceren-landelijke-capaciteitskaart-voor-producenten-duurzame-energie--1449>.
- [18] JF Meirink. “Algorithm Theoretical Basis Document, Cloud Physical Products, SEVIRI”. In: *EUMETSAT Satellite Application Facility on Climate Monitoring. Available online at: www.cmsaf.eu*. doi 10 (2013).
- [19] J. R. Jing et al. “AENN: A GENERATIVE ADVERSARIAL NEURAL NETWORK for WEATHER RADAR ECHO EXTRAPOLATION”. In: *International Archives of the Photogrammetry, Remote Sensing and Spatial Information Sciences - ISPRS Archives* 42 (3/W9 Oct. 2019), pp. 89–94. ISSN: 16821750. DOI: [10.5194/isprs-archives-XLII-3-W9-89-2019](https://doi.org/10.5194/isprs-archives-XLII-3-W9-89-2019).
- [20] Ties van der Heijden et al. “Electricity Price Forecasting in European Day Ahead Markets: A Greedy Consideration of Market Integration”. In: *IEEE Access* 9 (2021), pp. 119954–119966. ISSN: 21693536. DOI: [10.1109/ACCESS.2021.3108629](https://doi.org/10.1109/ACCESS.2021.3108629).
- [21] W.C. de Rooy et al. *Harmonie verification and evaluation*. Tech. rep. Koninklijk Nederlands Meteorologisch Instituut, 2016.
- [22] J Bergstra, D Yamins, and D D Cox. *Making a Science of Model Search: Hyperparameter Optimization in Hundreds of Dimensions for Vision Architectures*. 2013.

- [23] Lisha Li et al. “Hyperband: A Novel Bandit-Based Approach to Hyperparameter Optimization”. In: *Journal of Machine Learning Research* 18 (2018), pp. 1–52. URL: <http://jmlr.org/papers/v18/16-558.html>.
- [24] Donald Shepard. “A Two-Dimensional Interpolation Function for Irregularly-Spaced Data”. In: *Proceedings of the 1968 23rd ACM National Conference*. ACM '68. New York, NY, USA: Association for Computing Machinery, 1968, pp. 517–524. ISBN: 9781450374866. DOI: [10.1145/800186.810616](https://doi.org/10.1145/800186.810616). URL: <https://doi.org/10.1145/800186.810616>.
- [25] Jerome H. Friedman. “Greedy function approximation: A gradient boosting machine.” In: *The Annals of Statistics* 29.5 (2001), pp. 1189–1232. DOI: [10.1214/aos/1013203451](https://doi.org/10.1214/aos/1013203451). URL: <https://doi.org/10.1214/aos/1013203451>.
- [26] Jerome H. Friedman. “Stochastic gradient boosting”. In: *Computational Statistics & Data Analysis* 38.4 (2002). Nonlinear Methods and Data Mining, pp. 367–378. ISSN: 0167-9473. DOI: [https://doi.org/10.1016/S0167-9473\(01\)00065-2](https://doi.org/10.1016/S0167-9473(01)00065-2). URL: <https://www.sciencedirect.com/science/article/pii/S0167947301000652>.
- [27] L. Breiman. “Random Forests”. In: *Machine Learning* 45.1 (2001), pp. 5–32. ISSN: 1098-6596. DOI: [10.1023/A:1010933404324](https://doi.org/10.1023/A:1010933404324). arXiv: [arXiv:1011.1669v3](https://arxiv.org/abs/1011.1669v3).



7

CONCLUSIONS AND RECOMMENDATIONS

*Everything's got to end sometime.
Otherwise, nothing would ever get started.*

Dr. Who

7.1. CONCLUSIONS

The integration of *Variable Renewable Energy* (VRE) is a necessary but challenging task. As the penetration of VRE into the energy system increases, efficient electricity grid management becomes difficult. The inherent uncertainty and intermittency of VRE increases the need for flexibility in the energy system, which can be (partially) met with *Demand Response* (DR) services. This thesis considers the modelling of uncertainty, as well as risk-aware decision-making approaches to unlock flexibility in assets and enable DR participation and more efficient electricity grid management. It provides a framework that allows for describing and connecting uncertainty from weather, markets, and operations, and how to leverage these to inform risk-aware decision-making for complex systems. As such, it aims to contribute to the further integration of VRE and speed up the transition to a renewable energy system. The main contributions of this thesis are:

- **Receding horizon Model Predictive Control approach for multi-market participation from pumping stations.**

Motivated by the available flexibility in storage in the Dutch open canal system and its significant energy and power consumption, we propose a new pump-scheduling strategy that optimizes the energy cost of pumping based on *Day Ahead Market* (DAM) and *Intraday Market* (IDM) participation in Chapter 2. We perform an analysis of the cost-saving potential through DR, showing significant benefits to be gained by exploiting the flexibility in the water system where perfect foresight of market prices is assumed. By analysing both the Dutch and German markets

over multiple years, we also show that as renewable energy penetration increases, the potential benefits are expected to increase as well. This contribution shows how existing pump infrastructure can be leveraged to participate in DR services and quantifies the potential benefits while serving as a benchmark method for DR participation under uncertainty.

- **Modelling market integration in electricity price forecasting models.**

Within the context of the increasing European market integration, this contribution shows how market integration affects price settlement and Electricity Price Forecasting performance in DAMs. In Chapter 4, we performed an EU-wide data analysis on how European markets are affected by one another. We proposed a greedy search algorithm to find external market features that improve Dutch DAM price forecasting accuracy with statistical significance. Better forecasts allow for better planning and, thereby, more efficient energy use.

- **Deep learning techniques for estimating operational uncertainty.**

In Chapter 3, we propose a neural network architecture for quantile regression models to forecast multiple distribution quantiles simultaneously. The method is later applied to forecast DAM electricity prices, the water level of the North Sea, and pumped discharges from local water authorities in Chapter 5 and to model solar irradiance based on cloud characteristics in Chapter 6. This contribution has a broader application than energy- and water management by potentially supporting uncertainty modelling in general

- **Realistic and sparse uncertainty representations.**

Besides proposing a method for operational uncertainty estimation, we also propose methods for conditional sampling of the uncertainty space and making a sparse representation in Chapter 3. We sample time series from forecast marginal distributions while adhering to the observed auto-correlation in the data to efficiently generate a large number of realistic scenarios. We propose clustering methods to condense the scenario set into an optimal subset with redistributed weights based on the energy distance to reduce the computational complexity of large uncertainty representations. To further reduce computational complexity, we propose extending the method to generate scenario trees where uncertainty grows over time. This contribution facilitates optimal decision-making under uncertainty in a computational resource-constrained setting.

- **Optimal and risk-aware pump scheduling for DR participation under uncertainty.**

As our main case study for DR, in Chapter 5 we propose a framework for the control of pumping stations under uncertainty to participate in the DAM and IDM. We show the benefit of probabilistic control techniques compared to deterministic control, quantified by the energy cost for pumping. One key contribution is the application of Exceedance Risk (ER) constraints on water level bound violations, which constrains the tail of the water level distribution in a computationally efficient way. The formulation of ER constraints allows for the fine-tuning of risk

acceptance, giving decision-makers a button to optimally trade off system robustness and energy cost. This contribution allows pumping stations to participate in DR services, potentially transforming how the Dutch water system is managed. In addition, it allows for risk-aware operational decision-making, leading to risk-informed decisions and, ultimately, safer water systems.

- **Probabilistic irradiance nowcasting using satellite-derived cloud-characteristics.** As solar energy is becoming a dominant influence in the Dutch power system, local congestion is equally dominant. In Chapter 6, we developed a solar irradiance nowcast to forecast irradiance quantiles spatially up to 6h ahead at 15min resolution. We test our approach in a real case study using data from Dutch Distribution System Operator Alliander, where we develop probabilistic net-load forecasting models using the state-of-the-art (KNMI's Harmonie) and our irradiance forecast. The results show a significant performance increase in the ability of a net-load forecast to capture extreme loads without increasing the false alarms generated by the forecasts. This contribution benefits efficient grid management, where Alliander admits that uncertainty in solar generation is their largest hurdle towards efficient grid management. Our approach potentially benefits solar energy trading by allowing for a better estimation of the uncertainty in generation, benefiting portfolio optimization. This contribution aids in managing grid congestion, can help manage imbalance risk for energy traders and, thereby, reduce energy costs for consumers.

7.2. SOCIETAL IMPACT

The societal impact of the work presented in this thesis spans several areas, directly contributing to the global effort in combating climate change and enhancing the energy system's resilience and efficiency.

- **Climate change mitigation**
By advancing the integration of renewable energy sources through operational flexibility and improved forecasting, this research indirectly contributes to reducing greenhouse gas emissions. The development and application of optimized scheduling and DR participation facilitate a shift towards cleaner energy sources, thereby mitigating the adverse effects of climate change.
- **Climate change adaptation**
The developed probabilistic methods for uncertainty modelling and risk-aware operational strategies for managing operational uncertainty and optimizing water and/or energy systems underpin efforts to adapt to the changing climate. By ensuring that energy and water management systems are more resilient to variable and extreme weather conditions, this work supports societal adaptation to climate change impacts.

- **Energy cost reduction for consumers**

Our research shows that improving the efficiency and reliability of energy systems can lower energy costs. The strategies proposed for demand response and market participation can lead to significant savings in energy procurement and operational costs, benefits that can be passed on to consumers. Moreover, better forecasting and scheduling reduce the need for expensive peaking power plants or the occurrence of extreme imbalances, contributing to lower electricity prices.

- **Reliability of power systems**

The innovations in forecasting, scheduling, and risk management introduced in this thesis enhance the reliability of power systems. By accommodating the variability of renewable energy sources and improving operational decision-making, these contributions help ensure a stable and continuous energy supply, essential for modern societies' functioning.

7.3. SUGGESTIONS FOR FUTURE RESEARCH

ENHANCED OPERATIONAL UNCERTAINTY MODELLING

- **Generative time series modelling**

In this thesis, we propose scenario generation for control purposes in two steps; first, the *Combined Quantile Regression Deep Neural Network* (CQRDNN) (Section 3.1.1) to forecast distributions, and second the *Non-parametric Bayesian Network* (NPBN) (Section 3.2.1) to sample with realistic temporal dependency. Future research could explore generative AI models for producing time series data immediately. This could streamline the generation of time series data, enabling direct forecasting that encapsulates realistic temporal dynamics without resorting to intermediary sampling stages. The NPBN proposed in Chapter 3 is limited to Gaussian copula's, where a neural network could potentially infer any statistical dependency. Investigating models that can inherently capture complex patterns and dependencies within time series data promises a more integrated approach to forecasting and scenario generation that requires fewer assumptions about the data.

- **Modelling market integration with Graph Neural Networks**

Considering the interconnected nature of EU energy markets, *Graph Neural Networks* (GNNs) are a promising tool for capturing the physical and operational constraints enforced by grid topology. Future studies could leverage GNNs to model the complex interdependencies between markets and energy flows across borders.

- **Modelling of the Intraday market**

While the DAM has been extensively studied in a modelling context, the Intraday Market remains relatively underexplored. Challenges related to data scarcity and the dynamic nature of IDM necessitate a focused investigation into its operational mechanisms and the potential for renewable energy integration. The proposed Bayesian Network in Chapter 5 leaves room for improvement in conditional IDM modelling. In practice, the IDM market would be highly affected by the Day Ahead forecast errors of market participants and their speculation on future imbalances.

Further research could uncover strategies to harness IDM dynamics, optimise energy portfolios more efficiently, and lower operational energy costs.

- **Comparative evaluation of weather forecast models**

A systematic assessment of weather prediction models across diverse climates and geographic regions could significantly refine forecasting accuracy for energy and water resource management. By identifying the strengths and limitations of current models, researchers can tailor forecasting techniques to specific environmental conditions, improving the reliability and efficiency of renewable energy systems.

- **Assessing the value of data on forecasting performance**

Shifting the research emphasis from model innovation to the quality and accessibility of underlying data could provide new insights into the drivers of forecasting accuracy. A comparative study assessing the relative contributions of data quality versus model complexity to performance outcomes would inform more effective resource allocation in research and development efforts.

- **Standardising operational performance benchmarks**

Traditional statistical measures often fall short of capturing the practical value of forecasts in operational settings. As Goodhart's law states '*any observed statistical regularity will tend to collapse once pressure is placed upon it for control purposes*'; a metric will become less valuable as it becomes the objective to solely minimize it without regard for further usefulness. Proposing new standard benchmarks, such as the efficacy of battery storage strategies in exploiting electricity price volatility, would offer a more relevant evaluation of forecast models from a practical perspective.

- **Exploration of advanced conditional sampling techniques**

Extending beyond the use of Gaussian copulas as applied in the NPBs proposed in Chapter 3, exploring alternative methods, such as vine copulas or composite distributions, could improve scenario generation. This research would enhance the representation of uncertainties in forecasting, providing a more nuanced understanding of potential future states.

OPERATIONAL WATER MANAGEMENT

- **Adaptation of strategies for local water management**

The *Noordzeekanaal-Amsterdam-Rijnkanaal* (NZK-ARK) is, interesting as it may be, not very representative of local or regional water management. Local systems are characterized by networks of smaller canals, smaller and staged pumping stations, and more local objectives like lowering salinity. Investigating the applicability of the proposed strategies to local and regional water management systems is necessary for addressing the diverse challenges faced by these systems. This research could identify scale-able and adaptable solutions that align with different water management contexts' specific objectives and constraints.

- **Exploring the potential of collaborative water management**

In this thesis, we model the incoming fluxes on the NZK-ARK as stochastic variables. However, it is expected that there would be benefits through cooperative efforts among water authorities, including shared market participation and operational coordination. Such collaboration could unlock new efficiencies and resilience in the water system, increasing overall safety and lowering energy costs.

- **Application of Reinforcement learning in operational water management**

Given the complexity and temporal constraints of water management objectives, reinforcement learning promises to optimize decision-making processes. This approach could facilitate more adaptive and efficient management strategies that respond to evolving conditions and emerging challenges, especially in a computational resource-constrained environment.

- **Extending methodologies to hydropower systems**

Applying the insights gained from this thesis to hydropower could provide valuable perspectives on balancing long-term hydrological planning with short-term market opportunities. This research might reveal novel approaches to enhancing the sustainability and profitability of hydropower operations, possibly combined with environmental flow operations.

- **Virtual Power Plant concepts in water management**

Integrating local generation, energy storage capabilities, and energy use of pumping into a Virtual Power Plant framework could enhance the flexibility and resilience of water and energy systems. In this thesis, we only consider the pumping station as a controllable asset. Including local generation and storage could lead to improved operational strategies, unlocking more flexibility in the water system.

- **Energy management in urban water systems**

The demand response potential within urban water treatment and distribution systems, especially in energy-intensive processes such as wastewater aeration, presents an interesting area for investigation. Optimizing energy use in these systems could lead to efficiency gains and cost savings, contributing to more sustainable urban water infrastructure.

- **DR from an aggregator perspective**

In this thesis, we approach DR from the perspective of a single large energy-consuming asset. However, it would be interesting to research more scale-able approaches that can run on many smaller assets in a coordinated manner. It would be interesting to investigate how well the proposed approaches in this thesis can be extrapolated to coordinated assets that operate under localized constraints and objectives.

ENERGY FLEXIBILITY

- **Optimizing battery management for grid stability**

Translating the insights from this thesis into practical battery management strategies could enhance energy storage efficiency and grid stability. This would involve developing algorithms that optimize charge/discharge cycles in response to uncertain grid demands and market signals, facilitating a smoother integration of renewable energy sources. Physical grid constraints could be formulated in a risk-aware fashion, for example, by constraining a maximum net load to the grid.

- **Addressing imbalances with DR**

Future research should focus on developing mechanisms to actively address energy imbalances. In the Netherlands, this could relatively easily be achieved through passive imbalance due to its low entry requirements. It would, however, be interesting to see what amount of aggregated DR volume could be supplied on, for example, the aFRR, and with what certainty.

- **Comprehensive market modelling for enhanced trading strategies**

An in-depth study of the bidding processes and dynamics of continuous trading within energy markets could lead to developing more sophisticated and advantageous trading strategies. In this thesis, we assume that bids are accepted for the ID₃ price. In practice, this is no guarantee, and all contracts are closed for distinct prices and volumes. Further research on how the market could be better represented would provide insights into the operational and economic factors that influence market behaviour and enable more informed and efficient IDM trading.

7.4. PRACTICAL CONSIDERATIONS FOR OPERATIONAL WATER RESOURCES MANAGEMENT

In this section, I will describe some practical considerations for water resources management. It is aimed at the Dutch water sector and, therefore, written in Dutch.

In deze paragraaf heb ik het over praktische overwegingen voor operationeel waterbeheer. Ik beschrijf een in paar - in mijn ogen - noodzakelijke stappen om richting een robuust en duurzaam watersysteem te gaan. Ik eindig met suggesties voor overwegingen in systeemontwerp.

DE TOEKOMST VAN OPERATIONEEL WATERBEHEER IN EEN DUURZAAM ENERGIESYSTEEM

De integratie van duurzame energie is essentieel voor de energietransitie, maar vraagt meer van de spelers in het energiesysteem dan voorheen. Er zal meer flexibiliteit nodig zijn om het grillige karakter van duurzame bronnen te faciliteren. Dit biedt kansen voor een efficiënter waterbeheer waarbij op operationele energiekosten kan worden bespaard.

Flexibiliteit binnen het energiesysteem maakt het mogelijk voor kritieke infrastructuur, waaronder ons watersysteem, om betrouwbaar te functioneren, zelfs tijdens piekmomenten van duurzame energieproductie of -consumptie. Het meest recente voorbeeld van hoe de wederzijdse afhankelijkheid tussen water- en energiebeheer fout kan lopen zijn de boze brieven die sommige waterschappen hebben gehad van de netbeheerders. Gemalen hebben een hoger vermogen dan waar ze voor gecontracteerd zijn, welke capaciteit ten tijde van netcongestie niet meer vergeven kan worden zonder de leveringszekerheid van het net in gevaar te brengen. Gevolg: de netbeheerder overweegt gemalen af te sluiten. In tijden van hoogwater zal het toch echt niet anders kunnen, het is dan pompen of verzuipen. Dit zal flexibiliteit van andere spelers in het energiesysteem vragen om die piekvraag te kunnen faciliteren. Maar wanneer je van anderen wilt kunnen verwachten dat zij het net ontlasten wanneer het moet, is het niet meer dan redelijk om zelf ook de pompcapaciteit te beperken als het moet en wanneer het kan. Een tijdsafhankelijke randvoorwaarde op het pompvermogen kan goed worden opgelegd binnen het framework dat is beschreven in dit proefschrift, naast de optimalisatie op uurprijzen.

In de afgelopen jaren hebben we gezien dat de situatie op de energiemarkt soms erg extreem kan worden, in dit geval met name door hoge gasprijzen. Hoewel de energiemarkt onderhevig is aan schommelingen, biedt een strategische benadering kansen op besparingen, zelfs in tijden van energieschaarste. Een harde voorwaarde hieraan is dat de manier van energie inkoop verandert. Vaste contracten moeten worden ingeruild voor flexibele contracten die op uur- of kwartierbasis werken. Hier zal wel een risicoacceptatie moeten ontstaan voor enkele uitschieters in uurlijkse of dagelijkse kosten door hoge uurprijzen of eventueel veroorzaakte onbalans. Die bestaan echter ook de andere kant op, waar je in sommige gevallen betaald kan worden om je verbruik aan te passen. De energierekening zal dus niet tot op de euro nauwkeurig en een jaar van tevoren te begroten zijn. Wat uiteindelijk niet alleen goed is voor de portemonnee, maar ook voor de onbalans in het systeem.

In sommige gebieden zijn de gemalen namelijk grote bronnen van onbalans voor energieleveranciers. Onbalans komt door verbruik dat niet goed een dag van tevoren was voorzien. De energieleverancier heeft vaak geen hydrologische of systeemspecifieke kennis, dus wordt een verwachting van de benodigde energie voor malen lastig. In dit proefschrift laat ik ook zien dat het niet altijd even gemakkelijk is om het gedrag van een gemaal te voorspellen. Door als waterbeheerder die verwachting (of planning) zelf te maken en flexibel energie in te kopen weet een leverancier beter wat er in het portfolio gaat gebeuren en zal de totale onbalans in het systeem lager worden.

Om verder bij te dragen aan het realtime balanceren van het energiesysteem middels onbalansmechanismen hebben watersystemen naar verwachting een beperkt vermogen. Door slim in te spelen op onbalanssignalen kunnen ze helpen het net te stabiliseren, voornamelijk door middel van afregeling (minder gaan verbruiken). Echter wordt de onbalansmarkt naar verwachting een markt voor snel reagerende en extreem flexibele spelers (e.g. batterijen), terwijl een goede verwachting van de onbalansstatus en/of prijs nog niet bestaat (als dat er al mogelijk is) waardoor activatie slecht in de planning kan worden meegenomen. Daarnaast zijn de meeste gemalen nu niet geschikt om snel (e.g. binnen 5min) op- of af- te regelen.

De kwantificering van operationele onzekerheid en proactieve sturing hebben de potentie om ons water- en energiesysteem efficiënter én veiliger te beheren. Dit vraagt echter een paradigmaverschuiving in onze traditionele benaderingen. Prognosemodellen moeten geëvolueerd worden om onzekerheden adequaat te weerspiegelen, terwijl sturingssystemen meer complexiteit zullen ervaren waardoor meer rekenkracht en nieuwe software nodig zijn. Daarbij kan een stochastische output uit het systeem de interpretatie voor de gemaalbeheerder bemoeilijken. Het vergt vertrouwen in en de adoptie van geavanceerde algoritmen en technologieën, niet alleen met het oog op kostenreductie, maar ook als een actieve bijdrage aan de energietransitie.

Om op korte termijn stappen te zetten richting een efficiëntere samenwerking tussen de water- en energiesector zijn twee concrete oplossingen met relatief gemak te implementeren:

- **Dynamisch peilbeheer:** Implementeer en bevorder de toepassing van dynamisch peilbeheer, waarbij een grotere peilvariatie wordt toegestaan om aan de behoeften van het energiesysteem te voldoen. Dit vergt een verkenning van de toelaatbare variatie die wateroverlast niet in het geding brengt, maar opent mogelijkheden om de beschikbaarheid van duurzame energie en netcapaciteit in acht te nemen.
- **Data-uitwisseling:** Ontwikkel en implementeer systemen voor het uitwisselen van data tussen waterbeheerders, netbeheerders, en energiehandelaren om een betere planning en operationele afstemming mogelijk te maken. De data uitwisseling met de energieleverancier zou al vanzelf gaan wanneer Day Ahead wordt ingekocht. Dit zou bijdragen aan een lagere onbalans door betere inschatting van energieportfolio's, en waterbeheerders in staat stellen om op meer doelen te sturen. En wanneer het bij waterbeheer bekend is dat hoogwater en netcongestie gelijktijdig op zullen treden, kan er eerder worden gedacht aan de inzet van noodaggregaten of in een noodgeval de optie van het gebruik van bergingsgebieden te verkennen.

Naast deze twee concrete stappen richting integraal waterbeheer voor de huidige infrastructuur, kan flexibiliteit in het watersysteem ook mee worden genomen in systeemontwerp. Een aantal denkrichtingen voor systeemontwerp zijn:

- In de ontwerpfase kan operationele performance expliciet worden meegenomen. Alleen dan kan een weloverwogen keuze worden gemaakt tussen de investeringskosten van infrastructuur, de operationele kosten, en de maatschappelijke bijdrage die de infrastructuur kan leveren.
- Met de toenemende druk op het elektriciteitsnetwerk is het belangrijk om de netcapaciteit in overweging te nemen bij de uitbreiding van een gemeentelijk gebied. Proactieve strategieën, zoals capaciteitsbepurende contracten of het inzetten van energieopslag voor piekafvlakking, kunnen helpen netcongestie te verminderen en bij te dragen aan een efficiënter water- en energiebeheer. De gecontracteerde aansluitcapaciteit zal voortaan als harde randvoorwaarde moeten gelden. Overweeg om de congestie van het netwerk mee te nemen in de NBW-toetsing, waar zowel de faalkans van leveringszekerheid meegenomen kan worden in de faalkans van het watersysteem, als dat waterbeheerders de benodigde netcapaciteit in terugkeertijden kan uitdrukken.
- Flexibiliteit kan je inbouwen door dynamisch peilbeheer mogelijk te maken, het gebruik te maken van variabele snelheidspompen, of het aanschaffen van pompen die sneller op- en af- kunnen regelen. Dit vergroot je operationele handelingsperspectief en daarmee de mogelijkheden om bij te dragen op verschillende aspecten van het energiesysteem, zoals de onbalansmarkt of netcongestie. Door in de ontwerpfase al inschattingen te doen van de operationele voordelen van maatregelen (e.g. operationele kosten, bijdrage aan netcongestie, CO₂ uitstoot van de verbruikte elektriciteit) kunnen de extra kosten die worden gemaakt ten behoeve van de flexibiliteit worden afgewogen en verandwoord.



ACKNOWLEDGEMENTS

During the last few years, I've had the chance to be one of the lucky people who genuinely love what they're doing. The challenging and motivating research, the inspiring environment of academia, and the people who make it happen are all delightful. In this section, I'd like to thank some of the people who greatly influenced my experiences during this PhD adventure.

First, my promotors, Edo Abraham, Peter Palensky, and Nick van de Giesen, who have their fingerprints on this thesis. Edo, over the last 6 years, your role has evolved significantly. It transitioned from teacher to supervisor, then to mentor, and finally to friend. You were always available, friendly, patient, sharp, and challenging me to push my boundaries. You were sometimes afraid I got too occupied with my consultancy; I'll never forget you telling me that I should sometimes just go for a walk and think. A piece of advice I take at heart. You showed me the art of language by compressing text to a global optimum and politely disagreeing with ~~the~~ other views. We had countless meetings where we ended up in lively discussions, consumed by the topic and forgetting about time. Doing research can feel lonely sometimes, but after talking to you that feeling would be gone for a while. Nick, I felt supported by your interest in our work and to-the-point remarks. Even though the topics I was working on were sometimes quite far from your chair, you could always ask the fun questions. And Peter, your mix of kindness, entrepreneurial spirit, and crazy scientist is inspiring. You were always openly enthusiastic about our work while actively promoting it in academia and industry, which was a big support when founding Pythia. You know my money is on you if we ever find the walrus bar. Thank you all, let's find out where the rest of this journey takes us.

Another key figure in this adventure is Durk Klopstra. You played a key role in setting up this research by bringing the right people together and working on the proposal with me and Edo. You were always interested in my activities (and the usefulness of results) and ready to brainstorm ideas or review material. You trusted me and mentored me in my entrepreneurial drive, taking us from Brabant Water to Pythia. Thanks for all your support over the years. This story doesn't end here.

I also had the pleasure to collaborate with others during this thesis. Joost Heijkers, Ben Staring, Kees Vlak, René van der Zwan, Ciska Blom, Jochem Hermans, Pieter Buijs Heine, thank you for your involvement and collaboration before and throughout this research. Dorien and Ronald, thank you for your enthusiasm and support from my MSc thesis up to now. Jesus, thank you for the interesting discussions and for putting a high bar to pull up to. Your rigorousness has been an example to me ever since our collaboration. Mike; our collaboration is solid anecdotal evidence for Proposition 10. Thank you, for explaining BNs and helping me with the application. Frank, our scientific and industry collaborations are a joy. Your support has been instrumental to our results; thank you. Mattijn; your plotting and geospatial skills and scientific curiosity are admirable. Your support was invaluable in the early days of RayCast. And my brother in

arms; Thomas. The day you arrived at HKV, my life became a lot easier and more fun. We have some long nights of coding behind us to get RayCast where it is now. I'm sure we have a few more lined up as well.

There is one person who knew I was going to do a PhD before I did; Jerom. I can't count the amount of times we ended up discussing science over beers and am happy that we at least have one scientific collaboration to prove it wasn't all nonsense. And Chelsea, my academic sister. Thanks for letting me disturb you all the times I was drinking my coffee and looking for a person to talk with. However, there are plenty more people who made my life at TU a joy. Simon, who adopted me in his IEPG team. Su, whom I had bottomless coffees with. Bart, bringing glühwein to our *buitenborrels* in winter. Carol, my energy market insider who's never shy for some market talk over good food. Juan, who's always up to discuss the latest ML news or a (heated) philosophical discussion. My office mates Bas, Paul, Kizje, Judith, Ibrahim, and Derya, with whom I fought for the office balcony and enjoy it with ever since. And of course all the *Thursday PSOR people*; Jeroen, Robert, Jessica, Boran, David, Oswaldo, Monica, Antonella, Carina, Patricia, Davide, Johanna, Kutay, Mert, Job, Roberto, Akshit, and Mario, who I blame for many *kapsali* and rough Friday mornings. Besides the regular Thursday drinks, many people contributed to the university feeling like a welcome home. Thom, Jeroen, Fransje, Erik, Markus, Saket, Remko, Coco, Alireza, Bahareh, Luuk, Bas, Thijs, and many others. Thank you for the many drinks, walks, lunches, and cookie breaks.

Some of my beloved (ex-)colleagues at HKV deserve a special mention. Joost; *energie maatje* and current business partner, working with you was and is truly energizing. David, Paulina, Carolien, and Nils, who always keep the *gezelligheid* alive and who I largely attribute my mental sanity during COVID to. And Dorien 'H', who always thoughtfully checks in.

I got to enjoy the warm support of a large group of friends and family during the process of this PhD (and before). Mom and dad, even though you don't always fully comprehend what I do; you're always excited and proud to hear about it, preferably over a beer. Thanks for your support and, of course, explaining my work to Cora and André. Kim, as a kid I once admitted that you were the example to beat at school. I think I'll stop now. Thanks for your support throughout the way. Then there are many friends who I traveled with, blew of steam with, or even - at times - discussed science with: Jeroen, Jeroen, Ruben, Timo, Teunis, Jochem, Luuk, Ebbe, Niels, Jordy, Casper, Noortje, Joeri, Sandra, Floris, Niek, Cameron, Marta, Sam, Maud, Fenno, Kizje, Erkki, Patrick, the whole Erasmus and Liquicity crew, and everybody else who feels like a member of this set. Your contributions to this manuscript were invaluable.

ABOUT THE AUTHOR

Teunis Johannes Theodorus VAN DER HEIJDEN

Ties van der Heijden was born on the 10th of February 1993 in Wageningen, the Netherlands. After finishing his education at the Christelijk Lyceum Veenendaal in 2011, he moved to Delft in pursuit of a degree in Civil Engineering from Delft University of Technology. In 2019, he was awarded an MSc degree in Civil Engineering with a specialty in Water Resources Management and Hydrology, after finishing a thesis on energy flexibility from flood infrastructure in the Netherlands. Later that year he started his PhD that resulted into this thesis. Throughout his PhD he was active in industry as a part-time Water & Energy consultant at HKV Lijn in Water, where he applied his research in practice.



LIST OF PUBLICATIONS

PEER-REVIEWED SCIENTIFIC PUBLICATIONS

6. **T. van der Heijden**, P. Palensky, N. van de Giesen, and E. Abraham, *Closed-loop simulation testing of a probabilistic DR framework for Day Ahead Market participation applied to Battery Energy Storage Systems*, *The 32nd International Symposium on Industrial Electronics* (2023).
5. **T. van der Heijden**, P. Palensky, N. van de Giesen, and E. Abraham, *Day Ahead Market price scenario generation using a combined quantile regression deep neural network and a non-parametric bayesian network*, *The 2022 IEEE Conference on Power System Technology* (2022).
4. **T. van der Heijden**, D. Lugt, R. van Nooijen, P. Palensky, and E. Abraham, *Multi-market demand response from pump-controlled open canal systems: an economic MPC approach to pump scheduling*, *Journal of Hydroinformatics* **24** (2022).
3. **T. van der Heijden**, P. Palensky, and E. Abraham, *Probabilistic DAM price forecasting using a combined quantile regression deep neural network with less-crossing quantiles*, *Annual Conference of the IEEE Industrial Electronics Society* (2021).
2. **T. van der Heijden**, J. Lago, P. Palensky, and E. Abraham, *Electricity price forecasting in European Day Ahead Markets: a greedy consideration of market integration*, *IEEE Access* **9** (2021).
1. **T. van der Heijden**, D. Lugt, R. van Nooijen, P. Palensky, and E. Abraham, *Demand response from pumping infrastructure in the Dutch delta*, *International Conference on Applied Energy* (2019).

PENDING PEER-REVIEWED SCIENTIFIC PUBLICATIONS

3. **T. van der Heijden**, M. Mendoza-Lugo, P. Palensky, N. van de Giesen, and E. Abraham, *Incorporating risk in operational water resources management: Probabilistic forecasting, scenario generation, and optimal control.*, Under review at *Water Resources Research* (2024).
2. J. Aerts, **T. van der Heijden**, A. Weerts, N. van de Giesen, R. Hut, *Advancing hydrological model diagnostics: An exploratory approach using random forest models and large-sample catchment dataset*, Under review at *Hydrological Sciences Journal* (2024).
1. **T. van der Heijden**, T. Stolp, M. van Hoek, F. Kreuwel, P. Palensky, N. van de Giesen, and E. Abraham, *Raycast: A satellite-based quantile regression irradiance nowcast*, Under review at *IEEE Transactions on Sustainable Energy* (2023).

NON-PEER-REVIEWED SCIENTIFIC PUBLICATIONS

4. **T. van der Heijden**, N. van de Giesen, P. Palensky, and E. Abraham, *A stochastic MPC framework for the control of pumping stations in polder systems with regard for uncertainty in inflow and hourly electricity prices*, [European Geosciences Union General Assembly \(2023\)](#).
3. **T. van der Heijden**, N. van de Giesen, P. Palensky, and E. Abraham, *Probabilistic forecasting and scenario generation of pumped discharge in polder systems*, [European Geosciences Union General Assembly \(2022\)](#).
2. **T. van der Heijden**, D. Lugt, R. van Nooijen, P. Palensky, and E. Abraham, *Demand Response from Flood Defences in the Dutch Delta*, 1st IFAC Workshop on Control Methods for Water Resource Systems (2019).
1. **T. van der Heijden**, D. Lugt, R. van Nooijen, P. Palensky, and E. Abraham, *Energy markets and sustainable water management: pumping and demand response in the Dutch delta*, [European Geosciences Union General Assembly \(2019\)](#).

NON-SCIENTIFIC PUBLICATIONS

3. **T. van der Heijden**, *Virtuele energieopslag met slim waterbeheer*, [Land+Water \(2023\)](#).
2. **T. van der Heijden**, D. Klopstra, and E. Abraham, *Optimizing water system operations, blue storage and the energy transition*, [TU Delft Delta Links \(2019\)](#).
1. **T. van der Heijden**, P. Palensky, and E. Abraham, *Control of flood defense infrastructure for demand response purposes*, [IEEE Smart Grid Newsletter \(2019\)](#).

